SAPIENZA
UNIVERSITÀ DI ROMA

OTN/WDM Technology Application for Implementing Xhaul Architecture in C-RAN Environment

Dipartimento di Ingegneria dell'Informazione,
Elettronica e Telecomunicazioni

Dottorato di ricerca in
Ingegneria dell'Informazione e della Comunicazione
XXIX Ciclo

Advisor
Prof. Vincenzo Eramo

Candidate
Francesco Giacinto Lavacca

October, 2016

Abstract

Very often reading and talking about 5G or the next generation network, we have an idea as huge as confused.

We could find in many papers in literacy a lots of several issues and several facets that describe the new access network generation; from these ones, for example, we can mention an expected number of connected devices and forecast traffic that are more than 1000-fold actual values. This increasing number of wireless devices, the increasing required traffic bandwidth and the high power consumption lead to a revolution of mobile access networks, that will be not a simple evolution of traditional ones.

Another point of difference with the actual network will be the presence of different classes and qualities of service necessary for providing different service types.

As consequences of the intense research studies done in these years, a large number of emerging technologies that could achieve the above requirements are developed. One of these technologies is Cloud Radio Access Network (C-RAN), that is seen as promising solution in order to deal with the heavy requirements of bandwidth capacity and energy efficiency, defined for 5G mobile networks. The introduction of the Common Public Radio Interface (CPRI) technology allows for a centralization in Base Bandwidth Unit (BBU) of some access functions, with advantages in terms of power consumption saving when switching off algorithms are implemented. Unfortunately, the advantages of the CPRI technology is to be paid with an increase in bandwidth to be carried between the BBU and the Radio Remote Unit (RRU), in which only the radio functions are implemented.

However, one of the most import factors, that could sign a great boost in the new generation network, will be how these technologies could work together in order to improve the whole network performance and, consequently, the possibility to have a "network slicing", in which different service types could be managed by a carrier client. Thus, it is simple to think that one

of the most important key drivers in 5G networks has to be the flexibility in managing of different radio access technologies.

The OTN/WDM technology application could be important to achieve a great level of flexibility and to save resources in the 5G access network, where there will be a dense deployment of network elements like Base Station or WiFi access points. In this scenario, a trade-off solution between power and bandwidth consumption may be needed.

In this thesis, it is proposed and evaluated a network solution that consists in handling and carrying the traffic generated by the RRUs and RBSs (CPRI and Ethernet flows) with a reconfigurable network based on Optical Transport Network (OTN) technology.

After proposing some energy and cost-efficient OTN/WDM switch architectures and resource dimensioning analytical models, it is shown how the sum of the bandwidth and power consumption may be minimized with the deployment of a given percentage of RRU out of the total number of radio elements. It is important to note that the achievement of this results is only possible if the network has the capacity to efficiently manage a large number of base stations and, thus, it is able to exploit the gain related to the statistical multiplexing effects.

Contents

List of Figures

List of Tables

Chapter 1

Introduction

In the last decades, the vision of a transparent all-optical network is superseded by a more versatile and pragmatic idea of an hybrid network solution. Also 5G access networks follow this trend due to the very large number of key drivers and requirements that are outlined for the next generation network: demands for higher mobile networks capacity, for increased data rates and for larger number of simultaneously connected devices are, in fact, just few of the requirements posed in the evolution of the radio access network.

The scope of this thesis is to embrace some topics that analyze this evolution trend and contribute to it with the proposal of a radio access architecture that achieves some goals like energy and bandwidth efficiencies, low cost systems and high level of flexibility for managing different radio access technologies in the same network.

1.1 Motivations and scope of the work

The main motivations of this thesis are to analyze the different solutions come out from the intense research studies in order to deal the very strict requirements for the 5G access networks and to propose a versatile network architecture that could achieve simultaneously several ones of them.

To deal the very high capacity and coverage demand, one of the most commonly solutions could be the strong radio site densification (e.g. through small, pico, femto cells), that could be also obtained by different deployment architectures. Unfortunately, although this solutions complies the capacity and coverage demands, it could be not efficient enough to pursue the other important requirements about energy consumption and cost of systems.

The widespread availability of mobile devices, such as tablets and smartphones, and a lots of dedicated applications has led to quickly increase mobile data traffic in the last few years. Furthermore, based on different studies and predictions [3], it is possible to conclude that beyond 2020, mobile networks will be asked to support more than 1,000 times todays traffic volume. Demands for higher mobile networks capacity, for increased data rates and for larger number of simultaneously connected devices are just few of the requirements posed in the evolution of radio access networks. Other fundamental factors are energy consumption and cost of systems, latency, spectrum availability and spectral efficiency. Naturally, one of the solutions to deal the very high capacity and coverage demand is the strong radio site densification (e.g. through small, pico, femto cells), that could be also obtained by different deployment architectures.

Unfortunately, although the continuous radio site densification allows requirements about high capacity, short latency and reliability to be satisfied, we could not achieve the needed features about energy consumption, being this solution not energy and cost efficient: in fact, in traditional mobile networks nodes and components are always active to be immediately available where and when needed, and are not very dependent on traffic load.

As a promising solution to deal these requirements, Cloud Radio Access Network (C-RAN) or Centralized RAN could be considered for its efficiency and flexibility [4, 5]. Based on the idea to physically separate the traditional base station in the two different entities Base Band Unit (BBU) and Remote Radio Unit (RRU), C-RAN leads to important advantages, as energy saving, Total Cost of Ownership (TCO) saving, improving security and deployment of infrastructure ready to support advanced features, like Coordinated Multi-Point (CoMP), enhanced inter-cell interference coordination (eICIC), carrier aggregation and more complex and dynamic multiple-input multiple-output (MIMO) schemes [6, 7].

The network between the BBUs and RRUs is called fronthaul network. Furthermore, there are three noted standard interfaces to encapsulate radio samples between RRU and BBU: Common Public Radio Interface (CPRI)[8], Open Base Station Architecture Initiative (OBSAI)[9] and Open Radio equipment Interface [10]. Both standards introduce an important feature in C-RAN, the possibility to switch off or switch on the BBU when the traffic changes during the day [11]. As disadvantages to be paid, the C-RAN solution needs much bandwidth to carry the CPRI flows that have a bit rate up

to ten times higher than the total capacity of a traditional base station.

Another important section in 5G networks that has to be improved, especially in flexibility, is the transport network, which acts as backhaul and/or fronthaul for the radio traffic. With traffic expectation in the order of magnitude of several $Tbps/km^2$, a radical optimization of the transport network is unavoidable. It is clear that the network architecture, both access and transport, and its control need to be rethought.

An emerging network paradigm, labeled as "Xhaul" [12, 13], wraps fronthaul and backhaul in a common connectivity segment providing a joint optimization opportunity, especially in sharing transport resources for different purposes and protocols. Xhaul unifies and enhances the traditional backhaul and fronthaul areas by enabling a flexible deployment and reconfiguration of network elements and networking functions. It also facilitates the baseband processing centralization, achieved by pools of digital units. The role of the Xhaul transport network is to convey Ethernet traffic and CPRI traffic on the same network infrastructure. A relevant case is the use of a Wavelength Division Multiplexing (WDM) optical network to transport Ethernet and CPRI over optical channels possibly sharing the same channel for heterogeneous traffic. Transport of future protocols will be similarly possible on Xhaul, for example in support of alternative splitting strategies in the radio layer.

1.2 Research Contributions

Based on these motivations, this treatise addresses a complete solution for next generation access network, starting from a deep study of an switch architecture that integrates with low costs and complexity two switching levels, Optical Transport Network (OTN) and Wavelength Division Multiplexing (WDM), and arriving to a proposal of network architecture that jointly optimizes the access and the transport segments of a future network.

Founded by the definition of an integrated WDM-OTN switch that allows for significantly lower complexity and cost at the price of relaxing the non-blocking ideal performance requirements normally required to such a kind of switch [14], Chapter 3 treats the investigation of the impact that the switch blocking has on the network performance in static and dynamic scenario for different metropolitan networks.

Different architectures are proposed and analyzed by means of the formulations of routing problems in integrated OTN/WDM networks, the definitions

of efficient heuristics to evaluate the blocking performance in static traffic scenario. For this studies, the results show how no blocking degradation occurs in case of different metropolitan networks. In particular it is shown that the degradation of 2-3 orders of magnitude in blocking probability occurring under dynamic traffic scenario can be mitigated with the introduction of a spatial speedup of value 1.5.

Furthermore, with the definition of a low complexity and integrated switching architecture for metropolitan networks, it is possible to obtain a reduction in OTN switches as small as 50%, that could be reached when the traffic needing sub-wavelengths switching is less than 40%.

In the Chapter , a network solution in which the radio component is composed by RRU and traditional Radio Base Station (RBS) has been analyzed. The conducted study shows that the solution in which only RRUs are used are not cost effectiveness because the low power consumption achieved with the switching off of the centralized components does not compensate the high bandwidth consumption. Conversely the use of only RBSs would lead to bandwidth efficient solutions but very poor in terms of power consumption.

The main contributions of the analysis [15] could be summarized in the following way:

i) the definition of analytical models, validated by simulation, for the resource dimensioning of the Xhaul network;

ii) the evaluation of power/bandwidth trade-off solutions based on the optimal determination of the percentage of RRUs to be used in order to minimize the sum of the bandwidth and power costs.

The first objective is to determine the total cost of radio access network, deployed over a Xhaul transport solution, by considering the cost of bandwidth and power consumption. Costs are evaluated for a dense urban scenario starting from a statistical modelling of radio traffic over time and space.

The development of analytical models quantifies the advantages and allows finding a trade-off between the employment of RRUs and RBSs at sub areas level, so as to minimize the total cost depending on both the bandwidth and consumption consumption. It leads to determine the right percentage of RRUs to be used as a function of the traffic and network parameters. The most appropriate mix could depend on several factors and, for instance, it could be driven by radio coordination and coverage needs, but this thesis deals with only the required bandwidth to carry and the energy consumed. In this

case, the radio network is assumed to be arranged as a set of RRUs and RBS, serving sub-areas, and transmitting CPRI and Ethernet flows respectively across the re-configurable Xhaul transport segment towards the core. The most appropriate mix depends on several factors and, for instance, it could be driven by radio coordination and coverage needs. In order to save energy, the centralized component of the CPRI technology is activated/deactivated to follow the traffic demand.

Several traffic models characterizing the statistical of the peak traffic values [3] are introduced. According to these traffic models, a dimensioning procedure is illustrated allowing significantly lower number of CPRI circuits as well as the number of BBUs needed, with respect to the case in which that number is statically fixed to the number of installed RRUs. This study aims at quantifying the potential advantages in terms of bandwidth and energy saving obtainable via:

i) an activation/deactivation policy of BBUs associated to the sub-areas;

ii) a full sharing of transport capacity in the Xhaul network.

1.3 Organization

The rest of the thesis is organized as follows. In Chapter 2, there is a literature review with a detailed context exploration for all the areas covered in this treatise. In Section 2.1 there is an introduction to the Xhaul environment; in particular, the main facets of the next generation network are reported. In Section 2.2, the Cloud - Radio Access Networks (C-RAN) are described reporting the benefits and the drawbacks. Section 2.3 deals with the possible splitting solutions for the C-RAN architecture, starting from the classical definition in BBU and RRU to the traditional base station. In Section 2.4, it is reported the evolution of the optical transport network. Section 2.5 treats the multiple implementation of an optical-node, in particular the benefits of the OTN/WDM switching are explained.

Chapter 3 deals with the definition of OTN/WDM integrated switching architectures. In particular, the OTN/WDM switch node architecture is described in Section 3.1 and the complexity evaluation is reported in Section 3.1.2. In Section 3.2, the optimal problem of the Switch Resource Assignment and Routing (SRAR) in OTN/WDM networks is stated. The ILP problem is NP-complete, thus an heuristic, named Maximizing Shortest Path Traffic

(MSPT), is defined in Section 3.3. Then the numerical results of the analysis are report in Section 3.4. Section 3.5 treats the definition of a new OTN/WDM switching node architecture with a reduced number of elements. The formulation of an ILP problem and the description of an heuristic are reported in Section 3.6 and Section 3.7 respectively. Then the most important results of the performance analysis of the proposed architecture in metropolitan networks are reported in Section 3.8.

Hence Chapter 3 deals with all the theoretic models and theoretic analysis created to verify the benefits of an OTN/WDM integrated node architecture that is flexible and efficient. While keeping those in mind, a solution for a reconfigurable Xhaul network is proposed and investigated in Chap. 4. In Section 4.2, the reference scenario is explained. Then the cost evaluation model and the analytical models for resource dimensioning are reported in Section 4.3 and 4.4 respectively. The main results for 4G and forecast 5G network areas are illustrated in Section 4.5 in both Xhaul and fronthaul scenarios. In Section 4.5.4, the optimal bandwidth/power consumption trade-off analysis is reported.

Finally conclusions and future research items are illustrated in Chapter 5.

Chapter 2

Background and Literature Overview

The chapter reports a complete introduction to the OTN/WDM switching and to the Xhaul reference scenario.

2.1 Introduction to Xhaul Environment

The widespread availability of mobile devices, such as tablets and smartphones, and a lots of dedicated applications has led to quickly increase mobile data traffic in the last few years. Furthermore, based on different studies and predictions [3], it is possible to conclude that beyond 2020, mobile networks will be asked to support more than 1,000 times todays traffic volume. Demands for higher mobile networks capacity, for increased data rates and for larger number of simultaneously connected devices are just few of the requirements posed in the evolution of radio access networks. Other fundamental factors are energy consumption and cost of systems, latency, spectrum availability and spectral efficiency. Naturally, one of the solutions to deal the very high capacity and coverage demand is the strong radio site densification (e.g. through small, pico, femto cells), that could be also obtained by different deployment architectures.

Many documents in literature propose, as solution for a Fixed and Mobile Convergence (FMC), the Next Generation Passive Optical Network (NGPON2), that is technology compliant with the cost figures and operational needs for running optical access networks. Usually NGPON2 could be divided in structural convergence (regarding the infrastructure) and functional

convergence (regarding the necessary functionalities required in fixed and mobile networks). In particular, in [12, 16] authors address five use cases that have structural convergence as a driver and suggest NGPON2 as evolution network to support and trigger this kind of convergence, in which the access network infrastructure is used for all kind of services, extending the access reach towards the aggregation network.

Unfortunately, the previous solutions could be not efficient enough to pursue the discussed requirements about energy consumption and cost of systems. In fact, although the continuous radio site densification allows requirements about high capacity, short latency and reliability to be satisfied, we could not achieve the needed features about energy consumption, considering that in mobile networks nodes and components are today always active to be immediately available where and when needed. Hence in traditional base stations, the energy consumption is not very dependent on traffic load. As said above, for deployment of 5G networks, there are stronger and more clearly defined requirements on high energy performance than before. Operators explicitly mention a reduction of total network energy consumption by 50% despite the expected 1,000-fold traffic increase. These results can be achieved only by temporary deactivating network resources, like small cells, when the traffic demand is reduced.

As a promising solution to deal these requirements, Cloud Radio Access Network (C-RAN) or Centralized RAN could be considered for its efficiency and flexibility [4, 5]. Based on the idea to physically separate the traditional base station in the two different entities Base Band Unit (BBU) and Remote Radio Unit (RRU), C-RAN leads to important advantages, as energy saving, Total Cost of Ownership (TCO) saving, improving security and deployment of infrastructure ready to support advanced features, like Coordinated Multi-Point (CoMP), enhanced inter-cell interference coordination (eICIC), carrier aggregation and more complex and dynamic multiple-input multiple-output (MIMO) schemes [6, 7, 17]. There are several architectures to implement the C-RAN and they differ regarding some aspects like the cooperation between RRUs and BBUs or the implementation of the BBU functionalities [18]. In particular there are three groups of classification:

- *BBU hotel*: many BBUs are collocated in the same place, but remain physically separate and each of them is individually connected to a dedicate RRU;

- *BBU pool*: it is a cluster of collocated and cooperating BBUs that serves a cluster of RRUs;

- *BBU cloud*: the processing functions of a BBU pool are implemented on servers that can be flexibly configured and located in different place.

In the proposed analysis and in the proposed architecture, the concept of a flexible cluster of BBUs is considered in order to achieve a very high level of efficiency in energy consumption and management.

The network between the BBUs and RRUs is called fronthaul network. There are two noted standard interfaces to encapsulating radio samples between RRU and BBU: Common Public Radio Interface (CPRI) and Open Base Station Architecture Initiative (OBSAI). Both standards introduce an important feature in C-RAN, the possibility to switch off or switch on the BBU when the traffic changes during the day [11].

The C-RAN solution needs much bandwidth to carry the CPRI flows that have a bit rate up to ten times higher than the total capacity of a traditional base station. For multi-sector and multi-antenna configurations, the total bit rate for the CPRI fronthaul links could be evaluated as follow [18]:

$$B_{CPRI} = S \cdot A \cdot f_s \cdot b_s \cdot 2 \cdot (16/15) \cdot LC \tag{2.1}$$

wherein, S and A are the number of sectors and antennas per sectors respectively; f_s is the sample rate (equal to 30.72 MS/s per 20 MHz radio bandwidth) and b_s is the number of bits per sample (we have 15 for LTE and 8 for UMTS). The remaining factors in the expression take into account the separate processiong of In-phase and Quadrature (I/Q) sample (factor 2), the additional overhead information (factor 16/15), and the rate increase caused by line coding (LC = 10/8 or 66/64, dipending on the CPRI net bit rate option). For instance, for a tower with 20 MHz LTE bandwidth, 1 sector and MIMO 2x2, we have a CPRI flow of about 2.5 Gbps. [19]

To reduce the amount of data transmitted through the fronthaul network it was proposed that the functional splitting point between a BBU and an RRU be changed [4, 20, 21]. Splitting between the MAC and Physical layers in Long Term Evolution (LTE) has been proposed that can achieve the most significant bandwidth reduction. In particular a split whiting the physical layer is compatible with both good wireless performance and significant bandwidth reduction near the MAC and physical splitting solution.

Another important facet in 5G networks that has to be improved, not only in the capacity but also in flexibility, is the transport network, which acts as backhaul and/or fronthaul for the radio traffic. With traffic expectation in the order of magnitude of several $Tbps/km^2$, a radical optimization of the transport network is unavoidable. As reported in [7], there some key drivers that force the RAN transport network to widely reinvent itself:

- the need for immense amounts of bandwidth in the RAN (expected data transmission for tower more than 10 Gbps);
- energy efficiency;
- the requirement for extremely low latency to provide for a better user experience;
- the addition of different classes of service for different service types;
- centralization of control to accommodate more complex network planning and optimization;
- a push toward virtualization and standardization to simplify network hardware.

It is clear that the network architecture, both access and transport, and its control need to be rethought. And it is well-known that the only use of a fronthaul solution does not address all requirements listed above. Based on this assumption, it is proposed an emerging network paradigm, labeled as "Xhaul" [13], that wraps fronthaul and backhaul in a common connectivity segment providing a joint optimization opportunity, especially in sharing transport resources for different purposes and protocols. Xhaul unifies and enhances the traditional backhaul and fronthaul areas by enabling a flexible deployment and reconfiguration of network elements and networking functions. It also facilitates the baseband processing centralization, achieved by pools of digital units. The role of the Xhaul transport network is to convey Ethernet traffic and CPRI traffic on the same network infrastructure. A relevant case is the use of a Wavelength Division Multiplexing (WDM) optical network to transport Ethernet and CPRI over optical channels possibly sharing the same channel for heterogeneous traffic. Transport of future protocols will be similarly possible on Xhaul, for example in support of alternative splitting strategies in the radio layer.

2.2 Cloud Radio Access Network

Traditional C-RANs are organized as a three element network, that contains BBU pool, RRUs network and the transport network (commonly defined as fronthaul network). As mandatory requirements, the most important aspects are good jitter, short latency, high bandwidth and good error ratio performance.

There are many papers in literature that debate various solutions for the implementation of the fronthaul network, especially to overcome the disadvantages of the simple deployment of dedicated fiber for every fronthaul link, being this one not efficient in terms of fiber utilization and fiber costs.

In [22], authors propose a single fiber Coarse Wavelength Division Multiplexing (CWDM) solution, that is a low cost option that allows multiplexing CPRI links over one fiber. Small Form factor Pluggable (SFP) let fronthaul network be implemented in a single fiber with up to 4.9 Gbps capacity including an innovative monitoring scheme. Also in [23], a Dense Wavelength Division Multiplexing SubCarriers Modulation-Passive Optical Network (SCM-PON) solution has been proposed, where 60 subcarriers, each carrying a 20 MHz-LTE signal with 64 Quadrature Amplitude Modulation (QAM), are transmitted on a single wavelength. It is important to note that the use of WDM techniques for the multiplexing of the multiple fronthaul connections fixes the fiber efficiency requirements and adds the capacity to add-drop fronthaul links in a flexible way, which is particularly important in dense urban areas where fronthaul is likely to be used and where cells are for instance at the tops of buildings. Moreover these solutions overcome the limitations of the passive WDM option that do not provide management capabilities, such as fault isolation ones.

In [24], authors consider, as transport technologies, Radio-over-Fiber (RoF) that is an analog transmission, instead of the digital transmission subsystems as CPRI and OBSAI. Each fiber has 4 cores and each Multiple Input Multiple Output (MIMO) signals is transmitted by radio-over-fiber technology in a given core. Considering the carrier aggregation, each fiber could support up to 12 MIMO signals. Also in [25] - [26], authors consider RoF as technology for the last miles to implement an optical backhaul for 5G wireless broadband connections; several architectures for RoF systems are available, but their employment is related to the number of users (RRUs) and the number of optical resources (optical transceivers). Wireless fronthaul

cannot provide the same performance as optical fiber, in terms of latency and throughput. In [27], authors consider to employ the same technology in transport network, furthermore they treat the benefits on reconfigurable fronthaul networks and the need of a reconfigurable electrical switch very close to the BBU pool.

In [28], authors consider a Mobile Fronthaul RoF (MFH RoF) transceivers with the capability to transport Digital RoF (D-RoF). As transport system architecture, they consider Next Generation Passive Optical Network (NG-PON2) based on SCM. In order to increase the number of transported D-RoF channels, they suggest the use of WDM in conjunction of SCM technique: the increasing factor of supported RRUs is equal to the number of sub-carriers per optical wavelength.

In [29], authors propose a solution for next generation cost-effective mobile fronthaul network based on Intermediate Frequency over Fiber (IFoF) technique. In IFoF systems, multiple radio signals can be allocated onto the same number of IFs within a particular bandwidth: compared to D-RoF, it is not necessary to utilize relatively larger bandwidth. The maximum number of IFs per wavelength has been evaluated as 12, that correspond to 10.32 Gbps digital rate based on CPRI interface.

Recently, the Radio-over-Ethernet project (IEEE 1914.3) [30] has been proposed to elaborate a standard for mapping and encapsulating the I/Q samples into standard Ethernet frames, allowing for reusing low cost Ethernet equipment for transmission and in the long run for also applying Ethernet based networking [31]. For this case the latency-related requirements have to be kept in mind, being the traditional Ethernet not complaint with the very strict time constraints introduced by 5G scenarios [32, 33]. The Ethernet standard has to be enhanced to support time sensitive applications in order to support the demanding latency and the synchronization requirements of a fronthaul network [18].

All discussed solutions about deploying technologies in fronthaul networks have some critical points: first of all the static approach for connecting the RRUs with the BBU pool with dedicated links and the very high bandwidth required by CPRI signals; in fact, the CPRI flows require a transport bandwidth that is more that 15 times higher [11] than the capacity offered to the users. Efficient solutions have to be identified to carry the CPRI flows in both link and network levels. For instance, related to the first one, it is simple to think about the increase of the fronthaul capacity, by means of single fiber

bidirection, wavelength-division multiplexing, and etc [34]. Another way is to reduce the required data rate on the fronthaul, by means of baseband signal compression [35], RRU-BBU functionality splitting [36], radio resource allocation [37], dynamic Rate configuration [38] and etc. On the network level, packet switching can provide hierarchical and flexible fronthaul networking [39, 40]

In [41], authors focus on the key transport challenges with respect to future 5G mobile networks in five future scenarios, such as very high data rate or very dense crowds of users. They consider a 5G transport network divided in two different segments, *small cell transport* and *metro/aggregation*. For the latter one, authors advise as promising solution the DWDM-centric network, that offer high capacity and lower energy consumption than their packet-centric counterparts. For the first one, a dedicated network segment, they treat many options that differs in performance, costs (in terms of CapEx and OpEx) and deployment maturity. In that analysis, fiber-based solutions are seen as a good and long term candidate for 5G small cells transport networks. In [42], authors analyses a number of architectural options for optical 5G transport networks, with the objective of understanding which alternatives are the most promising in terms of total power consumption and equipment costs. But in this analysis, the several cost models do not consider the effects of the required bandwidth into different scenarios. In [43], authors show the benefits in terms of statistical multiplexing gain for efficient two-segment fronthaul deployment.

Finally, treating about 5G networks, virtualization aspects need to be mentioned. For instance, Network Function Virtualization (NFV) or Software Defined Network (SDN) are two technologies that enable the definition of logically isolated networks over physical networks, sharing the physical resources in a flexible and dynamic way. In this scenarion, a good example might be RAN-as-a-Service (RANaaS [44]) paradigm that introduces a great level of flexibility about the radio access functionalities, but do not overcome the big issue of a very high capacity infrastructure. Indeed every network entities has to support the full-centralization as the typical C-RAN.

2.3 Functional Splitting in Crosshaul Network Architecture

In C-RAN environment, the In-phase and Quadrature (IQ) samples of the baseband signals are transmitted in the fronthaul network across a common public radio interface (CPRI) [11, 6]. The amount of IQ sampled data becomes at least ten times than that of the RF signal maximum bandwidth and it must be transmitted via an optical link [6, 11]. For this reason new solutions have been proposed in literature in order to save the used bandwidth and at the same time by maintaining the advantages of power consumption saving and interference management of the centralized solution. [45, 46]

The most interesting solutions have been proposed for the Long Term Evolution (LTE) network case and their basic idea is to reduce the used bandwidth by making the optical transmission rate proportional to the wireless link data rate [47]. The reduction can be obtained with a different functional split with respect to the traditional solution. The functional split options, which can achieve a significant bandwidth reduction are the Split MAC Physical (SMP) and Split Physical Processing (SPP) solutions reported in Fig. 2.1.a and 2.1.b respectively.

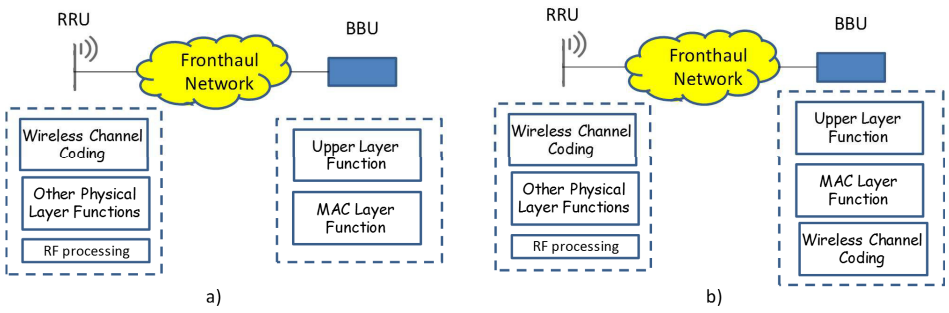

Figure 2.1: Split MAC Physical (a) and Split Physical Processing (b) solutions

In the SMP solution all of the physical layer functions are implemented in the RRU. Conversely the MAC layer functions are implemented in the BBU. With this solution, LTE MAC frames called transport blocks, and control signals in the physical layer are forwarded through the fronthaul network, rather than IQ samples as occurring in the traditional solution. The optical transmission rate is greatly reduced to approximately the wireless transmission data rate. The drawbacks of the the SMP solution is the difficulty of implementing centralized processing for joint transmission and reception.

In the SPP solution, the wireless channel coding is migrated towards the BBU while the others physical layer functions as modulation and Multiple Input Multiple Output (MIMO) are implemented in the RRU. This solution allows the inter-cell interference management and the required optical link capacity can be reduced to nearly that of the SMP solution and it depends on the wireless transmission coding rate.

2.4 Evolution of Optical Transport Networks

Transport networks are migrating towards a simplified architecture basically composed of three layers [48, 49, 50]:

i) the Multi-protocol Label Switching (MPLS) layer, which is the connection-oriented packet technology able to harmonize IP with circuit-based worlds;

ii) the Optical Transport Network (OTN) layer [51, 52, 53], needed to handle simultaneously packet and circuit-based services, with the right granularity, while providing a level of performance monitoring, network surveillance and fault recovery operations similar to the one provided by the Synchronous Digital Hierarchy (SDH) network;

iii) the Wavelength Division Multiplexing (WDM) layer allowing routing of individual wavelengths carrying high capacity channels benefiting from the huge transmission bandwidth of the optical fiber.

This simplified transport network layering came out to simultaneously fulfill key requirements such as to migrate the network towards the all-IP paradigm and to reduce complexity and costs associated to traditional transport technology based on circuit-switching (SDH/SONET). As a result, all the transport functions that were assigned to SDH/SONET are now distributed across different layers, partly in the optical (OTN and WDM) and partly in the packet (MPLS).

The introduction of OTN switching [54]-[55] was a topic largely debated, and many operators came to the conclusion that its use is needed to aggregate, with an efficient bandwidth utilization, packet service data flows (from router client interfaces) at lower rate into WDM data flows at higher rates in order to lower the cost per transported bit [56, 57, 58]. Possible applications of the OTN switching is in metropolitan area networks to aggregate both fixed and

mobile traffic in a ring or mesh network topology. In fact in such networks an higher level of functionalities are required but keeping at the same time the cost acceptably low. In such applications the advantages offered to the operators by the proposed node are the possibility to bring up services dynamically, the support of enhanced network applications such as protection and restoration [59] and the provision of an extra level of flexibility by the OTN subwavelength multiplexing and switching. Another case where OTN switch can be important is in those applications where tough requirements on latency are given.

Regarding a generic node of the transport network, it will contain multiple switching layers, according to the level of switching and granularity needed in that specific node. The most generic case is represented by a node logically composed of three stacked switches, handling data flows at different levels of traffic aggregation, namely MPLS (LSP: label switching paths tunnels), OTN (ODU: optical channel data unit tunnels), and WDM (wavelength channels). The ODU channels, defined by the G.709 standard [60, 61, 62] carry traffic at medium-high sub-wavelength granularity, are cross-connected by the OTN switch, while wavelength channels, carrying higher order data flows, are optical switched typically by a ROADM (reconfigurable optical add-drop multiplexer) [63, 64, 65, 66]. The finest granularity is so handled by the MPLS switch.

There could be different levels of integration of the different layers, at either data plane, or control plane, or even management plane; but in any the real benefit of packet-optical integration is to offload the job of packet switch/routers (e.g. MPLS), by routing bypass traffic in each node down to the optical layer (either OTN or WDM) so as to save a significant number of switch/routers ports leading to relevant reduction of power consumption and costs [67, 68, 69].

A new concept of switch architecture referred to as Integrated OTN/WDM switch [56, 57] assumes an OTN switch having integrated WDM interfaces in the same system chassis as the switching functionality. This results in the convergence of the WDM and OTN transmission functionality into a single system, and has the benefit of eliminating any need for short-reach interconnections between separate WDM and OTN systems, while also reducing the rack space and power consumption.

More recently, the development and widespread deployment of multichannel Photonic Integrated Circuit (PIC) technology [70]-[71], that enables the

integration of all the optical functions required for WDM transmission into a single device, has helped to address these OTN/WDM integration.

2.5 Optical Node Architecture Options

Several packet-optical node architectures have been developed and put on the field, and many other have been proposed in literature [72, 73]. They differs each other from different points of view: number of switching layers, switching architectures at the different layers, and related technologies, degree of integration etc. Without loosing generality, they can be basically classified into three main categories, as depicted in Fig. 2.2.

The first alternative is illustrated in Fig. 2.2.a where Packet-optical nodes incorporates transparent wavelength switching (OOO), OTN cross-connect to perform switching at medium granularities, and on top of those a MPLS layer is used to switch client traffic at low granularity.

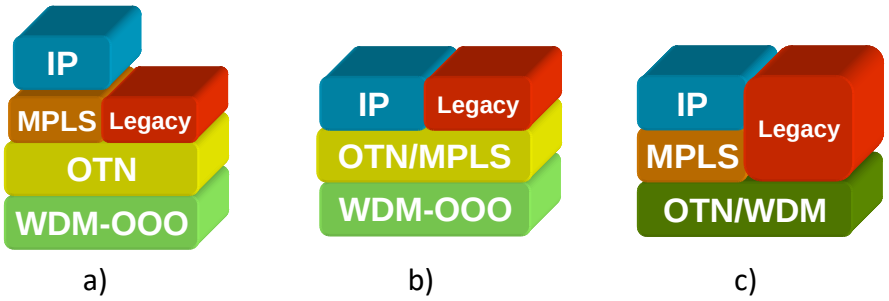

Figure 2.2: Packet-Optical Node Architectural Options. First Option (a): Transparent WDM switching layer and separated MPLS, OTN WDM functionalities. Second Option (b): Transparent WDM switching layer and integrated MPLS/OTN functionalities. Third Option (c): Integrated OTN/WDM functionalities realized in digital technology.

This architecture fits particularly for all those network applications when a considerable amount of OTN switching is needed. In this case the OTN switch play a role similar to the SDH/SONET cross-connect of the legacy transport nodes. The WDM switch just by-pass in an all-optical way those wavelength channels that do not need to be dropped and processed. This option combines all the pros and cons of transparent optical transport layer. Pros are basically the independence of the transmission rate and the highest level in scalability and capacity. The main disadvantages are the low manageability in terms of signal quality monitoring [74, 75] and the limitation in the flexibility of

the optical layer at the end points where the transponders are connected to the optical switching equipment that is, in most cases, a Reconfigurable Add and Drop Multiplexer (ROADM). The switching element in a ROADM is the Wavelength Selective Switch (WSS) that bases its operations on free space optics technology [76]. In basic ROADMs the transponders are rigidly connected to a colored ROADM port and are assigned to a fixed ROADM direction and any color or direction change can be only performed by manual re-wiring operations. To provide the optical switching layer with high level of flexibility in terms of colorless, directionless and contentionless characteristics [76], new costly components like more WSSs, multicast switches, tuneable filters have to be added rising the cost of the complete node to a level that is in most cases unacceptable for access and metro network applications.

The second alternative is illustrated in Fig. 2.2.b where Packet-optical node incorporates packet and OTN layers in the same platform based on a agnostic (packet-based) switching fabric, and transparent wavelength switching. This means that the same packet-based fabric is used to perform both packet and OTN switching. This is clearly not optimal for cost and power consumption in those cases when it is expected to switch high volumes of OTN flows. Instead become very flexible and low cost when the mixture of packet and OTN switching is required with a reasonable low percentage of OTN switching, or to have a single platform to apply in different network contexts without re-design the node. For the WDM layer applies the same considerations discussed in case of the first node option [77].

Finally, the third alternative is illustrated in Fig. 2.2.c where Packet-optical nodes incorporates packet, OTN, and WDM switching, being this latter based on Optical/Electrical/Optical (OEO) technology (opto-electronic conversion in each node for all channels) . In this case, since all wavelength channels are converted into electrical signals at each node, the same OTN fabric can switch at both wavelength and sub-wavelength level [78, 71, 79]. Those types of nodes typically use a cross-point switch as switching fabric. The main advantage is flexibility in terms of colorless. directionless and contentionless features (provided by the electrical switch), manageability, and relaxed transmission requirements, due to digital regenerated optical transport layer. Main drawback is that all incoming traffic has to be electrically converted and OTN processed. Thus there is more power consumption with respect to the previous solutions. In addition this option is not independent of the bit rate, due to OEO conversion.

The first two categories are based on traditional transparent optical transport, whose switches make use of all-optical costly devices such as wavelength selective switches (WSS). Wavelength Selective Switches have reached the development maturity and a cost reduction has become difficult due to the many internal free-space optics parts to be aligned with high precision during the assembly, and due to the hermetic and thermally compensated package required. In those cases the optical layer is essentially an analogue layer that suffers from transmission impairments accumulation along the transmission span. In addition they do not allow any real integration at HW level being completely different technologies.

Differently, the third category is based on digital optical transport approach, which basically means to reconvert optical signal at each node and to switch them in the electrical domain as any other digital electrical layer with the consequence that a new opportunity come out: the possibility to further integrate the WDM and the OTN switching layers, since they share transceivers and cross-point switches, in order to further lower cost and energy consumption.

The solutions proposed in [70] are based on strictly non-blocking high-capacity OTN switches able to switch ODU sub-flows from low order (e.g. ODU0) to high order (ODU3 ODU4). In those cases the OTN switches (or cross-connect) are fully accessible, in the sense that each sub-flow, coming from any input port can be routed to any output port at any ODU level. This means that the architecture of the OTN switches are quite complex, includes big switch fabrics, and thus are quite costly and energy consuming.

To reduce the switching fabric complexity, it is proposed the structure of a scalable core switch [14, 80] composed of low capacity OTN switches and one high capacity space switching fabric. It has shown [14] how the switching architecture can be implemented by means of low cost market devices, in particular 12×12 OTN switches of $120Gbps$ capacity [1] and 144×144 crosspoints of $1.44Tbps$ capacity [2].

A simplified integrated OTN/WDM switching architecture equipped with reduced number of OTN switches has been also proposed in [81] where it has shown how the introduction of OTN switches assignment policies can lead to a remarkable reduction in number of OTN switches used. The analytical evaluation of the blocking probability of the proposed integrated OTN/WDM switches [14] shows how the blocking can be much high in some traffic scenario. Its impact on the network blocking probability has been only marginally in-

vestigated [82] in the case of very simple routing strategies.

To reduce the blocking, in [83] it is proposed a more general integrated OTN/WDM switching architecture that can be provided with a spatial speedup able to improve the blocking performance. Obviously the introduction of this speedup increases the switch complexity and, in this case, the objective becomes to find the right trade-off between blocking degradation and complexity increase. The impact of the switch blocking on the network performance in static and dynamic traffic scenario has been investigated. Furthermore, it is formulated the switch resource assignment and routing problem as an Integer Linear Problem (ILP) and, to evaluate the blocking performance for large networks and in static traffic scenario, an efficient heuristic has been introduced. Finally the network blocking probability has been be evaluated by simulation in dynamic traffic scenario.

Chapter 3

OTN/WDM Integrated Switching Architecture

The introduction of Optical Transport Network (OTN) switching technology in metropolitan networks enables an efficient wavelength bandwidth utilization and reduces the number of wavelengths, leading to reduced network costs. It has been shown [83] that the use of integrated OTN/WDM switch architecture is cost effective because it reduces the number of short-reach client interfaces and the rack space compared to an architecture that uses a reconfigurable optical adddrop multiplexer and a separate standalone OTN switch or one that uses back-to-back muxponder connections to perform manual grooming. As seen in the Chapter 2, an integrated WDM-OTN switch that allows for significantly lower complexity and cost at the price of relaxing the non-blocking ideal performance requirements normally required to such a kind of switch has been proposed [14].

This chapter treats the investigation of the impact that the switch blocking has on the network performance in static and dynamic scenario for different metropolitan networks. The routing problem in the integrated OTN/WDM network as an Integer Linear Problem has been formulated in Section 3.2 and an efficient heuristic to evaluate the blocking performance in static traffic scenario has been developed in Section 3.3. The Section 3.4 shows how no blocking degradation occurs in a case study of different metropolitan networks. In particular it shows that the degradation of 2-3 orders of magnitude in blocking probability occurring under dynamic traffic scenario can be mitigated with the introduction of a spatial speedup of value 1.5.

Furthermore a low complexity and integrated OTN/WDM switching ar-

chitecture for metropolitan networks has been proposed in Section 3.5. This switch is scalable and composed by small capacity OTN switches and one space switch. The architecture reduces the number of OTN switches with respect to other solutions proposed in literature with the consequence of optimizing the used OTN switching resources and the complexity of the space switch. To study the impact on the blocking performance of the reduced number of OTN switches, an Integer Linear Problem that models the routing and switch resource assignment problem in a network equipped with the proposed switches has been introduced in Section 3.6. Being the problem NP-hard, an heuristic is defined to evaluate the network request blocking in static traffic scenario in Section 3.8. The obtained results show how a reduction in OTN switches as small as 50% can be reached when the percentage of traffic needing sub-wavelength switching is 40%.

Next Section 3.1 reports the proposed integrated OTN/WDM switching architecture and carries out a complexity analysis of the switching fabric as a function of the spatial speedup. Finally conclusions and future research items are illustrated in Section 3.10.

3.1 OTN/WDM Integrated Switching Node

A possible implementation of an OTN/WDM integrated switching node of degree N=4 is depicted in Fig. 3.1 [14].

It comprises four bi-directional fiber lines for a mesh optical network connection named North, South, West, and East. In each fiber line, up to W=48 wavelength channels are multiplexed and transported. Optical signals are generated and received by multichannel 12×10 Gbps photonic integrated circuit (PIC) devices to lower the cost and energy consumption of the optical interfaces. To multiplex/demultiplex the WDM channels of the four PIC devices, four-band mux/demux devices are used at the node input/output. In this type of node, that is a digital photonic node, all incoming traffic, regardless if it is local traffic that needs to be terminated or transit traffic to be routed toward other nodes, is converted in the electrical domain by PIC devices. The wavelength signals carrying sub-wavelength signals enter the switch core for OTN/WDM switching. Traffic that needs to be terminated is routed towards the packet client interfaces that are implemented by using high-density $N \times 10$ Gbps parallel optics transceivers. Transit traffic coming from one direction, after optical-to-electrical conversion by one PIC device and switching in the

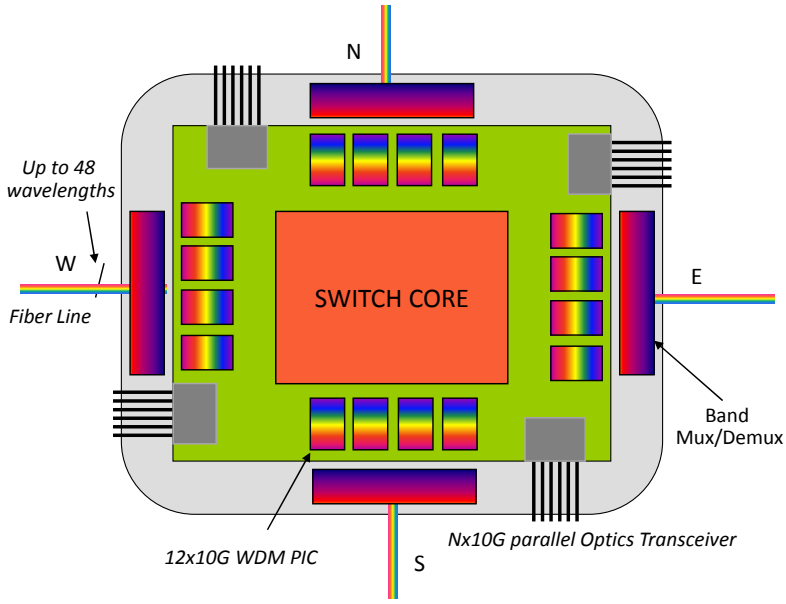

Figure 3.1: Implementation of an integrated OTN/WDM Switching Node

switch core, is routed toward another PIC connected to another direction for electrical-to-optical conversion and transmission through the network.

The main limitation of the proposed node is the high processing capacity required to the switch core that should be of $1.92Tbps$ to process express transit only. Today's technology provides much lower processing capacity, for instance switch core chip of up to $120Gbps$ has been realized [1]. For this reason, a multilayer switching architecture composed by some basic blocks that the actual technology makes available has been proposed and evaluated in [14] in terms of internal blocking probability. In particular two main basic blocks, today implementable with market devices, will be used: $K \times K$ OTN switching modules ([1] with $K = 12$) and $Q \times Q$ space switching modules ([2] with $Q = 144$). As above mentioned the first block is able to perform both time and space switching and it is implementable with an OTN chip supporting up to $K = 12$ input/output lines of $10Gbps$ rate [1]. The second block performing space switching only is realizable with several crosspoint chips whose maximum processing capacity is actually of $1.44Tbps$ with $Q = 144$ input/output lines of $10Gbps$ rate [2]. Section 3.1.1 deals with the proposed architecture and its complexity has been evaluated in Section 3.1.2 in terms of number needed of OTN, crosspoint chips and interconnection links between chips.

Parameter	Description
N	node degree
W	number of wavelengths
f_H	H-ODU bit-rate
f_L	L-ODU bit-rate
F	multiplexing ratio of f_H to f_L
C_W	wavelength capacity
K	OTN switch size
H	number of OTN switches per input/output line
T	number of OTN switches in each ADD/DROP section
C_{IL}	interstage link capacity
S	spatial speedup
Q	size of the basic switching module

Table 3.1: Switch Parameters

3.1.1 Switch Core Architecture

This section deals with the proposed switch core for hierarchical two-level OTN transport architecture and able to switch two types of Optical Data Units (ODU) referred to as higher order ODU (H-ODU) and lower order ODU (L-ODU) respectively.

Next some switch parameters whose meaning is reported in Table 3.1 are introduced.

The bit-rate of the H-ODU and L-ODU are denoted with f_H and f_L respectively. furthermore the multiplexing ratio F of the H-ODU bit-rate to the L-ODU bit-rate has been introduced. Here an important assumption is that any input/output wavelength is characterized by a capacity C_W equal to f_H and is hence able to carry either one H-ODU or up to F L-ODUs. The switch can handle two typed of H-ODU. If an H-ODU needs only space switching, it is referred to as "Direct" H-ODU (DH-ODU). Conversely if it carries L-ODUs needing time switching it is referred to as "Switched" H-ODU (SH-ODU).

The proposed switch core architecture, described in Fig. 3.2 [83], is composed by three stages: $K \times K$ OTN switching modules are placed in the first

and third stages and are able to perform both space and time switching. Conversely the middle stage is able to perform space switching only and hence to handle the switching among H-ODUs only.

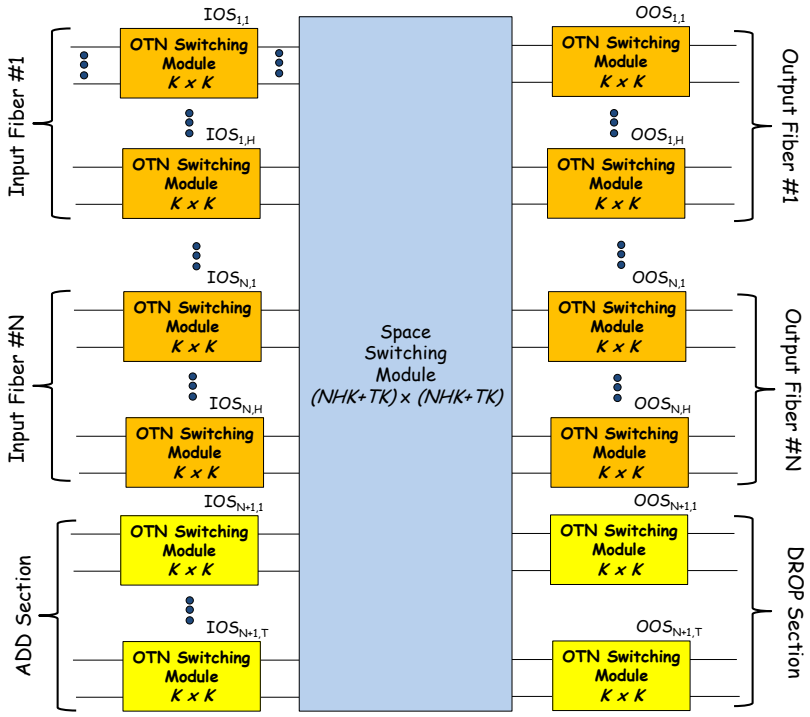

Figure 3.2: Switch core architecture equipped with $K \times K$ OTN switching modules and one $(NHK + TK) \times (NHK + TK)$ space switching module

If the switch is equipped with N input/output lines each supporting W wavelengths, the H OTN switching modules of the first (third) stage are used to switch L-ODU and H-ODU coming (directed) from (to) any input (output) line. As one can note in the architecture, the j-th $(j = 1, \cdots, H)$ Input (Output) OTN switching module assigned to the i-th $(i = 1, \cdots, N)$ input (output) fiber is denoted with $IOS_{i,j}$ $(OOS_{i,j})$. In Fig. 3.2 the ADD and DROP sections are also reported. Each one of those is composed by T OTN switching modules that are denoted as $IOS_{N+1,j}$ $(j = 1, \cdots, T)$ and $OOS_{N+1,j}$ $(j = 1, \cdots, T)$ for the ADD and DROP sections respectively. The input/output OTN switching modules are connected by means of interstage links provided by the $(NHK+TK) \times (NHK+TK)$ space switching module. Each interstage link is characterized by the capacity C_{IL} equal to f_H and hence it is able to carry either one DH-ODU or up to F L-ODUs.

The blocking performance of the switch core architecture has been investigated [14] when the condition $W = HK$ holds, that is when the number of

wavelengths carried on any input (output) line is equal to the sum of the number of inputs (outputs) relative to the H OTN switching modules assigned to that input (output) line. However this choice, that minimizes the switch cost, does not guarantee the switch core architecture to be non blocking. The penalization in terms of blocking probability has been studied in [14] and can be much high in traffic scenario in which DH-ODU traffic is prevalent. To mitigate the blocking a spatial speedup $S = \frac{HK}{W}$ has been introduced and it is defined as the ratio of the maximum number NHK of interstage links to the total number NW of input/output wavelengths. Obviously a speedup greater than 1 increases the switch complexity but allows for lower blocking probability. In the case of W multiple of H, the same number $\frac{W}{H}$ of wavelengths of any input (output) line are assigned to each of the H input (output) OTN switching modules dedicated to that input (output) line. In Fig. 3.3 it is illustrated an example of switch core in the case in which the parameter values $N = 2$, $W = 4$, $H = 2$, $K = 4$ are chosen with a speedup value $S = 2$. In this case, it is not reported the ADD and DROP section, while the E/O and O/E conversion modules that as before mentioned are illustrated. They will be realized with optical multiplexer/demultiplexer and PICs.

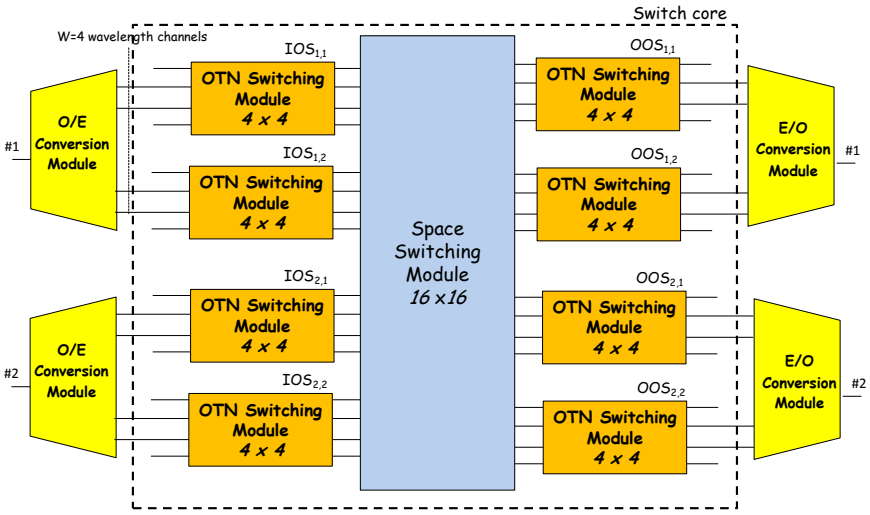

Figure 3.3: OTN/WDM integrated switching node with N=2 input/output lines each one supporting W=4 wavelengths. The node is equipped with H=2 4×4 OTN switching modules per input/output line and one 16×16 space switching module. The speedup S is equal to 2.

It is important to note that there is a minimum value S_{SSNB} of the speedup such as to make the switch core Strict Sense Non Blocking (SSNB). In particular this aspect is proved by the following lemma:

Lemma 1. *Under the constraint of W multiple of H, the proposed switch core architecture is SSNB if the speedup S is greater than or equal to*

$$S_{SSNB} = \lceil \frac{K}{\lfloor \frac{K}{F} \rfloor} \rceil$$

.

The proof of the lemma 1 is reported in Appendix A.1.

3.1.2 Switch Core Complexity Evaluation

The increase in speedup S can lead to better blocking performance and even to a SSNB switch configuration when S is greater than or equal to S_{SSNB}. However the consequence is the complexity increase of the switch core that we characterize with three indexes. The first complexity index n_{OTN} is characterized by the total number of $K \times K$ OTN switching modules used. Because the space switching module is too big to be implemented with a single chip, the second complexity index n_{SW} is characterized by the total number of $Q \times Q$ space switching modules needed to realize the space switching module of the proposed switch core, being Q depending on the availability of market devices. Finally the third complexity index n_{IL} characterizes the number of interconnection links between the switching modules.

Next it is reported the evaluation of the indexes n_{OTN}, n_{SW} and n_{IL} as a function of the speedup S when the ADD and DROP sections are neglected. n_{OTN} is simply given by $2HN$ and expressing H as a function of the speedup S:

$$n_{OTN} = 2S\frac{W}{K}N \tag{3.1}$$

The parameter n_{SW} is evaluated in the case in which the space switching module has a three stages SSNB Clos network structure and characterizes the least number of $Q \times Q$ switching modules needed to realize the space switch. As preliminary result of the evaluation of n_{SW}, the following lemma can be enunciated:

Lemma 2. *A $U \times U$ switching module with a three stages SSNB Clos network structure can be realized with the least number $N_{Q\times Q}$ of $Q \times Q$ ($U > Q$) switching modules given by:*

$$N_{Q\times Q} = min_{n\in\Theta}\left(2\left\lceil\frac{\lceil\frac{U}{n}\rceil}{\lfloor\frac{Q}{2n-1}\rfloor}\right\rceil + \left\lceil\frac{2n-1}{\left\lfloor\frac{Q}{\lceil\frac{U}{n}\rceil}\right\rfloor}\right\rceil\right) \tag{3.2}$$

where Θ *is a set of positive integer numbers given by:*

$$\Theta = \{i \in Z^+ \ / \ Q \geq max(2i-1, \left\lceil\frac{U}{i}\right\rceil)\} \tag{3.3}$$

The proof of the lemma 2 is reported in Appendix A.2.

The switch core is equipped with a space switching module of size NHK when the ADD and DROP sections are neglected. According to (3.2) and (3.3) and introducing the speedup $S = \frac{HK}{W}$, the following expression for n_{SW} can be written:

$$n_{SW} = min_{n\in\Pi}\left(2\left\lceil\frac{\lceil\frac{NSW}{n}\rceil}{\lfloor\frac{Q}{2n-1}\rfloor}\right\rceil + \left\lceil\frac{2n-1}{\left\lfloor\frac{Q}{\lceil\frac{NSW}{n}\rceil}\right\rfloor}\right\rceil\right) \tag{3.4}$$

where Π is a set of positive integer numbers given by:

$$\Pi = \{i \in Z^+ \ / \ Q \geq max(2i-1, \left\lfloor\frac{NSW}{i}\right\rfloor)\} \tag{3.5}$$

Finally we introduce the third performance index n_{IL} that characterizes the number of interconnection links between OTN switching modules and $Q \times Q$ switching modules. The index n_{IL} is expressed as a function of the speedup S and the parameter n_{opt} characterizing the optimal dimension of the switching elements of the Clos network and minimizing the expression (3.4):

$$n_{IL} = 2NSW + 2(2n_{opt} - 1)\left\lfloor\frac{NSW}{n_{opt}}\right\rfloor \tag{3.6}$$

3.2 Optimal Switch Resource Assignment and Routing Problem in OTN/WDM Networks

The optimal problem of the Switch Resource Assignment and Routing (SRAR) in OTN/WDM networks is stated below. The following inputs are

considered:

- $\mathcal{G} = (\mathcal{V}, \mathcal{E})$: graph representing a physical topology where $\mathcal{V}$ is the set of nodes and $\mathcal{E}$ is the set of links; the nodes correspond to the OTN/WDM integrated switching nodes and the links correspond to the fibers between switching nodes; the degree of the node $v \in \mathcal{V}$ is assumed to be d_v that is the corresponding switching node has d_v express input/output fibers; the network is composed by $N_{\mathcal{V}}$ switching nodes, each one equipped with $K \times K$ OTN switches and provided with a speedup S.
- T: number of ADD/DROP OTN switches for each switching node;
- W: number of wavelength channels carried by each fiber where each channel has the capacity of carrying either one H-ODU or up to F L-ODUs;
- $\mathcal{T}^{DH} = [t_{sd}^{DH}], \mathcal{T}^{L} = [t_{sd}^{L}]$: $N_{\mathcal{V}} \times N_{\mathcal{V}}$ traffic matrices for the DH-ODUs and L-ODUs traffic offered between the network nodes respectively. In particular t_{sd}^{DH} and t_{sd}^{L} denote the number of DH-ODUs and L-ODUs offered between the nodes $s \in \mathcal{V}$ and $d \in \mathcal{V}$;

The goals are to determine:

- which interstage links are set up between the OTN switching modules in the nodes $v \in \mathcal{V}$;
- where the accepted H-ODUs and L-ODUs traffic is routed in the OTN/WDM network.

The objective is to maximize the throughput given by total accepted bandwidth traffic demand normalized to the bandwidth f_L requested by one L-ODU. In particular notice that the acceptance of one DH-ODU request and one L-ODU request leads to a contribution of F and 1 respectively in the normalized total accepted bandwidth traffic demand.

Next the optimization problem is described.

1) Notations and parameters

To give formally the ILP formulation, the unconnected graph $\mathcal{G}^* = (\mathcal{V}^*, \mathcal{E}^*)$ where $\mathcal{V}^*$ and $\mathcal{E}^*$ are the set of nodes and the links respectively

has been introduced. The set $\mathcal{V}^*$ is the union of the sets Ψ_v^I, Ψ_v^O, Γ_v^I, Γ_v^O, A_v and D_v defined for each node $v \in \mathcal{V}$ and whose meaning is indicated in Fig. 3.4 for the OTN/WDM integrated switch of Fig. 3.2.

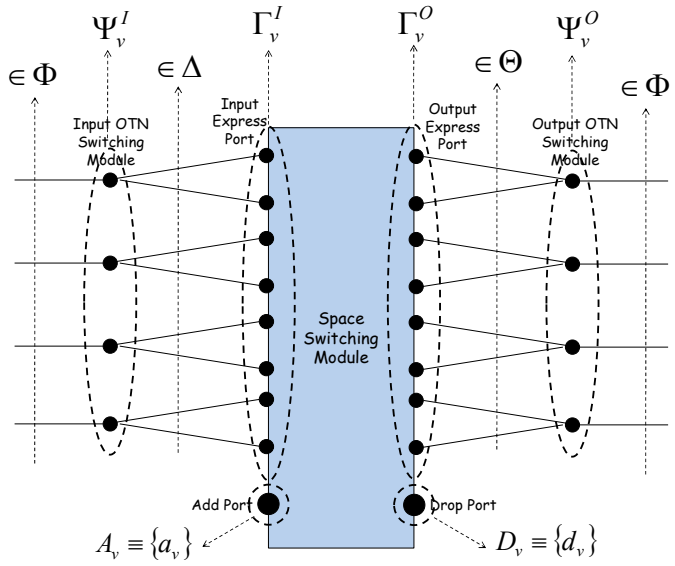

Figure 3.4: Sets of nodes and links of the node $v \in \mathcal{V}$ in the graph $\mathcal{G}^* = (\mathcal{V}^*, \mathcal{E}^*)$

The definition of these sets is shown below:

- $\Psi_v^I \equiv \{l_v^{i,j}, i = 1, \cdots d_v; j = 1, \cdots, H\}$: set of nodes $l_v^{i,j}$ $(i = 1, \cdots d_v; j = 1, \cdots, H)$ corresponding to the $j-th$ input OTN switching module of the $i-th$ input line in the node $v \in \mathcal{V}$;

- $\Psi_v^O \equiv \{o_v^{i,j}, i = 1, \cdots d_v; j = 1, \cdots, H\}$: set of nodes $o_v^{i,j}$ $(i = 1, \cdots d_v; j = 1, \cdots, H)$ corresponding to the $j-th$ output OTN switching module of the $i-th$ output line in the node $v \in \mathcal{V}$;

- $\Gamma_v^I \equiv \{p_v^{I,i,j,k}, i = 1, \cdots d_v; j = 1, \cdots, H; k = 1, \cdots K\}$: set of nodes $p_v^{I,i,j,k}$ $(i = 1, \cdots d_v; j = 1, \cdots, H; k = 1, \cdots K)$ corresponding to the input express port of the space switching module connected to the $k-th$ output of the $j-th$ input OTN switch of the $i-th$ line in the node $v \in \mathcal{V}$;

- $\Gamma_v^O \equiv \{p_v^{O,i,j,k}, i = 1, \cdots d_v; j = 1, \cdots, H; k = 1, \cdots K\}$: set of nodes $p_v^{O,i,j,k}$ $(i = 1, \cdots d_v; j = 1, \cdots, H; k = 1, \cdots K)$ corresponding to the output express port of the space switching module connected to the

$k-th$ input of the $j-th$ output OTN switch of the $i-th$ line in the node $v \in \mathcal{V}$;

- $A_v \equiv \{a_v\}$: set composed by the only node a_v that jointly represents the ADD OTN switches and the ADD ports of the space switch of the node $v \in \mathcal{V}$;

- $D_v \equiv \{d_v\}$: set composed by the only node d_v that jointly represents the DROP OTN switches and the DROP ports of the space switch of the node $v \in \mathcal{V}$;

The set $\mathcal{E}^*$ is composed by the following three sets of links:

- Φ: set of links $(o_v^{i_v,j}, l_u^{i_u,j})$ $((v,u) \in \mathcal{E}; j = 1, \cdots H)$ where the nodes v and u are adjacent in $\mathcal{G}$ and the corresponding switching nodes are interconnected with a fiber by the $i_v - th$ output line of the node v to the $i_u - th$ input line of the node u;

- Δ: set of links $(l_v^{i,j}, p_v^{I,i,j,k})$ $(v \in \mathcal{V}; i = 1, \cdots d_v; j = 1, \cdots, H; k = 1, \cdots K)$ connecting nodes corresponding to input OTN switches and input express ports;

- Θ: set of links $(p_v^{O,i,j,k}, o_v^{i,j})$ $(v \in \mathcal{V}; i = 1, \cdots d_v; j = 1, \cdots, H; k = 1, \cdots K)$ connecting nodes corresponding to output express ports and output OTN switches.

Furthermore for each node $w \in \mathcal{V}^*$ the sets $\Omega_w^{(-)}$ and $\Omega_w^{(+)}$ of the predecessor and successor nodes respectively have been introduced. Thus it is possible to write:

$$\Omega_w^{(-)} = \{t \in \mathcal{V}^* \ / \ (w,t) \in \mathcal{E}^*\}$$

$$\Omega_w^{(+)} = \{t \in \mathcal{V}^* \ / \ (t,w) \in \mathcal{E}^*\}$$

2) Optimization variables

- $S_{s,d}^{y,t} \in \{0,1\}$ $(s,d \in \mathcal{V}; y \in \{DH, L\}; t \in \{1..t_{sd}^y\})$: the variable assumes the value 1 if the $t-th$ y-ODU offered between the nodes s and d is successfully carried; otherwise it assumes the value 0;

- $\lambda_{s,d}^{w,u,y,t} \in \{0,1\}$ $(s,d \in \mathcal{V}; (w,u) \in \mathcal{E}^*; y \in \{DH, L\}, t \in \{1..t_{sd}^y\})$: the variable assumes the value 1 if the $t-th$ y-ODU offered between the nodes s and d is carried on the link (w,u); otherwise it assumes the value 0;

- $x_{w,u}^v \in \{0,1\}$ $(v \in \mathcal{V}; w \in \Gamma_v^I \cup A_v; u \in \Gamma_v^O \cup D_v)$: the variable assumes the value 1 if the ports of the space switch corresponding to the nodes w and u are interconnected by an interstage link.

3) Objective function

The objective is to maximize the throughput given by total accepted bandwidth traffic demand normalized to the bandwidth f_L requested by one L-ODU:

$$Maximize: \sum_{s,d \in \mathcal{V}} \sum_{t=1}^{t_{s,d}^L} S_{s,d}^{L,t} + F \sum_{s,d \in \mathcal{V}} \sum_{t=1}^{t_{s,d}^{DH}} S_{s,d}^{DH,t} \tag{3.7}$$

4) Constraints

Constraints are introduced to ensure that from an input and output express port of any space switch is activated only an interstage link. Conversely up to a maximum of KT interstage links can be activated from/to the ADD/DROP sections. These constraints can be expressed as follows:

$$\sum_{u \in \Gamma_v^O \cup D_v} x_{w,u}^v \leq 1 \quad v \in \mathcal{V} \;\; w \in \Gamma_v^I \tag{3.8}$$

$$\sum_{w \in \Gamma_v^I \cup A_v} x_{w,u}^v \leq 1 \quad v \in \mathcal{V} \;\; u \in \Gamma_v^O \tag{3.9}$$

$$\sum_{u \in \Gamma_v^O \cup D_v} x_{w,u}^v \leq KT \quad v \in \mathcal{V} \;\; w = a_v \tag{3.10}$$

$$\sum_{w \in \Gamma_v^I \cup A_v} x_{w,u}^v \leq KT \quad v \in \mathcal{V} \;\; u = d_v \tag{3.11}$$

For the t-th y-ODU $(y \in \{DH, L\}; t \in [1..t_{sv}^y])$ offered between the nodes $s, v \in \mathcal{V}$, flow conservation constraints in every node $w \in \mathcal{V}^*$ are introduced. The constraints may not be respected only in the ADD and DROP nodes a_s and d_v where the total flow is equal to 1 and -1 respectively if the y-ODU is successfully carried; otherwise is equal to 0. We can write:

$$\sum_{u\in\Omega_w^{(-)}} \lambda_{s,v}^{u,w,y,t} - \sum_{u\in\Omega_w^{(+)}} \lambda_{s,v}^{w,u,y,t} = \begin{cases} -S_{s,v}^{y,t} & if\ w = a_s \\ S_{s,v}^{y,t} & if\ w = d_v \\ 0 & otherwise \end{cases} \tag{3.12}$$

Further constraints are considered in order to guarantee that the traffic routed on any link $(w,u) \in \mathcal{E}^*$ in smaller than or equal to the link transport capacity normalized to the bandwidth f_L of one L-ODU. This capacity equals F for the links $(w,u) \in \Delta \cup \Theta$ that interconnect nodes corresponding to input/output OTN switches and output/input express ports. In the case of links $(w,u) \in \Phi$ interconnecting nodes corresponding to output OTN switch and input OTN switch, the capacity equals the sum of the capacities provided by the wavelength channels interconnecting them, that is $\frac{KF}{S}$. Finally another constraint that limits to F the normalized capacity of any activated interstage link has been added. In particular, it can be simply written as follow:

$$\sum_{s,d\in\mathcal{V}} \sum_{t=1}^{t_{s,d}^{L}} \lambda_{s,d}^{w,u.L,t} + F \sum_{s,d\in\mathcal{V}} \sum_{t=1}^{t_{s,d}^{DH}} \lambda_{s,d}^{w,u,DH,t} \leq C_L \tag{3.13}$$

where C_L is given by:

$$C_L = \begin{cases} F & if\ (w,u) \in \Delta \cup \Theta \\ \frac{KF}{S} & if\ (w,u) \in \Phi \\ Fx_{w,u}^{v} & if\ v \in \mathcal{V}; w \in \Gamma_v^I; u \in \Gamma_v^O \cup D_v \\ Fx_{w,u}^{v} & if\ v \in \mathcal{V}; w \in \Gamma_v^I \cup A_v; u \in \Gamma_v^O \end{cases} \tag{3.14}$$

This section is concluded with a computational complexity analysis. If we assume that only DH-ODUs are offered to the network and strict sense non blocking switching nodes are used, the studied SRAR problem becomes the Routing and Wavelength Assignment (RWA) optimization problem with wavelength conversion. Because it is well known the RWA problem is NP-complete [84], we can conclude that the SRAR problem is NP-complete too. As the number of variables and equations increases exponentially with the size of network, the speedup of the switch and the number of wavelengths on each fiber, the ILP formulation will allow us to provide results only in the case of small networks. In the next section an heuristic is introduced in order to evaluate the performance of the proposed switch node architecture in large

networks.

3.3 Maximizing Shortest Path Traffic (MSPT) Heuristic

The Maximizing Shortest Path Traffic (MSPT) heuristic attempts in the initial phase (Phase-1) to route the traffic on the shortest paths of the network by carrying on each of them either one DH-ODU or F L-ODUs. If there is not enough resources to carry all of the traffic on the shortest paths, the MSPT heuristic will try to carry in the successive phase (Phase-2) the remaining traffic on alternative paths. The main steps of the heuristic are illustrated in Algorithm 1.

In the initialization phase the graph $\mathcal{G}_{aux} = (\mathcal{V}_{aux}, \mathcal{E}_{aux})$ is built up (line 2) where $\mathcal{V}_{aux} = \mathcal{V}^*$ and $\mathcal{E}_{aux}$ is obtained from $\mathcal{E}^*$ with the addition of all of the possible interstage links that connect input express and add ports to output express and drop ports in any switching node. For instance the interstage links added to the switching node with the representation in Fig. 3.5.a is illustrated in Fig. 3.5.b.

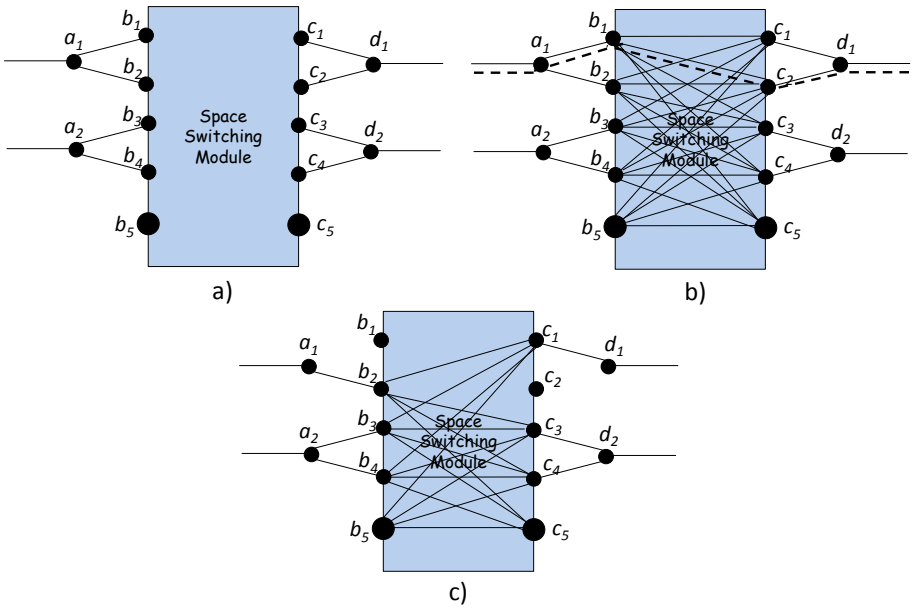

Figure 3.5: Sets of nodes and links of a node $v \in \mathcal{V}$ in the graph $\mathcal{G}^* = (\mathcal{V}^*, \mathcal{E}^*)$ (a); insertion of the interstage links in the graph $\mathcal{G}^* = (\mathcal{V}^*, \mathcal{E}^*)$ (b); deletion of links after that the least cost path crossing the nodes a_1,b_1,c_2,d_1 is evaluated by the MSPT heuristic.

Algorithm 1 MAXIMIZING SHORTEST PATH TRAFFIC (MSPT) HEURISTIC

/*Initialization*/
build up the auxiliary graph $\mathcal{G}_{aux} = (\mathcal{V}_{aux}, \mathcal{E}_{aux})$
for $s, u \in \mathcal{V}$ **do**
    $t_{su}^{DH,r} = t_{su}^{DH}$,$t_{su}^{L,r} = t_{su}^{L}$, $t_{su}^{tot,r} = t_{su}^{DH,r} + Ft_{su}^{L,r}$
end for
/*Phase-1. Routing of the DH-ODUs and the L-ODUs on the shortest paths of $\mathcal{G}_{aux}$ ****/***
label the links of $\mathcal{E}_{aux}$ with weight 1
evaluate in the graph $\mathcal{G}_{aux}$ the lengths c_{su} $(s, u \in \mathcal{V})$ between the nodes $a_s, d_u \in \mathcal{V}_{aux}$
insert into the list $\mathcal{L}$ in decreasing order the values $t_{su}^{tot,r}$ $(s, u \in \mathcal{V})$ greater than or equal to F
while $\mathcal{L} \neq \oslash$ **do**
    extract the first value $t_{wz}^{tot,r}$ in the list $\mathcal{L}$
    evaluate the least cost path $\mathcal{P}_{w,z}$ in $\mathcal{G}_{aux}$ and its length $c(\mathcal{P}_{w,z})$
    if $(\mathcal{P}_{w,z}\ exists)$ & &$(c(\mathcal{P}_{w,z}) = c_{wz})$ **then**
        remove the links of $\mathcal{G}_{aux}$ on the path $\mathcal{P}_{w,z}$ that become fully occupied
        remove the not admissible interstages links from $\mathcal{G}_{aux}$
        /*Update the traffic demands to be routed*/
        $t_{wz}^{tot,r}$=$t_{wz}^{tot,r}$-F
        if $t_{wz}^{tot,r} \geq F$ **then**
            insert the value $t_{wz}^{tot,r}$ into the list $\mathcal{L}$
        end if
        if one DH-ODU is routed **then**
            $t_{wz}^{DH,r}$=$t_{wz}^{DH,r}$-1
        else
            $t_{wz}^{L,r}$=$t_{wz}^{L,r} - F$
        end if
    end if
end while
/*Phase-2. Routing of the DH-ODUs and the L-ODUs on the alternative paths of $\mathcal{G}_{aux}$ ****/***
for $y \in \{DH, L\}$ **do**
    insert into the list $\mathcal{L}_y$ in decreasing order the values $t_{su}^{y,r}$ $(s, u \in \mathcal{V})$ greater than or equal to 1
    label the links in $\mathcal{G}_{aux}$ with weights equal to the available link capacity in terms of y-ODU the link can accept and deleting the links with no capacity
    while $\mathcal{L}_y \neq \oslash$ **do**
        extract the first value $t_{wz}^{y,r}$ in the list $\mathcal{L}_y$
        evaluate the least cost path $\mathcal{P}_{w,z}$ in $\mathcal{G}_{aux}$
        if $\mathcal{P}_{w,z}$ *exists* **then**
            update in $\mathcal{G}_{aux}$ the weight of the links of $\mathcal{P}_{w,z}$
            remove the full links of $\mathcal{G}_{aux}$
            remove the not admissible interstages links from $\mathcal{G}_{aux}$
            /*Update the traffic demands to be routed*/
            $t_{wz}^{y,r}$=$t_{wz}^{y,r}$-1
            if $t_{wz}^{y,r} \geq 0$ **then**
                insert the value $t_{wz}^{y,r}$ into the list $\mathcal{L}_y$
            end if
        end if
    end while
end for

In the initialization phase the variables $t_{su}^{DH,r}$,$t_{su}^{L,r}$ and $t_{su}^{tot,r}$ $(s,u \in \mathcal{V})$ are also initialized (line 4). They store during the execution of the MSPT heuristic the number of DH-ODUs, L-ODUs and the normalized total bandwidth traffic demand to be still routed respectively. At the beginning of the Phase-1 the links in $\mathcal{E}_{aux}$ are labeled with weight 1 (line 7) and the length of the shortest path $c_{su}(s,u \in \mathcal{V})$ between the nodes $a_s, d_u \in \mathcal{V}_{aux}$ are evaluated (line 8). The evaluation of c_{su} is important because during the execution of the MSPT heuristic some links could be removed by $\mathcal{G}_{aux}$ and the knowledge of c_{su} allow us to understand if a least cost path evaluated when some links are removed is or not a shortest path in the initial auxiliary graph $\mathcal{G}_{aux}$. The normalized total bandwidth traffic demands $t_{su}^{tot,r}$ $(s,u \in \mathcal{V})$ are stored in the list $\mathcal{L}$ according to a decreasing order (line 9). At each iteration of the Phase-1, the MSPT heuristic tries to route either one DH-ODU or F L-ODUs, on the shortest path between the nodes $w,z \in \mathcal{V}$ in which the higher normalized total bandwidth traffic demand $t_{wz}^{tot,r}$ (line 11) is remaining to be routed. In particular the least cost path $\mathcal{P}_{w,z}$ between the nodes $a_w, d_z \in \mathcal{V}^*$ is evaluated (line 12) and if both it exists and its length $c(\mathcal{P}_{w,z})$ equals c_{wz} (line 13) the traffic routing is successfully and the graph $\mathcal{G}_{aux}$ with the variables $t_{wz}^{DH,r}$,$t_{wz}^{L,r}$ and $t_{wz}^{tot,r}$ $(w,z \in \mathcal{V})$ are updated (lines 14-24). The updating of the graph $\mathcal{G}_{aux}$consists in deleting the links belonging to the shortest path $\mathcal{P}_{w,z}$ (line 14) and becoming fully occupied. Besides the interstage links belonging to $\mathcal{P}_{w,z}$, other interstage links have to be deleted (line 15) from $\mathcal{G}_{aux}$. They are referred to as not admissible interstage links and their deletion is needed to respect the constraints expressed by the Eqs (3.8)-(3.11). These constraints establish that when an interstage link is setup between an input and an output space switch port of any switching node, no other interstage links (not admissible interstage links) can be set up from these input and output ports. For instance if the shortest path crossing the nodes a_1, b_1, c_2, d_1 in Fig. 3.5.b is evaluated, the application of the MSPT heuristic leads to the deletion of the links (a_1,b_1), (b_1,c_2), (c_2,d_1). Furthermore the use of the interstage link (b_1,c_2) prevents from setting up other interstage links that have to be deleted, that is the links (b_1,c_1), (b_1,c_3), (b_1,c_4), (b_1,c_5), (b_2,c_2), (b_3,c_2), (b_4,c_2), (b_5,c_2). The representation of the switch core when the links are deleted is shown in Fig. 3.5.c. Any traffic demand $t_{wz}^{tot,r}$ is not more inserted in the list $\mathcal{L}$ when either a shortest path $\mathcal{P}_{w,z}$ is not available or when its value is smaller than F. The condition of list $\mathcal{L}$ empty (line 10) guarantees the end of the Phase-1.

At the beginning of the Phase-2, the traffic demands $t_{su}^{DH,r}$, $t_{su}^{L,r}$ $(s,u \in \mathcal{V})$

of DH-ODUs and L-ODUs not routed in the Phase-1 are stored in the lists $\mathcal{L}_{DH}$ and $\mathcal{L}_L$ in decreasing order (line 30) respectively. When the type y ($y \in \{DH, L\}$) of traffic (DH-ODU and L-ODU) is handled, each link of the graph $\mathcal{G}_{aux}$ is labeled with a weight denoting the available link capacity (line 31) given by the number of y-ODUs the link can accept. The links with capacity equal to zero are deleted. The MSPT heuristic tries to route the higher traffic demand $t_{wz}^{y,r}$ (line 33) on the least cost path $\mathcal{P}_{w,z}$ (line 34) of the graph $\mathcal{G}_{aux}$. If this operation is successfully (line 35), the graph and the variables are updated (line 36-40). The traffic demand $t_{wz}^{y,r}$ is again inserted in the list $\mathcal{L}_y$ only if it is greater than 0 (line 41-43). The Phase-2 ends when both the lists $\mathcal{L}_y$ ($y \in \{DH, L\}$) are empty (line 32).

This section is concluded with a computational time complexity evaluation of the MSPT heuristic. Before giving an expression of the complexity, the following observations could be done:

i) the heavier operation of MSPT is the evaluation of least cost paths;

ii) in the worst case MSPT evaluates a number of least cost paths as many times as the total sum $D^{tot} = \sum_{s,v \in V}(t_{sv}^{DH,r} + t_{sv}^{L,r})$ of the traffic demand;

iii) if a least cost path is evaluated in the graph $\mathcal{G}_{aux} = (\mathcal{V}_{aux}, \mathcal{E}_{aux})$ by using the Dijstra algorithm with binary heap implementation, its computational complexity is equal to $O(L_{aux} log N_{aux})$ where N_{aux} and L_{aux} are the number of nodes and links of $\mathcal{G}_{aux}$;

iv) it is easy to prove that in the worst case occurring in the initial phase the graph $\mathcal{G}_{aux}$ is composed by $N_{aux} = 4L_{\mathcal{E}}SW\frac{K+1}{K} + 2N_{\mathcal{V}}$ nodes and $L_{aux} = 2L_{\mathcal{E}}SW\frac{2K+1}{K} + 2N_{\mathcal{V}}(d_{max}SW)^2$ links, $N_{\mathcal{V}}$, $L_{\mathcal{E}}$ being the number of nodes and links of the network graph $\mathcal{G} = (\mathcal{V}, \mathcal{E})$ and d_{max} being the maximum node degree.

According to these remarks we can conclude that the computational time complexity of the MSPT heuristic is

$$O(D^{tot}SW(L_{\mathcal{E}} + N_{\mathcal{V}}d_{max}^2SW)log(SWL_{\mathcal{E}} + N_{\mathcal{V}}))$$

.

3.4 Numerical Results for the Proposed Architecture

In the first part, this section deals with a complexity analysis of the integrated OTN/WDM switching node versus the spatial speedup S. Then the impact that the parameter S has on the network blocking performance in static and dynamic traffic scenario will be evaluated.

In Table 3.2 some results on the hardware complexity as a function of the speedup S of the proposed integrated OTN/WDM switch are reported. As reference scenario, we can consider the case in which the DH-ODU and the L-ODU carry f_H=10 Gbs and f_L = 1.25 Gbs flows corresponding to ODU-2 and ODU-0 respectively of the OTN multiplexing hierarchical respectively [54]. This choice leads to a value of F equal to 8. In this evaluation, an integrated OTN/WDM switch with N=4 Input/Output lines each one carrying W=48 wavelengths is considered. Obviously this analysis can be carried out for other scenarios and can be easily extended to the case in which a number of OTN hierarchical levels greater than two is considered. An important assumption is about the availability of the following market devices needed to realize the proposed switch core:

i) OTN switching modules of size K=12 [1] with OTN processing and switching total capacity of 120 Gbps;

ii) space switching modules of size Q=144 with switching total capacity of 1.44 Tbps [2].

As said above, in Table 3.2 there are reported the values of the complexity parameters n_{OTN}, n_{SW} and n_{IL} introduced in Section 3.1.2 and denoting the number of 12×12 OTN switches used, the number 144×144 space switching modules and the number of interconnection links respectively. From the Table 3.2, where the values of n_{OTN}, n_{SW} and n_{IL} are reported versus the speedup S, we can observe how the realization of an SSNB (S=S_{SSNB}=12 according to lemma 1) switch needs the use of many components that makes it unfeasible.

In particular it would be needed n_{OTN}=384 12×12 OTN switches, n_{SW}=99 144×144 space switching modules and n_{IL}=13568 interconnection links. The complexity may be dramatically dropped if the speedup S is lowered from S=12 (SSNB case) to S=1.5. That would lead to the use of n_{OTN}=48 12×12 OTN switches, n_{SW}=9 144×144 space switching modules and n_{IL}=976

S	n_{OTN}	n_{SW}	n_{IL}
1	32	7	960
1.5	48	9	1440
2	64	15	2048
3	96	23	3168
4	128	31	4352
6	192	47	6624
12 (SSNB)	384	99	13568

Table 3.2: Evaluation of the complexity indexes n_{OTN}, n_{SW} and n_{IL} as a function of the spatial speedup S. The switch parameters are N=4, W=48, F=8. DH-ODU and L-ODU carrying 10 Gbps and 1.25 Gbps flows respectively are considered. The basic blocks of the integrated OTN/WDM switch are 12×12 OTN switching modules at 120 Gbps [1] and 144×144 space switching modules at 1.44 Tbps [2].

interconnection links with a reduction of 87.5%, 90.9% and 92.9% for each type of network element respectively. Obviously it is important to study the impact that the reduction in speedup S has on the network blocking performance. For this reason the blocking performance results in static and dynamic traffic scenarios will be shown in Section 3.4.1 and 3.4.2 respectively.

3.4.1 Blocking Performance in Static Traffic Scenario

In this section, the blocking performance is evaluated when the following static traffic model is used to generate the traffic matrices $\mathcal{T}^{DH} = [t_{sd}^{DH}]$ and $\mathcal{T}^{L} = [t_{sd}^{L}]$ that report the number of DH-ODUs and L-ODUs offered between each couple of nodes $s, v \in \mathcal{V}$.

The traffic model is characterized by the following two parameters:

- $A_{o,sn}$: the total offered bandwidth traffic demand normalized to the total network capacity; we have

$$A_{o,sn} = \frac{A_{0,s}}{C_{tot}}$$

  where $A_{o,s}$ is the total offered bandwidth traffic demand and C_{tot} is the total network capacity; because each wavelength is provided with a capacity equal to f_H we have C_{tot}=WLf_H, L and W being the number of network fibers and the number of wavelengths carried in any fiber respectively;

- u: the L-ODU fraction of offered bandwidth traffic demand.

Given a value of $A_{o,sn}$, L-ODU and H-ODU connection requests are generated with probabilities

$$\alpha_L = \frac{1}{1 + \frac{1-u}{uF}}$$

and α_{DH}=1-α_L respectively until the value of $A_{o,sn}$ is not exceeded. These requests are randomly assigned to any couple of network nodes $s, v \in \mathcal{V}$.

The network blocking performance in static traffic scenario is characterized with the performance index $P_{b,s}^{tot}$ denoting the rejected fraction of the offered bandwidth traffic demand.

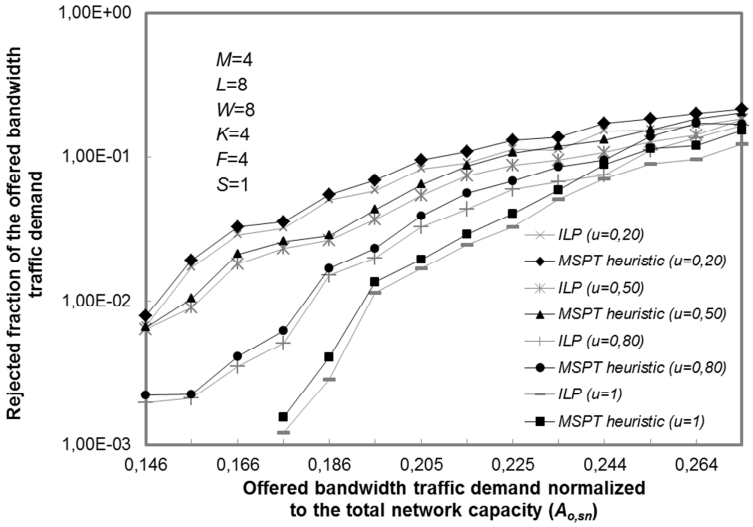

Figure 3.6: Comparison between the ILP and MSPT heuristic results. The rejected fraction of the offered bandwidth traffic demand ($P_{b,s}^{tot}$) is reported for ILP and MSPT heuristic as a function of the traffic parameter $A_{o,sn}$. The L-ODU fraction u of the offered bandwidth traffic demand is equal to 0.20, 0.50, 0.80 and 1. The simple ring network with M=4 nodes and L=8 fibers each one carrying W=8 wavelengths is considered. The multiplexing ratio F is equal to 4 and the integrated nodes are equipped with 4×4 OTN switching modules and they are not provided with speedup (S=1).

In this evaluation analysis, the first objective is to verify the effectiveness of the MSPT heuristic introduced in Section 3.3 by comparing its results to the ones obtained by solving the ILP problem illustrated in Section 3.2. Because of the ILP problem complexity, this comparison could be done only in the case of small networks. In particular, a 4 nodes ring network in which each fiber carries W=8 wavelengths has been considered. Furthermore it is considered the case in which the DH-ODU and the L-ODU carry f_H=10 Gbps

and f_L=2.4885 Gbps flows corresponding to ODU-2 and ODU-1 respectively of the OTN multiplexing hierarchical respectively [54]. This choice leads to a value of F equal to 4. The integrated OTN/WDM nodes are equipped with OTN switching modules of size K=4 and no speedup is implemented (S=1). The comparison between the ILP and MSPT heuristic results are shown in Fig. 3.6 where the performance index $P_{b,s}^{tot}$ is reported as a function of $A_{o,sn}$ and for various mix of L-ODUs and DH-ODUs traffic and in particular for u equal to 0.2, 0.5, 0.8 and 1. We can observe from Fig. 3.6 that the MSPT heuristic shows good performance when compared with the results obtained from the ILP solver with the further advantage to have computation complexity much lower than the ILP approach.

Next some results obtained with the MSPT heuristic in the case of a larger metropolitan networks are shown. Two large metropolitan networks are considered:

- the DENSE network [82] illustrated in Fig. 3.7 and composed by M=13 nodes and L=40 fibers each carrying W=48 wavelengths.
- the VERY LARGE network [85] illustrated in Fig. 3.8 and composed by M=34 nodes and L=114 fibers each carrying W=48 wavelengths.

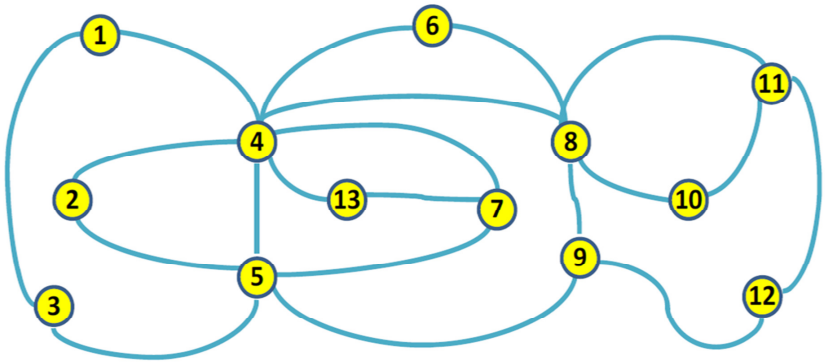

Figure 3.7: Topology of the DENSE metropolitan network with M=13 nodes and L=40 fibers.

In both networks, the case f_H=10 Gbps and f_L=1.25 Gbps that leads to a choice of F=8 has been considered. The nodes are equipped with 12 × 12 OTN switching nodes.

The DENSE metropolitan network is the first to be analyzed. In this scenario, the performance index $P_{b,s}^{tot}$ is reported as a function of $A_{o,sn}$ in

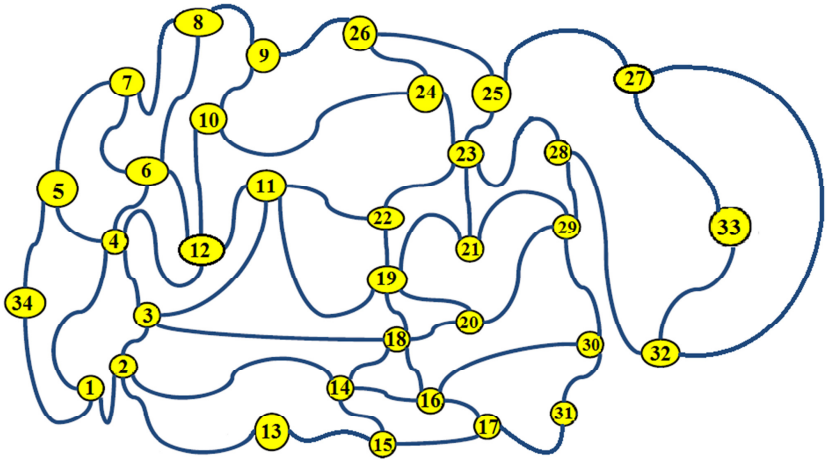

Figure 3.8: Topology of the VERY LARGE metropolitan network with M=34 nodes and L=114 fibers.

Figs 3.9-3.10 for speedup values S equal to 1, 1.5, 2, and 12 where S=12 corresponds to the SSNB switching node case. The traffic mix characterized by u equal to 0.2 and 0.8 is considered in Fig. 3.9 while the results for u equal to 0.5 and 1 are shown in Fig. 3.10. We can observe from Figs 3.9-3.10 that even in the case in which the speedup is not implemented (S=1) performance degradation does not occur and the same performance obtained with SSNB (S=12) nodes are reached.

Considering the scenario with the metropolitan networks in Fig. 3.8, the rejected fraction of the offered bandwidth traffic demand is reported in Fig. 3.11. In the VERY LARGE network, we can observe that when the speedup is not implemented (S=1), performance degradation of more than one order of magnitude occurs with respect to an SSNB switch. The performance degradation may be mitigated by introducing a spatial speedup value S=1.5.

3.4.2 Blocking Performance in Dynamic Traffic Scenario

The performance of the DENSE network of Fig. 3.7 with W=48 wavelengths carried on each fiber is investigated when the network is equipped with the integrated OTN/WDM switching nodes and in the case of dynamic traffic scenario. The first assumption is that the connection requests for carrying L-ODU and DH-ODU are presented with exponentially distributed inter-arrival times. The connection duration is also exponentially distributed and we assume that L-ODU and DH-ODU carry flows at f_L=1.25 Gbps and

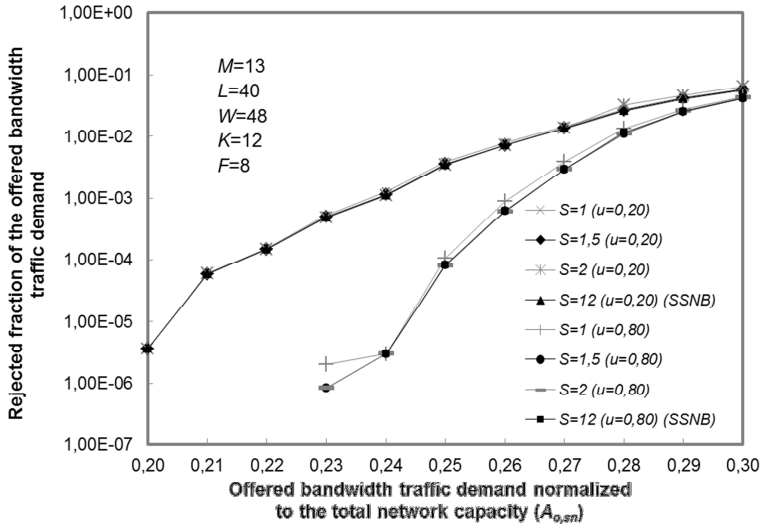

Figure 3.9: The rejected fraction of the offered bandwidth traffic demand ($P_{b,s}^{tot}$) is reported for the MSPT heuristic as a function of the traffic parameter $A_{o,sn}$. The L-ODU fraction u of the offered bandwidth traffic demand is equal to 0.20 and 0.80. The network parameter values are M=13, L=40, W=48, F=8. The integrated OTN/WDM nodes are equipped with 12×12 OTN switching modules and provided with speedup S varying from 1 to 12. The case S=12 corresponds to the case of SSNB switching nodes.

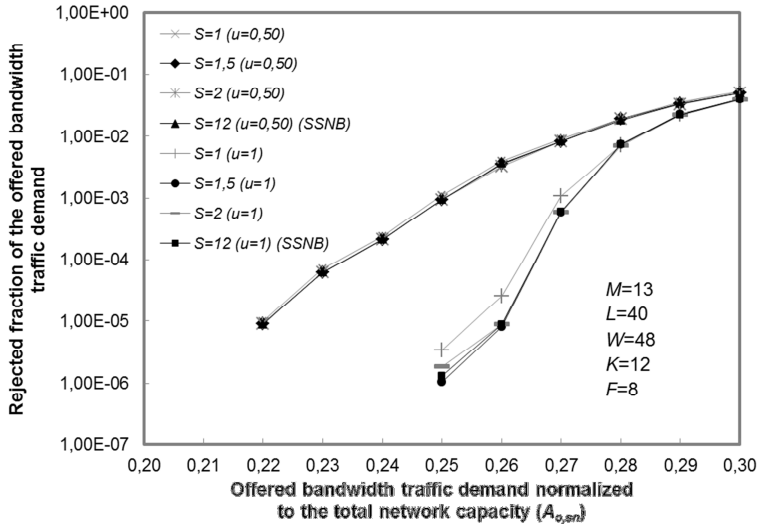

Figure 3.10: The rejected fraction of the offered bandwidth traffic demand ($P_{b,s}^{tot}$) is reported for the MSPT heuristic as a function of the traffic parameter $A_{o,sn}$. The L-ODU fraction u of the offered bandwidth traffic demand is equal to 0.50 and 1. The network parameter values are M=13, L=40, W=48, F=8. The integrated OTN/WDM nodes are equipped with 12×12 OTN switching modules and provided with speedup S varying from 1 to 12. The case S=12 corresponds to the case of SSNB switching nodes.

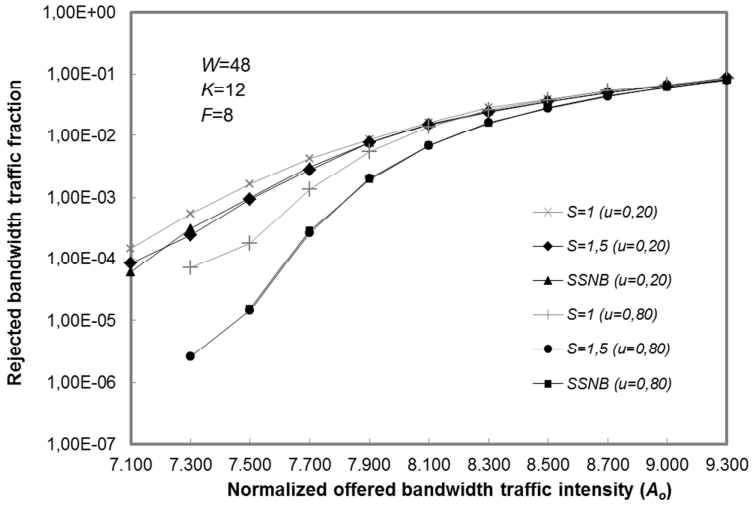

Figure 3.11: The rejected fraction of the offered bandwidth traffic demand ($P_{b,s}^{tot}$) is reported for the MSPT heuristic as a function of the normalized offered bandwidth traffic intensity $A_{o,sn}$. The L-ODU fraction u of the offered bandwidth traffic demand is equal to 0.20 and 0.80. The network parameter values are M=34, L=114, W=48, F=8. The integrated OTN/WDM nodes are equipped with 12×12 OTN switching modules and provided with speedup S varying from 1 to 12. The case S=12 corresponds to the case of SSNB switching nodes.

f_H=10 Gbps respectively that leads to a multiplexing ratio F=8.

Furthermore it is assumed uniformly distributed traffic between the network nodes and denote with λ_L and λ_{DH} the connection request inter-arrival rates of L-ODU and DH-ODU respectively. The same connection rate μ=1 is assumed for L-ODU and and DH-ODU.

The offered traffic is characterized with the parameter

$$A_{o,dn} = N(N-1)\frac{F\lambda_{DH} + \lambda_L}{WLF}$$

that indicates the offered bandwidth traffic intensity normalized to the total network capacity. In the dynamic traffic scenario, the expression could be written for the L-ODU fraction of the offered bandwidth traffic as follow:

$$u = \frac{\lambda_L}{\lambda_L + F\lambda_{DH}}$$

The adopted routing policy is based on the use of two auxiliary graphs $\mathcal{G}_{aux}^{DH}$ and $\mathcal{G}_{aux}^{L}$ for routing of L-ODU and DH-ODU respectively. The graphs are constructed as described in Section 3.3 and are updated all of times in which a connection carrying L-ODU or DH-ODU is set up or torn down.

At any instant the graph $\mathcal{G}_{aux}^{DH}$ ($\mathcal{G}_{aux}^{L}$) contains all of the links in which the allocation of one DH-ODU (L-ODU) is permitted. Each link is labeled with a weight denoting the number of DH-ODUs (L-ODUs) that the link can accept. When a DH-ODU (L-ODU) connection request arrives, the least cost path is evaluated in $\mathcal{G}_{aux}^{DH}$ ($\mathcal{G}_{aux}^{L}$) and if it exists then the weights of the graphs are updated and the links not able to accept at least one DH-ODU (L-ODU) are deleted from the graph $\mathcal{G}_{aux}^{DH}$ ($\mathcal{G}_{aux}^{L}$). As described in Section 3.3, the not admissible interstage links are also removed. When a connection is torn down, the graphs weights are updated and the links becoming newly available are inserted as well as the admissible interstage links.

In the analysis reported in this section, three performance indexes characterizing the network blocking under dynamic traffic scenario are introduced. The first index is the rejected bandwidth ratio $P_{b,d}^{tot}$ defined as the bandwidth blocking probability and characterizing the rejected fraction of the offered bandwidth traffic. The second (third) index is the L-ODU (DH-ODU) connection blocking probability $P_{b,d}^{L}$ ($P_{b,d}^{DH}$) defined as the ratio of the number of rejected L-ODU (DH-ODU) connection requests to the number of offered L-ODU (DH-ODDU) connection requests. The indexes $P_{b,d}^{tot}$, $P_{b,d}^{L}$ and $P_{b,d}^{DH}$ are evaluated as a function of $A_{o,dn}$ for speedup values S equal to 1, 1.5, 2, 12 where the case $S = S_{SSNB} = 12$ corresponds to the use of a Strict Sense Non Blocking (SSNB) switch according to the Lemma-1 of Section 3.1.2.

The curves of $P_{b,d}^{tot}$, $P_{b,d}^{DH}$ and $P_{b,d}^{L}$ evaluated with the analysis of the DENSE network are reported in Figs 3.12-3.14 for u=0.2 and u=0.8. Conversely the ones for u=0.5 and u=1 for the same network are illustrated in Figs 3.15-3.17. We can observe from Figs 3.12 and 3.15 a degradation of the bandwidth blocking probability $P_{b,d}^{tot}$ when no speedup is implemented (S=1). For instance when $A_{o,dn}$=0.091 and u=0.5, the bandwidth blocking probability $P_{b,d}^{tot}$ equals $1.44 \cdot 10^{-6}$ and $1.80 \cdot 10^{-4}$ for the SSNB (S=12) and S=1 cases with a worsening of two orders of magnitude. We can notice from Fig. 3.13 that the internal blocking of the switch and the lack of speedup lead especially a degradation in terms of the DH-ODU connection blocking probability. In this case $P_{b,d}^{DH}$ reaches values of $1.50 \cdot 10^{-6}$ and $3.59 \cdot 10^{-4}$ in the SSNB and S=1 cases respectively and for $A_{o,dn}$=0.091 and u=0.5. Notice that the higher reject rate of the DH-ODU connection requests leads to the possibility of accepting more L-ODU connection requests. That justifies why $P_{b,d}^{L}$ is lower in the case S=1 as shown in Figs 3.14 and 3.17.

Finally we can notice how a spatial speedup S equal to 1.5 leads to a lack

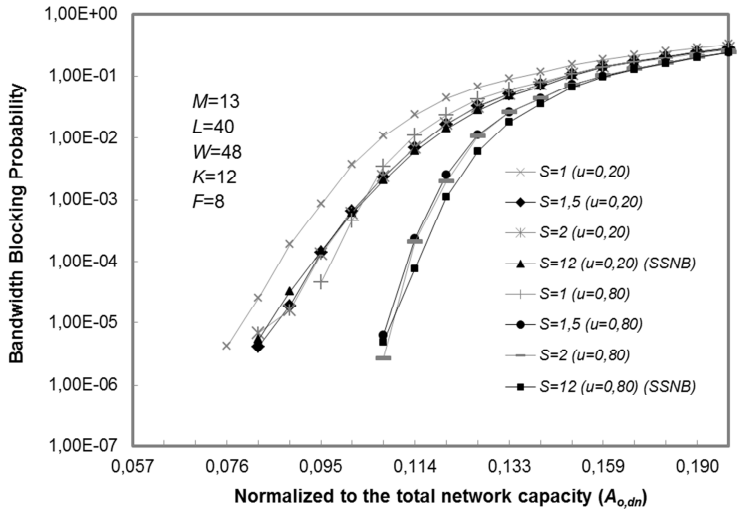

Figure 3.12: Bandwidth blocking probability $P_{b,d}^{tot}$ as a function of the normalized offered bandwidth traffic intensity $A_{o,dn}$. The switch and network parameters are M=13, L=40, F=8 and K=12. The L-ODU fraction of the offered bandwidth traffic u is equal to 0.2 and 0.8. The spatial speedup is varying from 1 to 12.

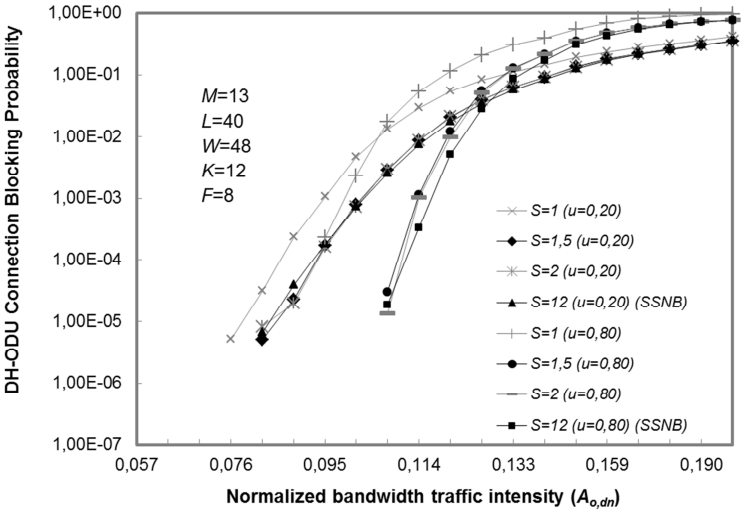

Figure 3.13: DH-ODU connection blocking probability $P_{b,d}^{DH}$ as a function of the normalized offered bandwidth traffic intensity $A_{o,dn}$. The switch and network parameters are M=13, L=40, F=8 and K=12. The L-ODU fraction of the offered bandwidth traffic u is equal to 0,2 and 0,8. The spatial speedup is varying from 1 to 12.

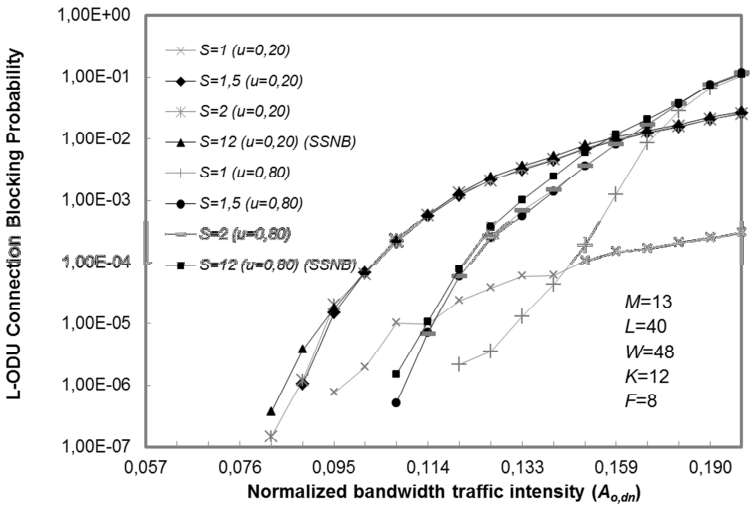

Figure 3.14: L-ODU connection blocking probability $P_{b,d}^{L}$ as a function of the normalized offered bandwidth traffic intensity $A_{o,dn}$. The switch and network parameters are M=13, L=40, F=8 and K=12. The L-ODU fraction of the offered bandwidth traffic u is equal to 0.2 and 0.8. The spatial speedup is varying from 1 to 12.

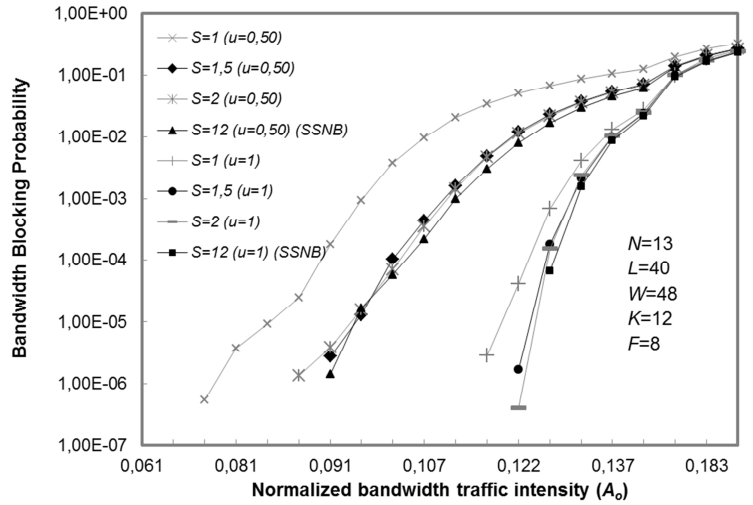

Figure 3.15: Bandwidth blocking probability $P_{b,d}^{tot}$ as a function of the normalized offered bandwidth traffic intensity $A_{o,dn}$. The switch and network parameters are M=13, L=40, F=8 and K=12. The L-ODU fraction of the offered bandwidth traffic u is equal to 0.5 and 1, whereas the spatial speedup is varying from 1 to 12.

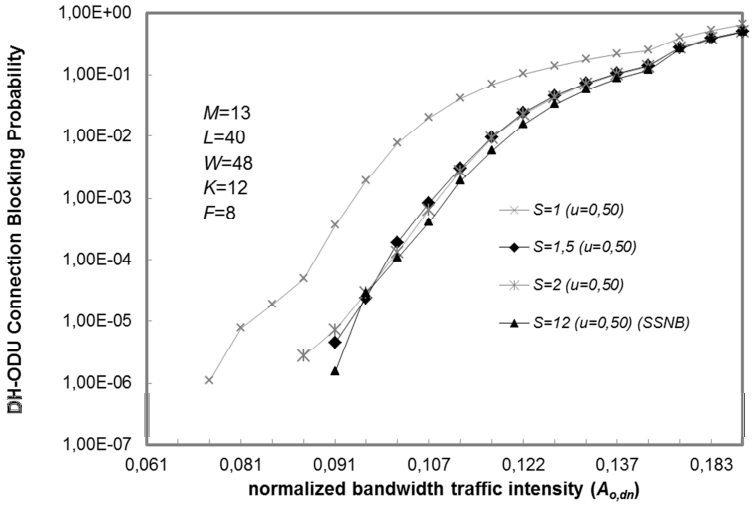

Figure 3.16: DH-ODU connection blocking probability $P_{b,d}^{DH}$ as a function of the normalized offered bandwidth traffic intensity $A_{o,dn}$. The switch and network parameters are M=13, L=40, F=8 and K=12. The L-ODU fraction of the offered bandwidth traffic u is equal to 0.5, whereas the spatial speedup is varying from 1 to 12.

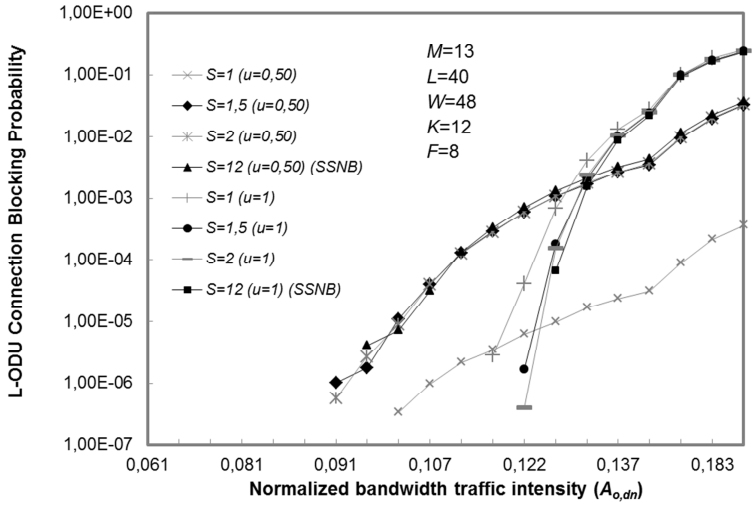

Figure 3.17: L-ODU connection blocking probability $P_{b,d}^{L}$ as a function of the normalized offered bandwidth traffic intensity $A_{o,dn}$. The switch and network parameters are M=13, L=40, F=8 and K=12. The L-ODU fraction of the offered bandwidth traffic u is equal to 0.5 and 1. The spatial speedup is varying from 1 to 12.

of degradation of the bandwidth blocking probability with performance equal to the one obtained with the use of SSNB switches.

Next the blocking performance in the case of dynamic traffic scenario for the VERY LARGE network is investigated.

In Fig. 3.18 it is reported the bandwidth blocking probability $P_{b,d}^{tot}$ evaluated with the same assumption considered for the DENSE network. We can observe from Fig. 3.18 a degradation of $P_{b,d}^{tot}$ when no speedup is implemented (S=1). For instance when A_o=6800 and u=0.8, the bandwidth blocking probability equals $4.36 \cdot 10^{-5}$ and $1,58 \cdot 10^{-2}$ for the SSNB and S=1 cases with a worsening of three orders of magnitude. Finally we can notice how a spatial speedup S equal to 1.5 leads to considerable reduction of degradation with the bandwidth blocking probability values equal to $2.17 \cdot 10^{-4}$ in the S=1.5 case.

Also in this network, the use of a spatial speedup S=1.5 leads to dramatically drop the switch complexity with respect to the SSNB case that can be implemented with the proposed architecture provided with speedup S=8 [83]. It has been proved that the choice of S=1.5 allows for a reduction of 81.2% [83] in term of number of 12×12 OTN switching modules [1]. The switch with $S = 1.5$ spatial speedup also allows for the saving of 144×144 space switching modules [2] needed to realize the switching fabric with respect to the SSNB ($S = 8$).

3.5 OTN/WDM Integrated Switch Architecture with a Less Number of Elements

In the previous sections, a possible implementation of an OTN/WDM integrated switching node has been introduced and an example of a 4-degree node is depicted in Fig. 3.1 [85]. In addition it has been proposed a switch core for two hierarchical levels OTN transport architecture and able to switch two types of Optical Data Units (ODU) referred to as higher order ODU (H-ODU) and lower order ODU (L-ODU) respectively.

This section deals with a new OTN/WDM switch architecture with a less number of elements. Here the proposed switch core architecture is described in Fig. 3.19 where N and W denote the number of Input/Output Fibers and the number of wavelengths respectively. Also in this new proposal, the switch is composed by three stages: $K \times K$ OTN switching modules are placed in the

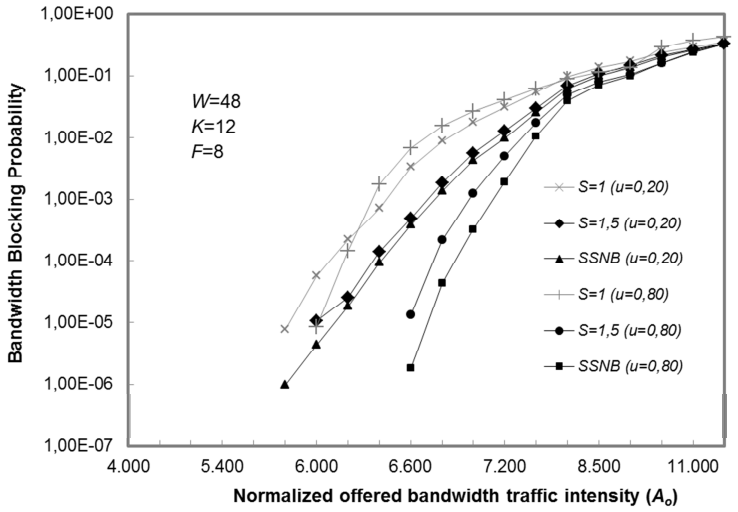

Figure 3.18: Bandwidth blocking probability $P_{b,d}^{tot}$ as a function of the normalized offered bandwidth traffic intensity $A_{o,dn}$. The switch and network parameters are M=34, L=114, F=8 and K=12. The L-ODU fraction of the offered bandwidth traffic u is equal to 0.2 and 0.8. The spatial speedup is varying from 1 to 12.

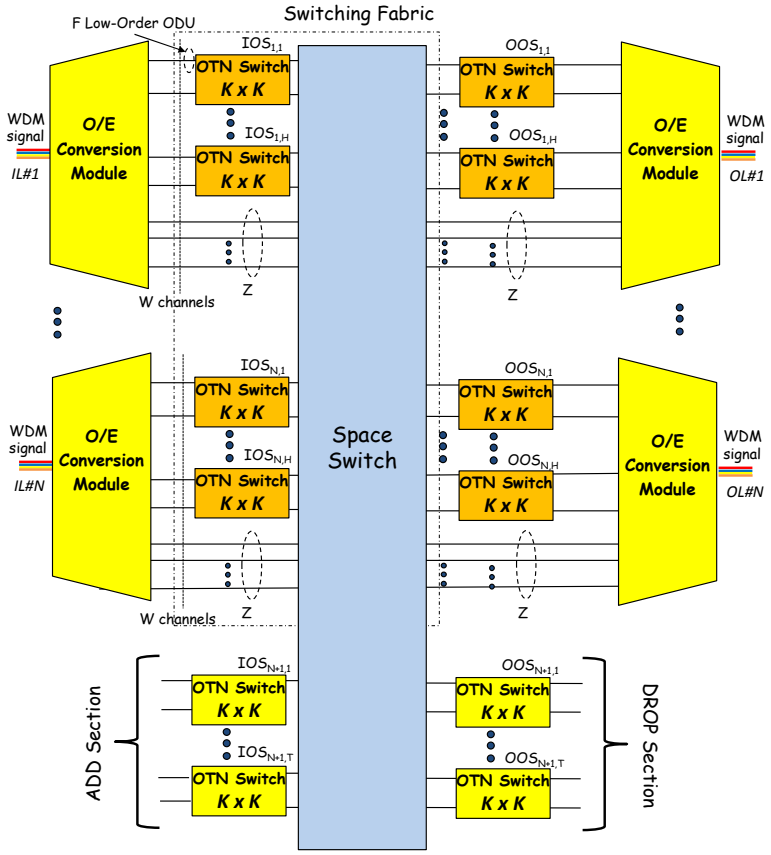

Figure 3.19: OTN/WDM Switching Architecture with low complexity switching fabric and a reduced number of OTN switches.

first and third stages and are able to perform both space and time switching. Conversely the middle stage is able to perform space switching only and hence to handle the switching among H-ODUs only.

In each of the N input/output lines, a number H of OTN switches are used while there are Z out of W wavelengths carried in each input/output line for which OTN switching is not allowed. We assume that the OTN switching modules of the first (third) stage are used to switch L-ODU and H-ODU coming (directed) from (to) any input (output) line.

In Fig. 3.19 it is also reported the ADD and DROP sections each one composed by T OTN switching modules. The input/output OTN switching modules are connected by means of interstage links provided by the $(NHK + NZ + TK) \times (NHK + NZ + TK)$ space switching module.

The blocking performance of the switch core architecture has been investigated [81] when the condition $\frac{W-Z}{H} = K$ holds that is the used number of inputs (outputs) of each input (output) OTN switch is equal to its size K. However this choice, that minimizes the switch cost, does not guarantee the switch core architecture to be non blocking. The penalization in terms of blocking probability has been studied in [81] and can be much high in some traffic scenario. To mitigate the blocking, it has been introduced a spatial speedup

$$S = \frac{K}{\frac{W-Z}{H}}$$

that is defined as the ratio of the OTN switch size to the used number of inputs (outputs) of each input (output) OTN switch.

Obviously a speedup S greater than 1 increases the switch complexity but allows for lower blocking probability. In the case of $W - Z$ multiple of H, we adopt the strategy of assigning the same number $\frac{W-Z}{H}$ of wavelengths of any input (output) line to each of the H input (output) OTN switching modules dedicated to that input (output) line.

In Fig. 3.20 an example of proposed switching architecture is illustrated in the case in which the parameter values $N = 2$, $W = 6$, $H = 1$, $K = 4$ are chosen with a speedup value $S = 2$.

In this case, it has neglected to report the ADD and DROP sections while we have illustrated the E/O and O/E conversion modules that as before mentioned will be realized with optical multiplexer/demultiplexer and PICs.

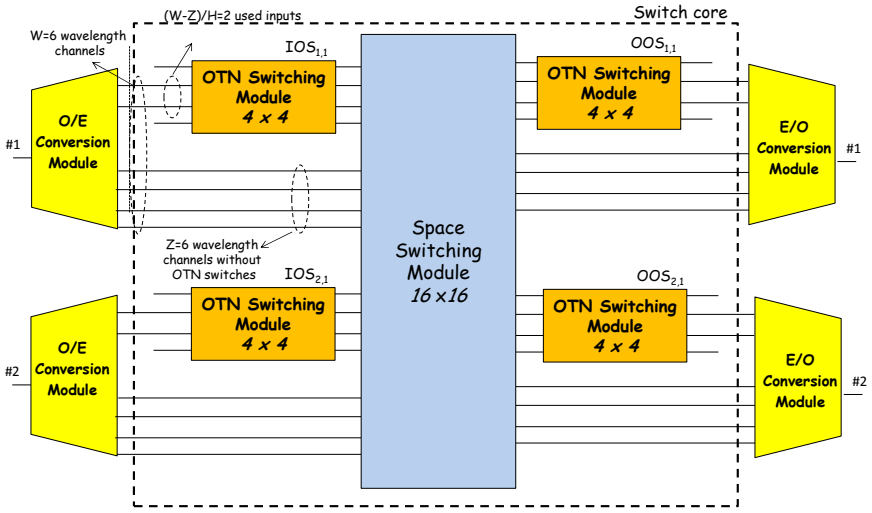

Figure 3.20: Integrated OTN/WDM switch with spatial speedup S=2 and $Z = 4$ wavelengths without OTN switches.

3.6 Switch Resource Assignment and Routing Problem

The optimal problem of the Switch Resource Assignment and Routing (SRAR) in OTN/WDM networks and nodes with a less number of elements is stated below. We have the following inputs:

- $\mathcal{G} = (\mathcal{V}, \mathcal{E})$: graph representing a physical topology where $\mathcal{V}$ is the set of nodes and $\mathcal{E}$ is the set of links; the nodes correspond to the OTN/WDM integrated switching nodes and the links correspond to the fibers between switching nodes; the degree of the node $v \in \mathcal{V}$ is assumed to be d_v that is the corresponding switching node has d_v express input/output fibers; the network is composed by $N_{\mathcal{V}}$ switching nodes, each one equipped with $K \times K$ OTN switches and provided with a speedup S.

- T: number of ADD/DROP OTN switches for each switching node;

- W: number of wavelength channels carried by each fiber where each channel has the capacity of carrying either one H-ODU or up to F L-ODUs;

- Z: number of wavelength channels carried by each fiber where OTN switching is not allowed;

- $\mathcal{T}^{DH} = [t_{sd}^{DH}], \mathcal{T}^{L} = [t_{sd}^{L}]$: $N_{\mathcal{V}} \times N_{\mathcal{V}}$ traffic matrices for the DH-ODUs and L-ODUs traffic offered between the network nodes respectively. In particular t_{sd}^{DH} and t_{sd}^{L} denote the number of DH-ODUs and L-ODUs offered between the nodes $s \in \mathcal{V}$ and $d \in \mathcal{V}$;

Also in this problem like the one reported in Section 3.2, the goal is to determine:

- where the accepted H-ODUs and L-ODUs traffic is routed in the OTN/WDM network;
- which interstage links are set up between the input and output ports of the space switches of the nodes $v \in \mathcal{V}$.

The objective is to maximize the throughput given by total accepted bandwidth traffic demand normalized to the bandwidth f_L requested by one L-ODU. In particular notice that the acceptance of one DH-ODU request and one L-ODU request leads to a contribution of F and 1 respectively in the normalized total accepted bandwidth traffic demand.

1) Notation and parameters

To give formally the ILP formulation, the unconnected graph $\mathcal{G}^* = (\mathcal{V}^*, \mathcal{E}^*)$ is introduced where $\mathcal{V}^*$ and $\mathcal{E}^*$ are the set of nodes and the links respectively. The set $\mathcal{V}^*$ is the union of the sets Ψ_v^I, Ψ_v^O, $\Gamma_v^{I,OTN}$, $\Gamma_v^{I,F}$, $\Gamma_v^{O,OTN}$, $\Gamma_v^{O,F}$, A_v and D_v defined for each node $v \in \mathcal{V}$ and whose meaning is indicated in Fig. 3.21 for the OTN/WDM integrated switch of Fig. 3.20.

In the following, the definition of these sets is provided:

- $\Psi_v^I \equiv \{l_v^{i,j}, i = 1, \cdots d_v; j = 1, \cdots, H\}$: set of nodes $l_v^{i,j}$ $(i = 1, \cdots d_v; j = 1, \cdots, H)$ corresponding to the $j-th$ input OTN switching module of the $i-th$ input line in the node $v \in \mathcal{V}$;
- $\Psi_v^O \equiv \{o_v^{i,j}, i = 1, \cdots d_v; j = 1, \cdots, H\}$: set of nodes $o_v^{i,j}$ $(i = 1, \cdots d_v; j = 1, \cdots, H)$ corresponding to the $j-th$ output OTN switching module of the $i-th$ output line in the node $v \in \mathcal{V}$;
- $\Gamma_v^{I,OTN} \equiv \{p_v^{I,OTN,i,j,k}, i = 1, \cdots d_v; j = 1, \cdots, H; k = 1, \cdots K\}$: set of nodes $p_v^{I,OTN,i,j,k}$ $(i = 1, \cdots d_v; j = 1, \cdots, H; k = 1, \cdots K)$ corresponding to the input express port of the space switching module connected to the $k-th$ output of the $j-th$ input OTN switch of the $i-th$ line in the node $v \in \mathcal{V}$;

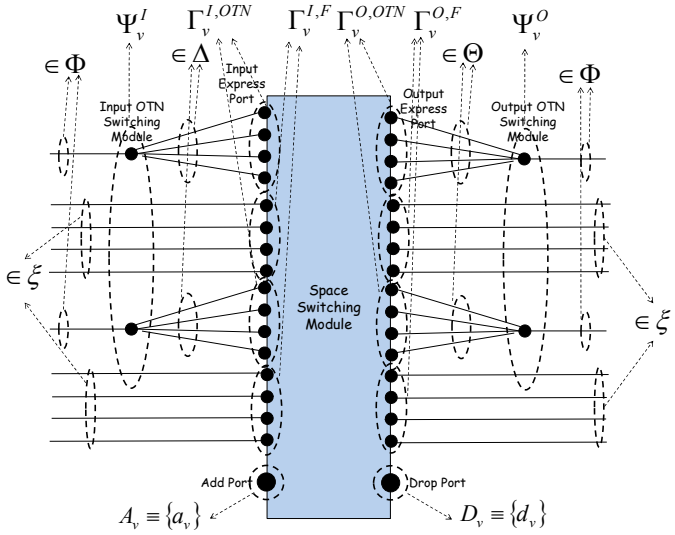

Figure 3.21: Sets of nodes and links of the node $v \in \mathcal{V}$ in the graph $\mathcal{G}^* = (\mathcal{V}^*, \mathcal{E}^*)$

- $\Gamma_v^{I,F} \equiv \{p_v^{I,F,i,j}, i = 1, \cdots d_v; j = 1, \cdots, Z\}$: set of nodes $p_v^{I,F,i,j}$ $(i = 1, \cdots d_v; j = 1, \cdots, Z)$ corresponding to the input express port of the space switching module connected to the $j-th$ wavelengths of the $i-th$ input line in the node $v \in \mathcal{V}$ in which OTN switch are absent;

- $\Gamma_v^{O,OTN} \equiv \{p_v^{O,OTN,i,j,k}, i = 1, \cdots d_v; j = 1, \cdots, H; k = 1, \cdots K\}$: set of nodes $p_v^{O,OTN,i,j,k}$ $(i = 1, \cdots d_v; j = 1, \cdots, H; k = 1, \cdots K)$ corresponding to the output express port of the space switching module connected to the $k-th$ input of the $j-th$ output OTN switch of the $i-th$ line in the node $v \in \mathcal{V}$;

- $\Gamma_v^{O,F} \equiv \{p_v^{O,F,i,j}, i = 1, \cdots d_v; j = 1, \cdots, Z\}$: set of nodes $p_v^{O,F,i,j}$ $(i = 1, \cdots d_v; j = 1, \cdots, H)$ corresponding to the output express port of the space switching module connected to the $j-th$ wavelengths of the $i-th$ output line in the node $v \in \mathcal{V}$ in which OTN switches are absent;

- $A_v \equiv \{a_v\}$: set composed by the only node a_v that jointly represents the ADD OTN switches and the ADD ports of the space switch of the node $v \in \mathcal{V}$;

- $D_v \equiv \{d_v\}$: set composed by the only node d_v that jointly represents the DROP OTN switches and the DROP ports of the space switch of the node $v \in \mathcal{V}$;

The set $\mathcal{E}^*$ is composed by the following four sets of links:

- Φ: set of links $(o_v^{i_v,j}, l_u^{i_u,j})$ $((v,u) \in \mathcal{E}; j = 1, \cdots H)$ where the nodes v and u are adjacent in $\mathcal{G}$ and the corresponding switching nodes are interconnected with a fiber by the $i_v - th$ output line of the node v to the $i_u - th$ input line of the node u;

- ξ: set of links $(p_v^{O,F,i_v,j}, p_u^{I,F,i_u,j})$ $((v,u) \in \mathcal{E}; j = 1, \cdots Z)$ where the nodes v and u are adjacent in $\mathcal{G}$ and the corresponding switching nodes are interconnected with a fiber by the $i_v - th$ output line of the node v to the $i_u - th$ input line of the node u;

- Δ: set of links $(l_v^{i,j}, p_v^{I,i,j,k})$ $(v \in \mathcal{V}; i = 1, \cdots d_v; j = 1, \cdots, H; k = 1, \cdots K)$ connecting nodes corresponding to input OTN switches and input express ports;

- Θ: set of links $(p_v^{O,i,j,k}, o_v^{i,j})$ $(v \in \mathcal{V}; i = 1, \cdots d_v; j = 1, \cdots, H; k = 1, \cdots K)$ connecting nodes corresponding to output express ports and output OTN switches.

For each node $w \in \mathcal{V}^*$ the sets $\Omega_w^{(-)}$ and $\Omega_w^{(+)}$ of the predecessor and successor nodes respectively have been introduced. thus we can write:

$$\Omega_w^{(-)} = \{t \in \mathcal{V}^* \ / \ (t,w) \in \mathcal{E}^*\}$$

$$\Omega_w^{(+)} = \{t \in \mathcal{V}^* \ / \ (w,t) \in \mathcal{E}^*\}$$

2) Optimization Variables

Next the variables of the optimization problem are reported:

- $S_{s,d}^{y,t} \in \{0,1\}$ $(s,d \in \mathcal{V}; y \in \{DH, L\}; t \in \{1..t_{sd}^y\})$: the variable assumes the value 1 if the $t - th$ y-ODU offered between the nodes s and d is successfully carried; otherwise it assumes the value 0;

- $\lambda_{s,d}^{w,u,y,t} \in \{0,1\}$ $(s,d \in \mathcal{V}; (w,u) \in \mathcal{E}^*; y \in \{DH, L\}, t \in \{1..t_{sd}^y\})$: the variable assumes the value 1 if the $t - th$ y-ODU offered between the nodes s and d is carried on the link (w,u); otherwise it assumes the value 0;

- $x_{w,u}^v \in \{0,1\}$ $(v \in \mathcal{V}; w \in \Gamma_v^{I,OTN} \cup \Gamma_v^{I,F} \cup A_v; u \in \Gamma_v^{O,OTN} \cup \Gamma_v^{O,F} \cup D_v)$: the variable assumes the value 1 if the ports of the space switch

corresponding to the nodes w and u are interconnected by an interstage link.

3) Constraints

Constraints are introduced to ensure that from an input and output express port of any space switch is activated only an interstage link. Conversely up to a maximum of KT interstage links can be activated from/to the ADD/DROP sections. These constraints can be expressed as follows:

$$\sum_{u \in \Gamma_v^{O,OTN} \cup \Gamma_v^{O,F} \cup D_v} x_{w,u}^v \leq 1 \quad v \in \mathcal{V} \;\; w \in \Gamma_v^{I,OTN} \cup \Gamma_v^{I,F} \tag{3.15}$$

$$\sum_{w \in \Gamma_v^{I,OTN} \cup \Gamma_v^{I,F} \cup A_v} x_{w,u}^v \leq 1 \quad v \in \mathcal{V} \;\; u \in \Gamma_v^{O,OTN} \cup \Gamma_v^{O,F} \tag{3.16}$$

$$\sum_{u \in \Gamma_v^{O,OTN} \cup \Gamma_v^{O,F} \cup D_v} x_{w,u}^v \leq KT \quad v \in \mathcal{V} \;\; w = a_v \tag{3.17}$$

$$\sum_{w \in \Gamma_v^{I,OTN} \cup \Gamma_v^{I,F} \cup A_v} x_{w,u}^v \leq KT \quad v \in \mathcal{V} \;\; u = d_v \tag{3.18}$$

For the t-th y-ODU ($y \in \{DH, L\}; t \in [1..t_{sv}^y]$) offered between the nodes $s, v \in \mathcal{V}$, flow conservation constraints are introduced in every node $w \in \mathcal{V}^*$. The constraint may not be respected only in the ADD and DROP nodes a_s and d_v where the total flow is equal to 1 and -1 respectively if the y-ODU is successfully carried; otherwise is equal to 0. So we can write:

$$\sum_{u \in \Omega_w^{(-)}} \lambda_{s,v}^{u,w,y,t} - \sum_{u \in \Omega_w^{(+)}} \lambda_{s,v}^{w,u,y,t} = \begin{cases} -S_{s,v}^{y,t} & if \;\; w = a_s \\ S_{s,v}^{y,t} & if \;\; w = d_v \\ 0 & otherwise \end{cases} \tag{3.19}$$

Further constraints are considered to guarantee that the traffic routed on any link $(w, u) \in \mathcal{E}^*$ in smaller than or equal to the link transport capacity normalized to the bandwidth f_L of one L-ODU. This capacity equals F for the links $(w, u) \in \Delta \cup \Theta \cup \xi$ that interconnect nodes corresponding to input/output OTN switches and output/input express ports. In the case of links $(w, u) \in \Phi$ interconnecting nodes corresponding to output OTN switch and input OTN switch, the capacity equals the sum of the capacities pro-

vided by the wavelength channels interconnecting them, that is $\frac{KF}{S}$. Finally another constraint is added that limits to F the normalized capacity of any activated interstage link. We can simply write:

$$\sum_{s,d\in\mathcal{V}}\sum_{t=1}^{t_{s,d}^{L}}\lambda_{s,d}^{w,u.L,t}+F\sum_{s,d\in\mathcal{V}}\sum_{t=1}^{t_{s,d}^{DH}}\lambda_{s,d}^{w,u,DH,t}\leq C_{L} \tag{3.20}$$

where C_L is given by:

$$C_{L}=\begin{cases}F & if\ (w,u)\in\Delta\cup\Theta\cup\xi\\ \frac{KF}{S} & if\ (w,u)\in\Phi\\ Fx_{w,u}^{v} & if\ v\in\mathcal{V};w\in\Gamma_{v}^{I,OTN}\cup\Gamma_{v}^{I,F};\\ & u\in\Gamma_{v}^{O,OTN}\cup\Gamma_{v}^{O,F}\cup D_{v}\\ Fx_{w,u}^{v} & if\ v\in\mathcal{V};w\in A_{v};\\ & u\in\Gamma_{v}^{O,OTN}\cup\Gamma_{v}^{O,F}\end{cases} \tag{3.21}$$

4) Objective Function

The objective is to maximize the throughput given by total accepted bandwidth traffic demand normalized to the bandwidth f_L requested by one L-ODU:

$$Maximize:\sum_{s,d\in\mathcal{V}}\sum_{t=1}^{t_{s,d}^{L}}S_{s,d}^{L,t}+F\sum_{s,d\in\mathcal{V}}\sum_{t=1}^{t_{s,d}^{DH}}S_{s,d}^{DH,t} \tag{3.22}$$

Ultimately this section is completed with a computational complexity analysis. If we assume that only DH-ODUs are offered to the network and strict sense non blocking switching nodes are used, the studied SRAR problem becomes the Routing and Wavelength Assignment (RWA) optimization problem with wavelength conversion. Because it is well known the RWA problem is NP-complete [84], we can conclude that the SRAR problem is NP-complete too. For this reason, in the next section, an heuristic is introduced to evaluate the performance of large networks in low computational time.

3.7 Minimizing OTN Switch Resource (MOSR) Heuristic

In the case of integrated OTN/WDM switching architectures equipped with the minimum number of OTN switches, it is very important to exploit wavelengths that are not supported by OTN switches, assigning to each of these either one DH-ODU or F L-ODUs. In the following in order to refer to these ones, the most generic term "H-ODU" is used.

The Minimizing OTN Switch Resource (MOSR) heuristic, shown in Algorithm 2, attempts in the first phase to route the traffic on the shortest paths of the network by carrying on each of them one H-ODU. Moreover among the available shortest paths, the one with minimum number of OTN switches used is selected.

If there is not enough resources to carry all of the traffic on the shortest paths, the MOSR heuristic will try to carry in Phase-2 the remaining traffic on alternative paths.

Before the Phase-1, there is an initialization phase, not shown in Algorithm 2, in which the auxiliary graph $\mathcal{G}_{aux} = (\mathcal{V}_{aux}, \mathcal{E}_{aux})$ is built up, where $\mathcal{V}_{aux} = \mathcal{V}^*$ and $\mathcal{E}_{aux}$ is obtained from $\mathcal{E}^*$ with the addition of all of the possible interstage links that connect input express and add ports to output express and drop ports in any switching node.

The normalized total bandwidth traffic demands t^{tot}_{su}=Ft^{DH}_{su}+t^{L}_{su} $(s, u \in \mathcal{V})$ are stored in the list $\mathcal{L}_1$ according to a decreasing order (line 2). At each iteration of the Phase-1, the MOSR heuristic tries to route either one DH-ODU or F L-ODUs, on the shortest path between the nodes $s^*, u^* \in \mathcal{V}$ in which the higher normalized total bandwidth traffic demand $t^{tot}_{s^*u^*}$ (line 4) is remaining to be routed. The shortest path with minimum number of OTN switches used is selected.

Any traffic demand $t^{tot}_{s^*u^*}$ is not more inserted in the list $\mathcal{L}_1$ when either a shortest path is not available or when its value is smaller than F. The condition of list $\mathcal{L}_1$ empty (line 3) guarantees the end of the Phase-1. At the beginning of the Phase-2, the traffic demands of DH-ODUs and L-ODUs not routed in the first phase are stored in the lists $\mathcal{L}_{DH}$ and $\mathcal{L}_L$ in decreasing order (line 12) respectively.

The MOSR heuristic tries to route the higher traffic demand on the path with minimum number of links (line 15). The alternative path with minimum

Algorithm 2 MINIMIZING OTN SWITCH RESOURCE (MSOR) HEURISTIC

/*Phase 1 - Routing of the H-ODUs on the shortest paths that minimize the number of OTN switches used*/
Sort the normalized bandwidth traffic demands t_{su}^{tot} $(s, u \in \mathcal{V})$ in deceasing order and **memorize** the values in list $\mathcal{L}_1$
while $\mathcal{L}_1$ is not empty **do**
    Try to setup a shortest path between the node pair (s^*, u^*) whose the traffic demand is the first element in $\mathcal{L}_1$; the shortest path with minimum number of OTN switches used is selected.
    if (the shortest path exists)**and**$(t_{s^*u^*}^{tot} \geq F)$ **then**
        $t_{s^*u^*}^{tot}$=$t_{s^*u^*}^{tot}$-F, update the list $\mathcal{L}_1$ and the graph $\mathcal{G}_{aux}$
    else
        the traffic demand $t_{s^*u^*}^{tot}$ is deleted from the list $\mathcal{L}_1$
    end if
end while

/*Phase 2 - Routing of the DH-ODUs and the L-ODU on the alternative paths that minimize the number of OTN switches used*/
Sort the remaining normalized bandwidth traffic demands $t_{s,u}^{y}$ $(s, u \in \mathcal{V}, y \in \{DH, L\})$ in deceasing order and **memorize** the values in list $\mathcal{L}_y$ $(y \in \{DH, L\})$

for $y \in \{DH, L\}$ **do**
    while $\mathcal{L}_y$ is not empty **do**
        Try to setup the path with the minimum number of links between the node pair (s^*, u^*) whose the traffic demand is the first element in $\mathcal{L}_y$; ; the alternative path with minimum number of OTN switches used is selected.
        if (the path exists)**and**$(t_{s^*u^*}^{y} \geq 1)$ **then**
            $t_{s^*u^*}^{y}$=$t_{s^*u^*}^{y}$-1, update the list $\mathcal{L}_y$ and the graph $\mathcal{G}_{aux}$
        else
            the traffic demand $t_{s^*u^*}^{y}$ is deleted from the list $\mathcal{L}_y$
        end if
    end while
end for

number of OTN switches used is selected. If this operation is successfully, the graph and the variables are updated (line 17). The Phase-2 ends when both the lists $\mathcal{L}_y$ ($y \in \{DH, L\}$) are empty (line 14).

3.8 Numerical Results for the Less Complex Architecture

Next this section deals with some results obtained with the MOSR heuristic in the case of a larger metropolitan network illustrated in Fig. 3.8, that is composed by M=34 nodes and L=114 fibers each carrying W=48 wavelengths.

The case f_H=10 Gbs and f_L=1.25 Gbs is considered, leading to a choice of F=8. The nodes are equipped with 12×12 OTN switching nodes.

The blocking performance has been evaluated when the following static traffic model is used to generate the traffic matrices $\mathcal{T}^{DH} = [t_{sd}^{DH}]$ and $\mathcal{T}^{L} = [t_{sd}^{L}]$ that report the number of DH-ODUs and L-ODUs offered between each couple of nodes $s, v \in \mathcal{V}$.

The traffic model is characterized by the two parameters:

- $A_{o,sn}$ that is defined as the total offered bandwidth traffic demand normalized to the total network capacity; we have

$$A_{o,sn} = \frac{A_{0,s}}{C_{tot}}$$

  where $A_{o,s}$ is the total offered bandwidth traffic demand and C_{tot} is the total network capacity; because each wavelength is provided with a capacity equal to f_H we have C_{tot}=WLf_H.

- u defined as the L-ODU fraction of offered bandwidth traffic demand.

Given a value of $A_{o,sn}$, L-ODU and H-ODU connection requests are generated with probabilities

$$u_L = \frac{1}{1 + \frac{1-u}{uF}}$$

and u_{DH}=1-α_L respectively until the value of $A_{o,sn}$ is not exceeded. These requests are randomly assigned to any couple of network nodes $s, v \in \mathcal{V}$.

The network blocking performance in static traffic scenario are characterized with the performance index $P_{b,s}^{tot}$ denoting the rejected fraction of the offered bandwidth traffic demand.

Fig. 3.22 plots the performance index $P_{b,s}^{tot}$ as a function of u when $A_{o,sn}$=0.57 and the network is equipped with integrated OTN/WDM optical switches provided with a spatial speedup S=1.5. The number H of OTN switches per Input/Output Fiber (IF/OF) is varied from 1 to 6, where H=6 corresponds to the case in which all of wavelengths are equipped with OTN switches.

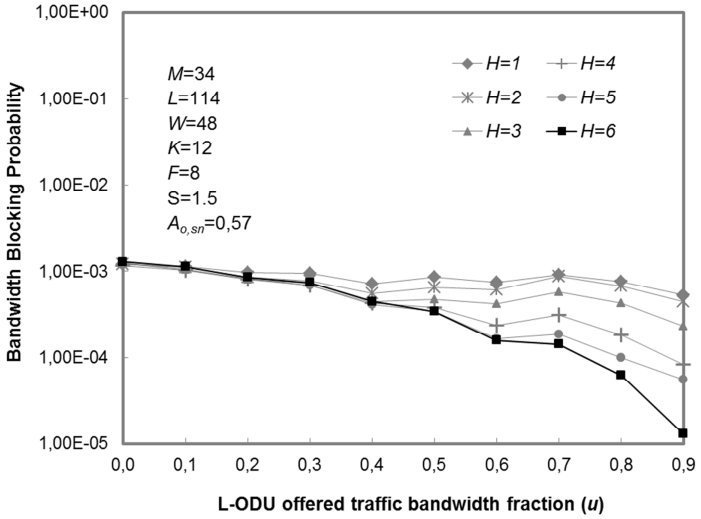

Figure 3.22: The rejected fraction of the offered bandwidth traffic demand ($P_{b,s}^{tot}$) is reported for the MOSR heuristic as a function of the L-ODU fraction u of offered bandwidth traffic demand and when $A_{o,sn}$=0.57.

u	n_{OTN}	α_{OTN}	n_{CP}	α_{CP}
0.1	228	83.3%	250	18.83%
0.2	456	66.7%	250	18.83%
0.3	456	66.7%	250	18.83%
0.4	684	50%	264	14.29%
0.5	912	33.3%	264	14.29%
0.6	1140	16.7%	306	0.64%

Table 3.3: Complexity indexes n_{OTN},α_{OTN},n_{CP} and α_{CP} as a function of the L-ODU fraction u of offered bandwidth traffic demand. The same parameter values of Fig. 3.22 are chosen and the space switch are realized with 144×144 crosspoints [2].

We can see from Fig. 3.22 that, increasing the value of u, the blocking probability $P_{b,s}^{tot}$ decreases due to the reduced granularity of the offered traffic bandwidth. For instance in the case H=6, we obtain values of $P_{b,s}^{tot}$ equal to $3.41 \cdot 10^{-4}$ and $1.29 \cdot 10^{-5}$ when the L-ODU fraction u of offered bandwidth

traffic demand equal to 0.5 and 0.9 respectively. Furthermore, increasing the value of u, we need to have an higher number of H and a greater space switch complexity as a consequence in order to guarantees the same performance of the case in which all of the wavelengths are provided with all of the OTN switches (H=6). For instance we need H=2 and H=3 OTN switches per IF/OF for u=0.3 and u=0.4 respectively in order to guarantee the minimum blocking probability of the case H=6.

To characterize the complexity reduction that the proposed architecture allows us to obtain with respect to the classical architecture using all of the OTN switches when the same bandwidth blocking probability $P_{b,s}^{tot}$ is guaranteed, in Table 3.3 for u varying from 0.1 to 0.6 the following indexes are reported:

- n_{OTN}, total number of OTN switches used;
- α_{OTN}, the percentage saving of OTN switches with respect to the case in which all of the OTN switches ate used (H=6);
- n_{CP}, total number of 144 × 144 crosspoints [2] needed to realize all of the space switches;
- α_{CP}, percentage saving of 144 × 144 crosspoints [2] with respect to the case H=6.

As a matter of example, in the case in which the L-ODU fraction u of offered bandwidth traffic demand is equal to 0.4, only half (H=3) of OTN switches per IF/OF can be used and saving of 50% and 14.29% of OTN switches and 144 × 144 crosspoints respectively are possible.

3.9 Further Analysis

In the previous sections, three-stages architecture for the OTN/WDM integrated switch are proposed and evaluated. In Fig. 3.23 [14, 81], in order to further reduce switch cost and power consumption, a new architecture with only two stages is proposed and the performance of the blocking switching fabric are investigated.

As said above, the architecture reported in Fig. 3.23, where N and W denote the number of Input/Output Lines (IL/OL) and the number of wavelengths supported per each IL/OL respectively, is composed by two stages.

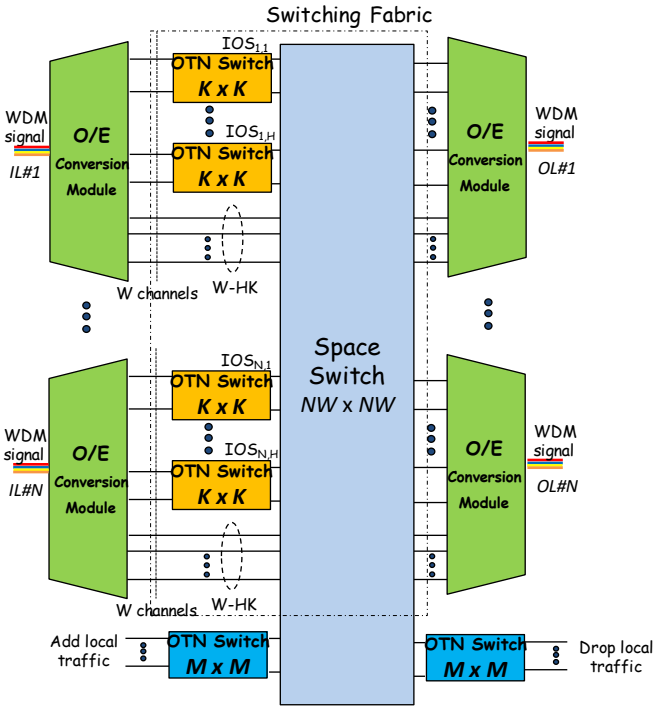

Figure 3.23: OTN/WDM Switching Architecture with low complexity switching fabric.

The first one performs both time and space switching by means of low capacity non-blocking OTN switches, each one of size K. Each IL is equipped with H OTN switches that perform time/space switching for the first HK input channels of the IL; OTN switches are not used for the $W - HK$ remaining input channels for which no time switching can be performed.

An OTN switch of size M is used to handle add/drop local traffic. The second stage of the OTN/WDM switch performs only space switching by means of an $(NW + M) \times (NW + M)$ non-blocking space switching fabric that connects inputs to outputs with high capacity switch links.

The OTN/WDM switching fabric can handle two type of flows. The first type of flow, referred to as Direct Flow (DF) carrying an high-order ODU, has to be switched without performing time switching. The second type of flow, referred to as Switched Flow (SF) is composed by up to maximum number F of sub-flows (SSF), carrying a low-order ODU. The SFs need of both time and space switching so that grooming can be performed and wavelength utilization efficiency is increased.

3.9.1 Numerical Results

The blocking performance of the 12-nodes RING and 13-nodes DENSE metropolitan networks, illustrated in Figs 3.24.a and 3.24.b respectively and assuming each wavelength channel carries ODU-2 at 10 Gbps, have been evaluated by simulation.

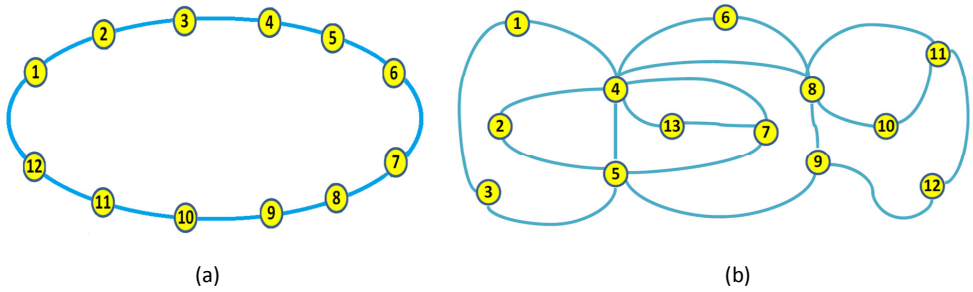

Figure 3.24: RING network (a) and DENSE network (b).

In these analysis, the networks are equipped with the integrated OTN/WDM switching nodes proposed in Section 3.9. To evaluate the performance degradation that the blocking switching fabric of the proposed solution introduces, the results are compared to the ones obtained when non blocking switching fabric are taken into account. Two typologies of flows are offered to the network nodes: flows carrying ODU-2 (10 Gbps) and subflows carrying ODU-0 (1.25 Gbps).

According to the OTN standard, up to F=8 ODU-0 can be carried on an ODU-2. In this case, the traffic is assumed to be uniformly distributed among all node pairs; both the request inter-arrival time and the connection duration are exponentially distributed. Let α the average bandwidth percentage of ODU-0 offered. The average offered bandwidth traffic intensity normalized to the network capacity is given by

$$A_0 = \frac{\Lambda}{FWL} \sum_{sd} h_{sd}$$

, where L is the number of bidirectional fiber links, W is the number of wavelength channels, Λ is the offered bandwidth traffic between two any nodes and h_{sd} is the hop count of the shortest path between the nodes s,d.

In this analysis, the important assumption is that the routing of any connection carrying ODU-0 (ODU-2) between the nodes s and d is performed according to the following steps:

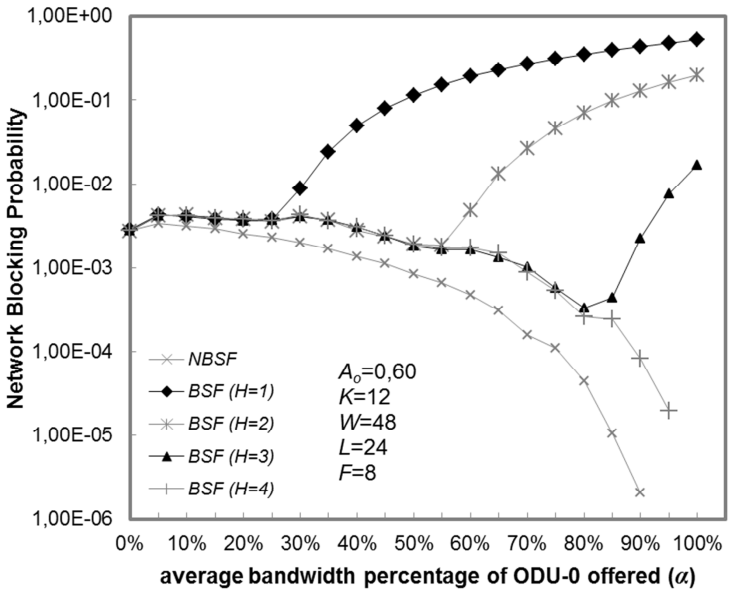

Figure 3.25: Network blocking probability versus the average bandwidth percentage of ODU-0 offered in the case of RING network, in the case of nodes equipped with Non Blocking Switching Fabric (NBSF) and the Blocking Switching Fabric (BSF) of Fig. 3.23 and H varying from 1 to 4.

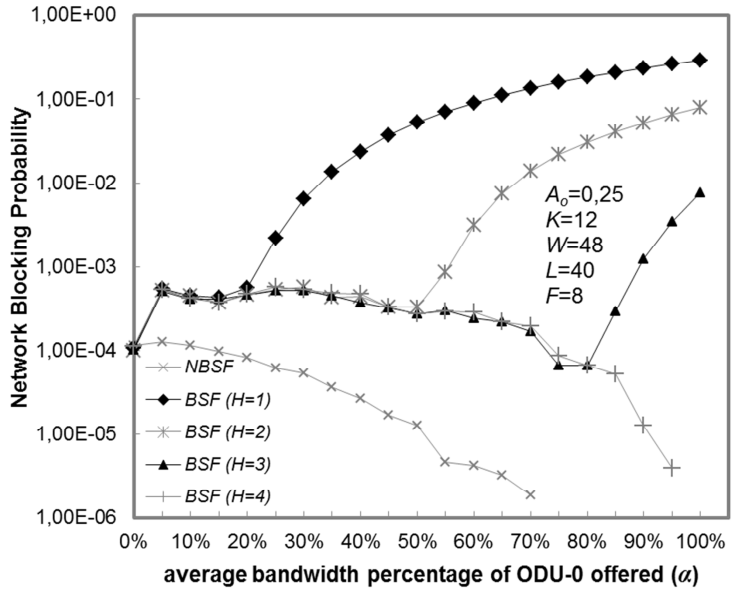

Figure 3.26: Network blocking probability versus the average bandwidth percentage of ODU-0 offered in the case of DENSE network, in the case of nodes equipped with Non Blocking Switching Fabric (NBSF) and the Blocking Switching Fabric (BSF) of Fig. 3.23 and H varying from 1 to 4.

i) the shortest path between the nodes s and d is chosen;

ii) an auxiliary graph is built having nodes representing OTN switches and fictitious nodes representing the wavelength bundle in which OTN switches are absent;

iii) two any graph nodes are connected if free resources (high capacity switch link and wavelengths) are available to carry ODU-0 (ODU-2) between the OTN switches/wavelength bundles representing the nodes;

iv) weights are assigned to the graph edge so that the routing of ODU-2 is performed by using preferably wavelengths in which OTN switches are absent and the routing of ODU-0 is performed by using preferably high capacity switch links and wavelengths already carrying other ODU-0's;

v) a new shortest path is evaluated in the auxiliary graph between the nodes representing the add and drop OTN switches of the nodes s and d respectively; if any shortest path exists, the connection is routed choosing at random free resources (wavelength and ODU container) through the OTN switches and the wavelength bundles corresponding to the nodes of the evaluated path, otherwise the connection request is rejected.

Figs 3.25 and 3.26 plot the network blocking probability as a function of α in the case of the RING and DENSE metropolitan networks having a number L of unidirectional fiber links equal to 24 and 40 respectively. Each link carries W=48 wavelengths and A_0 is equal to 0.60 and 0.25 for the RING and DENSE networks. In these figure, the blocking probability in the case of an integrated OTN/WDM optical switch with Blocking Switching Fabric (BSF) characterized by the use of available market OTN switches of size K=12 are reported. The number H of OTN switches is varied from 1 to 4 where H=4 corresponds to the case in which all of the wavelengths are equipped with OTN switches. It is also plotted the blocking probability obtained in the case in which Non Blocking Switching Fabrics (NBSF) are used. From Figs 3.25 and 3.26 we can observe that in the case H=4 the degradation in blocking probability due to the use of blocking switching fabrics is higher in the case of DENSE networks. This is due to its higher average network degree that leads to a lower average available number of high capacity switch links ongoing an OTN switch per Output Line [14] and consequently a higher blocking. We can notice from figs 3.25 and 3.26 that a correct dimensioning procedure can

lead to a reduction of OTN switches. As a matter of example we can use in the case of DENSE network only half (H=2) of the OTN switches per node when the average bandwidth percentage α of ODU-0 offered is smaller than or equal to 50%.

3.10 CONCLUSIONS

In Section 3.1. an integrated OTN/WDM switching architecture provided with spatial speedup has been studied and its complexity has been evaluated in terms of number of OTN switches and space switching modules used. The ILP formulation of the Switch Resource Assignment and Routing Problem allowed us to verify the effectiveness of an heuristic, referred to as Maximizing Shortest Path Traffic that it is used to evaluate the network blocking performance of large networks in static traffic scenario when ODU-2 and ODU-0 traffic is considered. The obtained results have shown that in these traffic conditions the use of spatial speedup is not needed because the basic switch without speedup allows for the same network blocking performance obtained with Strict Sense Non Blocking switches.

A simulation analysis has been carried out to evaluate the blocking probability of different metropolitan networks in dynamic traffic condition. In this case a remarkable performance degradation can occur. For example, in a network with 13 nodes and 40 fibers, equipped with W=48 wavelengths, and the normalized offered bandwidth traffic intensity is 0.091 the network blocking probability is equal to $1.80 \cdot 10^{-4}$ and $1.44 \cdot 10^{-6}$ in the case of basic and NBSS switches respectively. The results reported in Section 3.4 show that this performance degradation due to the switch internal blocking however can be overcome with the use of spatial speedup equal to 1.5 that consequently increases the hardware complexity of the proposed switch, but allowing for a high complexity reduction with respect to the case of Strict Sense Non Blocking switch.

Furthermore, Section 3.5 deals with an integrated OTN/WDM switching architecture with a reduced number of OTN switches. Then an heuristic, referred to as Minimizing OTN Switch Resource (MOSR), has been introduced to evaluate the network blocking performance in static traffic scenario. The results obtained in a 34-nodes metropolitan network show that when the L-ODU fraction of offered traffic bandwidth demand is equal to 0.4, it is possible to save the 50% and 15% of OTN switches and 144 $\times$ 144 crosspoints with

respect to the case in which all of the OTN switches are used.

Chapter 4

Xhaul Architecture in C-RAN Environment

4.1 Introduction

Cloud Radio Access Network (C-RAN) or Centralized RAN could be considered one of the most promising solutions for its efficiency and flexibility [4, 5]. Based on the idea to physically separate the traditional base station in the two different entities Base Band Unit (BBU) and Remote Radio Unit (RRU), C-RAN leads to important advantages, as energy saving, Total Cost of Ownership (TCO) saving, improving security and deployment of infrastructure ready to support advanced features, like Coordinated Multi-Point (CoMP), enhanced inter-cell interference coordination (eICIC), carrier aggregation and more complex and dynamic multiple-input multiple-output (MIMO) schemes [6, 7].

The access network is represented by the "fronthaul" that connects the BBUs with the RRUs. The most used standard to encapsulate radio samples is the Common Public Radio Interface (CPRI), that needs much bandwidth to carry the CPRI flows that have a bit rate up to ten times higher than the total capacity of a traditional base station. It is clear that the network architecture, both access and transport, and its control need to be rethought.

An emerging network paradigm, labeled as "Xhaul" [13], wraps fronthaul and backhaul in a common connectivity segment providing a joint optimization opportunity, especially in sharing transport resources for different purposes and protocols. Xhaul unifies and enhances the traditional backhaul and fronthaul areas by enabling a flexible deployment and reconfiguration of

network elements and networking functions. The role of the Xhaul transport network is to convey Ethernet traffic and CPRI traffic on the same network infrastructure.

In this chapter, a network solution in which the radio component is composed by RRU and traditional Radio Base Station (RBS) has been analyzed. The conducted study shows that the solution in which only RRUs are used are not cost effectiveness because the low power consumption achieved with the switching off of the centralized components does not compensate the high bandwidth consumption. Conversely the use of only RBSs would lead to bandwidth efficient solutions but very poor in terms of power consumption.

In the next sections, the main contributions of the analysis [15] are explained and, in particular, they could be summarized in the following way:

i) the definition of analytical models, validated by simulation, for the resource dimensioning of the Xhaul network;

ii) the evaluation of power/bandwidth trade-off solutions based on the optimal determination of the percentage of RRUs to be used in order to minimize the sum of the bandwidth and power costs.

Furthermore, several traffic models characterizing the statistical of the peak traffic values [3] are introduced. According to these traffic models, a dimensioning procedure is illustrated allowing significantly lower number of CPRI circuits as well as the number of BBUs needed, with respect to the case in which that number is statically fixed to the number of installed RRUs. This study aims at quantifying the potential advantages in terms of bandwidth and energy saving obtainable via:

i) an activation/deactivation policy of BBUs associated to the sub-areas;

ii) a full sharing of transport capacity in the Xhaul network.

The reference scenario considered in the reported analysis is reported in Section 4.2.

In the rest of chapter, two different solutions are considered and analyzed. The first reported solution is based on the use of a reconfigurable fronthaul network (only CPRI solution) that owing to statistical multiplexing advantages allows for bandwidth savings in order to balance the advantages in power saving and the remarkable bandwidth consumption. The proposed solution has been investigated with the introduction of an analytical model allowing

for the dimensioning of the needed CPRI flows and consequently the evaluation of the bandwidth and power consumptions. Then the main results for forecast 5G network areas are illustrated in Section 4.5.2.

To the other hand, a solution for a reconfigurable Xhaul network is also proposed and investigated. The cost evaluation model is reported in Section 4.3 and the dimensioning analytical models are reported in Section 4.4. In particular, the description of the traffic modeling, the network dimensioning procedure and the resource modeling are reported in Sections 4.4.1 and 4.4.2 for the CPRI and GEth flows respectively. The main results for 4G and forecast 5G network areas are illustrated in Section 4.5.

Finally conclusions and future research items are illustrated in Section 4.6.

4.2 Proposed Xhaul Architecture

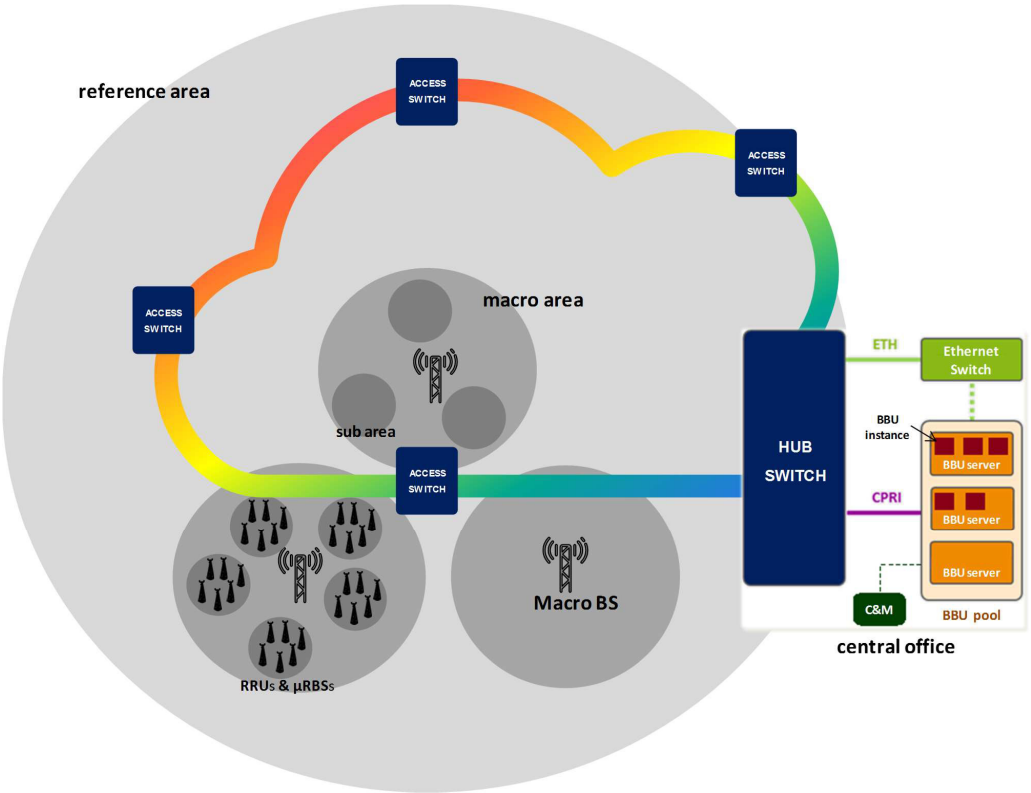

Figure 4.1: Xhaul Network Architecture

This section deals with the Xhaul architecture [15] reported in Fig. 4.1. As said in the introduction, the Xhaul architecture unifies the traditional backhaul and fronthaul areas by enabling a flexible deployment and recon-

Parameter	Description
B_{CPRI}	bandwidth required by one CPRI flow
K^{BBU}	maximum number of BBU instances supported in any BBU server
C^{RRU}	capacity of an RRU
C^{RBS}	capacity of a micro RBS
n_{RRU}	number of RRUs installed in a sub-area
n_{RBS}	number of micro RBSs installed in a sub-area
T	number of sub-areas handled by an AS
$n^{AS}_{RRU} = Tn_{RRU}$	number of RRUs installed in the region handled by the AS
$n^{AS}_{RBS} = Tn_{RBS}$	number of micro RBSs installed in the region handled by the AS

Table 4.1: Network parameters in Xhaul reference architecture

figuration of networks elements and networking functions, providing a joint optimization opportunity, especially between transport resources and energy consumption. It handles a reference area divided in macro areas, each one covered by macro base station (macro BS). Each macro area is divided into sub-areas, each one covered by a certain number of RRUs and traditional micro base stations (micro RBSs). A reference area is handled by a Central Office (CO) that contains a certain number of BBU servers managed by a Control and Management ("C&M") module. The "C&M" has the role of activating/deactivating/migrating BBU instances in the BBU servers with each BBU instance related to an active RRU, and moreover of implementing algorithms for the consolidation of BBU instances that lead to save energy. In the CO, Ethernet switch is also located to handle the Ethernet traffic generated by the micro RBSs.

Central office and radio stations (RRU and micro RBS) are connected to the BBUs by a reconfigurable transport network though some Access Switch (AS) and one HUB switch a shown in Fig. 4.1. Thus the Xhaul network has two levels:

- the first one, defined as "access network", connects the several RRUs and micro RBSs with the closest element of aggregation, referred to as Access Switch (AS);

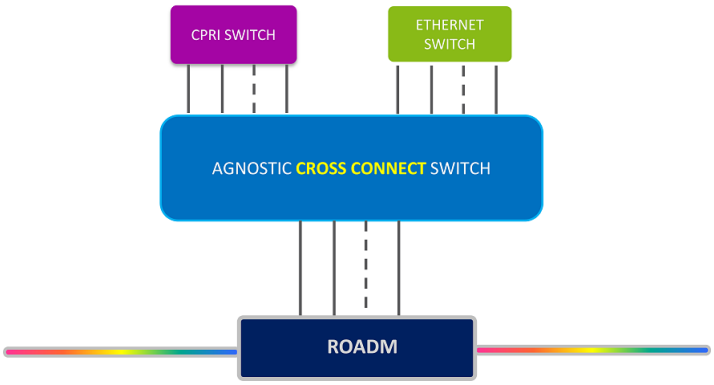

Figure 4.2: Access Switch Architecture

- the second one, defined as "reconfigurable network", connects the Access Nodes with the HUB switch placed in the Central Office.

The network reconfiguration allows for a bandwidth saving and this may occur on a hourly basis according to the traffic variations. The reconfiguration capability of ASs and the HUB switch provides a flexible allocation of the bandwidth and server resources to the RRUs and micro RBSs. Efficient implementations of reconfigurable networks consider solutions that combines DWDM and OTN, whose benefits are largely studied in several works [54, 56, 57, 58, 59, 71, 86, 87, 79], enabling hybrid transport of CPRI and Ethernet flows.

Example of AS and HUB switch architectures are reported in Figs 4.2 and 4.3 respectively. The AS is composed by a Reconfigurable Optical Add Drop Multiplexer (ROADM), an agnostic cross connect switch, the CPRI and Ethernet Switches. In particular the agnostic cross connect is inserted for scalability reasons and only allows for the spatial switching of CPRI and Ethernet aggregated flows. The flows generated by the RRU (micro RBS) are handled by the CPRI (Ethernet) switch, and forwarded towards the CO by appropriately configuring the agnostic cross connect switch and the ROADM. The HUB switch, as described in Fig. 4.3, is composed by an agnostic cross connect switch and by CPRI and Ethernet switches. Each input/output WDM interface of the agnostic cross connect switch is connected to a ROADM ring. The CPRI switch is connected to the BBU server pools.

An integrated OTN/WDM architecture could be used to implement the agnostic cross connect switches presented in the previous solutions, in order to manage the different kind of traffic in a large flexible way, guaranteeing the same performances as ROADM. [14, 80, 81, 82, 85, 83, 88].

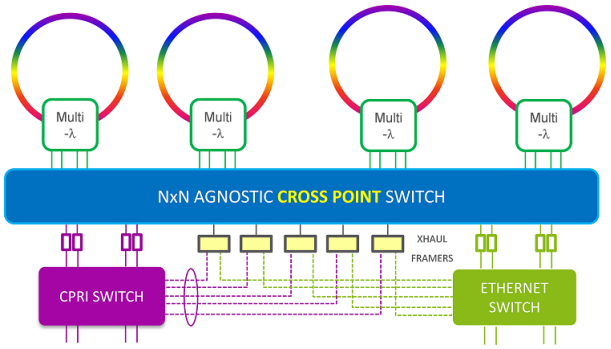

Figure 4.3: HUB Switch Architecture

The advantages of the proposed Xhaul architecture are threefold:

i) the use of an aggregation segment allows for the transport bandwidth sharing among RRUs and micro RBSs connected to the same AS that leads to a bandwidth saving if suited dimensioning procedures are applied;

ii) the Xhaul network is reconfigurable with the possibility of bandwidth saving in low traffic periods;

iii) the Xhaul network supports hybrid solution in which both CPRI and Ethernet technologies are employed in the access network with the possibility to optimize the total cost of bandwidth and power consumption.

In table 4.1, the network parameters of the Xhaul network architecture are summarized. In particular, B_{CPRI} is the bandwidth required by one CPRI flow, K^{BBU} is the maximum number of BBU instances supported in any server, C_{RRU} and C_{RBS} are the capacity of any RRU and any micro RBS, n_{RRU} and n_{RBS} are the number of RRUs and micro RBSs installed in a sub-area, n^{AS}_{RRU} and n^{AS}_{RBS} are the number of RRUs and micro RBSs in the region handled by the AS, that are related to the number T of sub-areas connected to a AS.

It is important to note that, for every different solutions, their effects on network complexity and costs should be evaluated and analyzed. Moreover an optimal dimensioning of access and aggregation networks is required. If we consider greater access networks, the number of RRUs and the length of the connections with these could lead to increase very quickly the complexity of the RSs.

Parameter	Description
C_{tot}^{avg}	average total cost during the cycle-stationary period
C_k^{BW}	bandwidth cost in the k-th stationary interval
C_k^{PWR}	power cost in the k-th stationary interval
μ_{BW}	cost per consumed bandwidth unit
$nc_{AS,CPRI}^k$	number of CPRI circuits needed between any AS and the CO in the k-th interval
$nc_{AS,GE}^k$	number of GEth circuits needed between any AS and the CO in the k-th interval
μ_{PWR}	cost per consumed power unit
P_{tot}^k	total power consumption in the k-th interval
P_{radio}	radio component of power consumption
P_k^{BBU}	baseband processing component of power consumption in the k-th interval
P_{RBS}	power consumption of a micro RBS
P_{RRU}	power consumption of an RRU
P_{server}	fixed power consumption associated to each server
P_{ins}^{BBU}	power consumption associated with one BBU instance

Table 4.2: Parameters related to the cost model

4.3 Cost Evaluation

An analytical model is introduced [15] in order to evaluate the total cost of the Xhaul solution as a function of the network and traffic parameters. The main components of the costs considered are:

i) the bandwidth consumption expressed in terms of CPRI and GEthernet circuits needed between any AS and the CO;

ii) the power consumption of both radio stations and servers.

In Table 4.2, the main parameters characterizing the cost model are reported. An important assumption is the cycle-stationary traffic scenario with N denoting the number of stationary intervals. As said in the Introduction, one of the objectives is to evaluate the average total cost defined by the following expression:

$$C_{tot}^{avg} = \frac{1}{TN} \sum_{k=0}^{N-1} (C_k^{BW} + C_k^{PWR}) \tag{4.1}$$

where C_k^{BW} and C_k^{PWR} denote the bandwidth and power consumption cost in the $k-th$ $(k = 0, \cdots, N-1)$ stationary interval. As you can notice from (4.1), the cost contribution due to MBS is not taken into account. This is due to the fact that this contribution has no significance impact on the cost optimization procedure that is carried out later.

For the contribution C_k^{BW} we can simply write:

$$C_k^{BW} = \mu_{BW}(nc_{AS,GE}^k + nc_{AS,CPRI}^k \cdot B_{CPRI}) \tag{4.2}$$

wherein μ_{BW} is the cost per consumed bandwidth unit, $nc_{AS,GE}^k$ and $nc_{AS,CPRI}^k$ are the number of GEth flows (that hold 1 Gbps traffic) and CPRI flows between any AS and the CO needed in the k-th interval respectively, B_{CPRI} is the bandwidth required (in Gbps) by one CPRI flow.

The second contribution C_k^{PWR} can be simply expressed as follows:

$$C_k^{PWR} = \mu_{PWR} P_k^{tot} \tag{4.3}$$

wherein μ_{PWR} is the cost per consumed power unit and P_k^{tot} is the total power consumption in the k-th stationary interval.

The total power consumption is evaluated considering the sum of several contributions, related to the radio and baseband processing components P_{radio} and P_k^{BBU} respectively. We can write:

$$P_k^{tot} = P_{radio} + P_k^{BBU} \tag{4.4}$$

For the radio component P_{radio}, the power consumption is assumed to be independent of the handled traffic according to the today's technology. Let us denote with P_{RBS} and P_{RRU} the power consumption of micro RBS and RRUs respectively. Thus we can simply write:

$$P_{radio} = P_{RBS} \cdot n_{RBS}^{AS} + P_{RRU} \cdot n_{RRU}^{AS} \tag{4.5}$$

wherein n_{RBS}^{AS} and n_{RRU}^{AS} are the parameters introduced in Section 4.2 and denoting the number of micro RBSs and RRUs handled by any AS respectively.

The second contribution P_k^{BBU} can be defined as the sum of a fixed contribution for the server rack (power supply, conditioned air, etc.) and a variable contribution related to the BBU instance processing. The fixed contribution is related to both the used number of servers and the fixed power consumption associated to each server (P_{server}), whereas the variable one is related to the number of BBU instances (equal to the number of needed CPRI flows) and the power consumption associated with one BBU instance (P_{ins}^{BBU}). In this analysis, the variable component of the power consumption is assumed to be a linear function of the processing capacity. Hence, the power consumption P_k^{BBU} related to the baseband processing can be expressed as follows:

$$P_k^{BBU} = P_{server} \cdot \left\lceil \frac{nc_{AS,CPRI}^k}{K_{BBU}} \right\rceil + P_{ins}^{BBU} \cdot nc_{AS,CPRI}^k \tag{4.6}$$

wherein K_{BBU} is the maximum number of BBU instances supported in any server.

Finally by inserting (4.5) and (4.6) in (4.4), (4.4) in (4.3), (4.2) and (4.3) in (4.1) we can achieve the average total cost C_{tot}^{avg}.

You can notice how the knowledge of $nc_{AS,GE}^k$ and $nc_{AS,CPRI}^k$ is needed for the evaluation of C_{tot}^{avg}. These parameters characterize the number of GEthernet and CPRI circuits needed between any AS and the CO and are determined according to a dimensioning procedure illustrated in the next Section 4.4.

4.4 Analytical Models for Resource Dimensioning in Xhaul Architecture

This section introduces the resource dimensioning models for the case in which the operation mode of the Xhaul architecture is the following:

- the installed micro RBSs are always turned on and provide a basic capacity for the coverage of the sub-area;
- the installed RRUs are always turned on and provides additional capacity needed in the intervals in which the traffic increases; the RRUs are only used when the basic capacity provides by the micro RBSs is not sufficient to support the user traffic; for this reason BBU instances are only instanced for the corresponding RRUs used; a server consolidation

algorithm is applied in order to minimize, in each stationary interval, the number of switched on servers.

The introduced analytical models allow us to evaluate the number $nc^k_{AS,GE}$ and $nc^k_{AS,CPRI}$ of GEthernet and CPRI circuits respectively needed between any AS and the CO. The number $nc^k_{AS,GE}$ and $nc^k_{AS,CPRI}$ are important to make the network planning of the access network in each hour interval that gives informations for dimensioning the transport network. The evaluation of the number of needed circuits is based on the following traffic assumptions:

- the traffic is cycle-stationary with N stationary periods; for instance N equals 24 when the classical daily traffic variation has to be reproduced;
- the user peak traffic generated in the sub-areas, expressed in Gbps, are independent and identically distributed (i.i.d.) variables; therefore the user peak traffic generated in any sub-area in the k-th stationary interval is characterized by a variable A^k that according to [89] we assume log-normal distributed of parameters (μ^k, σ^k);

Next the number $nc^k_{AS,GE}$ and $nc^k_{AS,CPRI}$ of GEthernet and CPRI circuits are evaluated in Subsections 4.4.1 and 4.4.2 respectively.

4.4.1 Evaluation of the number $nc^k_{AS,CPRI}$ of CPRI circuits

The decrease in offered traffic and the application of the switching off technique of BBU instances leads to the need of carrying a number of CPRI flows lower the number of installed RRUs.

To evaluate the values $nc^k_{AS,CPRI}$ $(k = 0, 1, ..., N-1)$, we could start by the knowledge of the statistical on the number N^k_{AS} $(k = 0, 1, ..., N-1)$, denoting the sum of used RRUs in the region handled by the AS in the k-th interval. In Appendix A.3.1, it is shown how it is possible to evaluate the probabilities $p_{N^k_{AS}}(j)$ $(j = 0, 1, ..., T \cdot n_{RRU})$ of the random variable N^k_{AS}. Hence the dimensioning of the number $nc^k_{AS,CPRI}$ of CPRI circuits between the AS and and CO in the k-th interval is performed by guaranteeing high the probability of the event that a number of used RRUs is lower than or equal to $nc^k_{AS,CPRI}$. In other words, $nc^k_{AS,CPRI}$ has been chosen as the α-th percentile of N^k_{AS} $(k = 0, 1, ..., N-1)$ that is the smallest value for which the following expression holds:

$$Pr(N_{AS}^{k} \leq nc_{AS,CPRI}^{k}) \geq 0.01 \cdot \alpha \quad (k = 0, 1, ..., N-1) \tag{4.7}$$

We can equivalently write (4.7) in terms of survivor function of N_{AS}^{k} as follows:

$$Pr(N_{AS}^{k} > nc_{AS,CPRI}^{k}) < 1 - 0.01 \cdot \alpha \quad (k = 0, 1, ..., N-1) \tag{4.8}$$

4.4.2 Evaluation of the number $nc_{AS,GE}^{k}$ of GEthernet circuits

In Appendix A.3.2, it is shown how it is possible to evaluate the statistical of the number $N_{AS,E}^{k}$ $(k = 0, 1, ..., N-1)$ of GEthernet flows to be carried between the AS and and CO. In particular we are able to evaluate the probabilities of $N_{AS,E}^{k}$ denoted as $p_{N_{AS,E}^{k}}(j)$ $(j = 0, 1, \cdots, \lceil T \cdot n_{RBS} \cdot C_{RBS} \rceil)$. As in the case of dimensioning of CPRI circuits, $nc_{AS,GE}^{k}$ has been chosen as the α-th of $N_{AS,E}^{k}$ $(k = 0, 1, ..., N-1)$ that is the smallest value for which the following expression holds:

$$Pr(N_{AS,E}^{k} > nc_{AS,GE}^{k}) < 1 - 0.01 \cdot \alpha \quad (k = 0, 1, ...N-1) \tag{4.9}$$

4.5 Numerical Results

The objective of this study is not only to evaluate the advantages in terms of CPRI flow bandwidth consumption saving that a reconfigurable optical network allows us to achieve when strategies for the BBU instance switching off are applied, but also to evaluate a trade-off between employment of RRUs and micro RBSs with regard to the energy and bandwidth consumption.

As depicted in Fig. 4.4, the reference scenario is an area of 1 km^2 handled by a central office that contains a certain number of BBU servers. We assume that the area is divided into squared sub-areas, where in each of them there is a building surrounded by streets and squares. Each sub-area is covered with a given number of RRUs and micro RBSs, that generate CPRI and GEthernet flows respectively.

This scenario assumption is suited to model a broadband access in dense urban areas [3]. In fact, the proposed study considers a dense outdoor area (streets, square) and an indoor ultra-high broadband access area, related to a

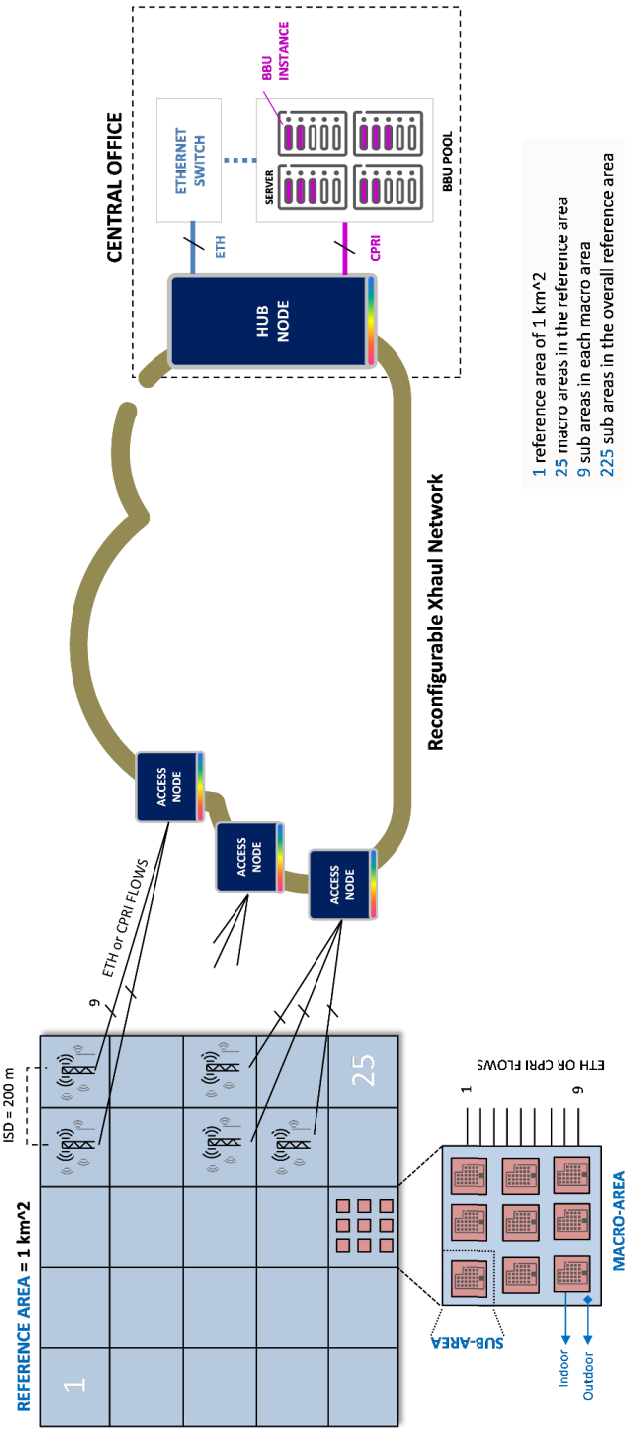

Figure 4.4: Reference Scenario for the Performance Evaluation

certain number of buildings positioned in that area. According to this model, 225 buildings are present in the reference area, each building having a floor surface of $1,600m^2$. The indoor area is $360,800\ m^2$, it means $\cong 36\%$ of the reference area. The remaining 64% is assumed as outdoor area.

One of the assumptions is that the traffic offered to each sub-area is cycle-stationary with N=24 stationary intervals modeling the daily traffic trend. The peak traffic offered to any sub-area is distributed according to a log-normal distribution [89] of parameters (μ^k, σ^k) for the k-th stationary interval. The trend of the average peak traffic versus the daily hours is assumed to be equal to the one measured for the City of London [90]. The trend normalized to the average peak traffic during the Peak Hour Interval (PHI) is reported in Fig. 4.5. The average peak traffic during the PHI is chosen to be equal to 0.52 Gbps and 26.16 Gbps that are typical values expected in 4G and 5G traffic scenarios [3] for each sub-area respectively. Finally the parameters μ^k and σ^k of the log-normal distribution are chosen so as to guarantee for the distribution matching of both the forecast average peak traffic and a typical standard deviation equal to 0.25 [89].

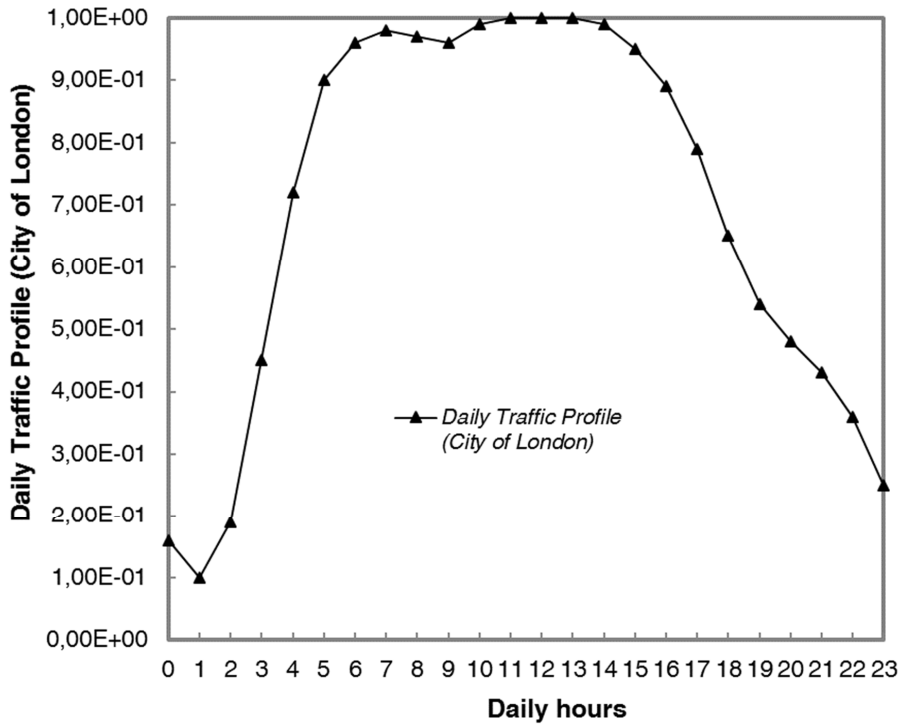

Figure 4.5: Daily Traffic Profile

To support the user traffic, the number n_{RRU} and n_{RBS} of RRUs and micro

RBSs installed in each sub-area are dimensioned according to the procedure illustrated in Appendix A.3.3. It is denoted with γ the ratio of the number n_{RRU} of RRUs to the total number $n_{RRU} + n_{RBS}$ of radio stations, that is:

$$\gamma = \frac{n_{RRU}}{n_{RBS} + n_{RRU}} \tag{4.10}$$

Next Sections 4.5.1 and 4.5.2 deal with the network resource dimensioning and bandwidth/power costs in the case of the reconfigurable fronthaul architecture in 5G scenario, in which only CPRI flows are carried. For the Xhaul architecture, some network resource dimensioning results are in Section 4.5.3 while bandwidth/power trade-off solutions will be investigated in Section 4.5.4.

4.5.1 Network Dimensioning in Fronthaul Architecture

In a fronthaul architecture, a traditional C-RAN solution is implemented, thus only RRUs are installed in the sub-areas. In this case, we can consider the same analytical models presented in the previous sections and a value of γ equal to 0.

For a 5G scenario, it is assumed that an LTE bandwidth equal to 20 MHz and MIMO $8x8$ are assigned to each station. RRUs are characterized by a capacity of C_{RRU}=600 $Mbps$. Each RRU generates one CPRI flow @10$Gbps$ [11]. If the dimensioning of RRUs is performed so as to guarantee the α=99.99th percentile of the user peak traffic offered to the sub-area, we achieve the values $n_{RRU} = 107$.

If RRU switching off strategies were not applied, it would be needed to guarantee a number of CPRI circuits equal to the number n_{AS}^{CPRI} of hardware elements generating CPRI traffic and tied to the AS. The values of n_{AS}^{CPRI} is equal to n_{RRU}^{AS} that is given by T times the value of n_{RRU}. In this case we achieve a value of 3375 for n_{AS}^{CPRI}. Conversely a remarkable reduction in CPRI circuits is possible to achieve if switching off algorithms are adopted.

In Appendix-A.3.1 the survivor function of the variable N_{AS}^{k} has been evaluated for each stationary interval and by applying the procedure mentioned in Section 4.3, the number of CPRI circuits to be supported between the Access Switch and the CO. It has verified that the application of the dimensioning procedure allows for a remarkable saving with respect to the case in which the dimensioning is performed on the number RRUs installed. For instance the percentage advantage in terms of CPRI circuits in the Peak Hour Interval

is in the order of 30%.

4.5.2 Bandwidth and Power Consumption Costs in Fronthaul Architecture

In Fig. 4.6 the average bandwidth consumption B^{avg}, expressed by Eq. 4.2, is reported as a function of the number T of sub-areas. The study considers the cases in which the number of CPRI flows is dimensioned for values of α in Eq. (4.7) equal to $1-10^{-3}$, $1-10^{-5}$, $1-10^{-7}$ and $1-10^{-9}$.

We can notice from Fig. 4.6 how the bandwidth decrease how the number T of sub-areas handled by any AS is increased. This is due to the high statistical multiplexing gain. Furthermore owing to the central limit theorem, the bandwidth and the power consumption tend to deterministic values for T tending to infinity and for this reason the decrease of the bandwidth reduces for values of T increasing and tends to an asymptotic value. The bandwidth saving percentage is expressed versus the number T of sub-areas in Fig. 4.7. We can notice remarkable bandwidth saving that varies from 45% to 70%. For instance in the case $\alpha = 1-10^{-5}$ and T=75 we achieve a percentage bandwidth saving in the order of 66%.

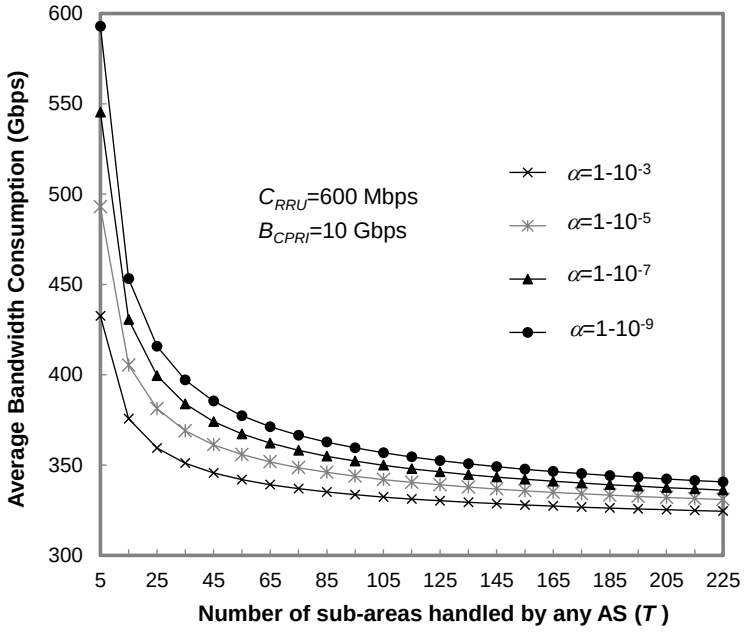

Figure 4.6: Average bandwidth consumption B^{avg} as a function of the number T of sub-area handled by any Access Switch.

Next some results on the average power consumption P^{avg} expressed by

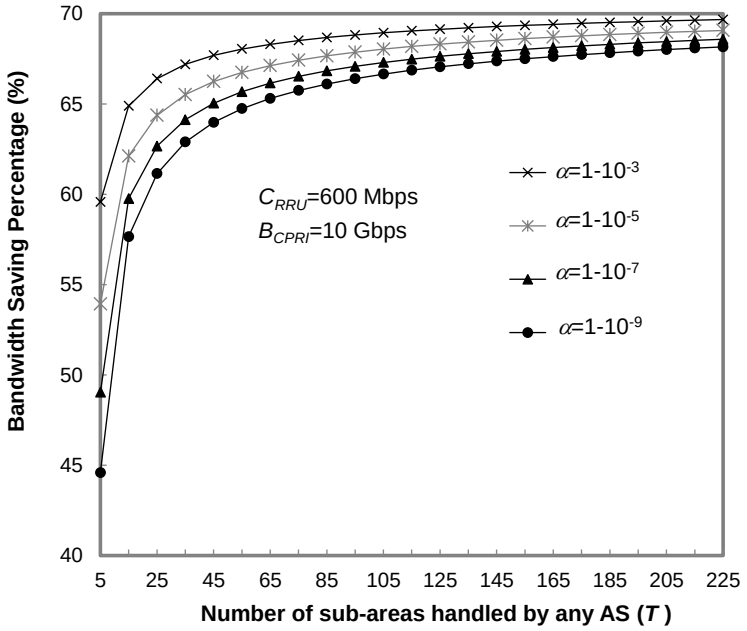

Figure 4.7: Bandwidth saving percentage as a function of the number T of sub-area handled by any Access Switch.

Eq. (4.3) are reported. The results are evaluated by considering the model reported in Section 4.3 and a total power consumption $P_{RRU,BBU}$ of a CPRI network element equal to the constant value 300 Watt. $P_{RRU,BBU}$ is expressed by:

$$P_{RRU,BBU} = P_{RRU} + P_{server}/K_{BBU} + P_{ins}^{BBU} \tag{4.11}$$

The value of K_{BBU} is chosen equal to 4 while the constant server power P_{server} is fixed equal to 30% of the maximum server power. Furthermore it is denoted with δ the ratio of the radio power consumption P_{RRU} to the total power consumption $P_{RRU,BBU}$. It is important to note that the RRU is always on, thus only the baseband processing component gives a variable contribution to the total power consumption.

The average power consumption P^{avg}, expressed by Eq. (4.3) is reported in Fig. 4.8 as a function of the number T of sub-area and varying the ratio δ of constant radio power consumption from 0.2 to 0.8. Even in this case we can notice how the statistical multiplexing effect, due to processing resource sharing of the BBU instances, leads to a decrease in power consumption for T increasing. Furthermore we notice how the power consumption is as much higher as the value of the radio power consumption P_{RRU}. As a matter of example, for T=45 we achieve values of P^{avg} equal to 154W and 279W for

$\delta = 0.2$ and $\delta = 0.8$ respectively. The reason of this effect is due to lower advantage in statistical multiplexing due to the increase in power consumption of the radio resources that are not shared.

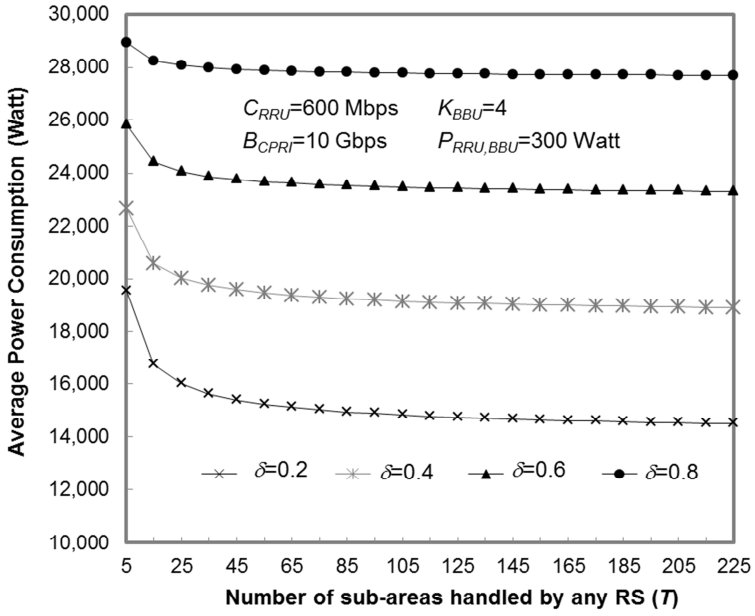

Figure 4.8: Average power consumption P^{avg} as a function of the number T of sub-area handled by any Access Switch. The ratio δ of the radio power consumption P_{RRU} to the total power consumption $P_{RRU,BBU}$ of an RRU is chosen equal to 0.2, 0.4, 0.6 and 0.8.

4.5.3 Network Dimensioning in Xhaul Architecture

Next some dimensioning results for the Xhaul architecture are reported in the case of a AS handling the traffic of T=45 sub-areas. Both 4G and 5G traffic scenario will be considered in order to show the very high differences between these two scenarios and the goodness of our approach in both of them.

In the 4G scenario case, the considered assumption is that an LTE bandwidth equal to 20 MHz and MIMO $2x2$ are assigned to each station. RRUs are characterized by a capacity of C_{RRU}=150 $Mbps$. Each RRU generates one CPRI flow @2.5$Gbps$ [11]. Micro RBSs are also employed with capacity of $C_{RBS} = 150$ $Mbps$. The ratio γ of the number of RRUs to the total number of radio stations is chosen equal to 0.7. If the dimensioning of RRUs and micro RBSs is performed so as to guarantee the α=99.99th percentile of the

	4G	**5G**
n_{RRU}	7	75
n_{RBS}	2	32

Table 4.3: Dimensioning values n_{RRU} and n_{RBS} of installed RRUs and micro RBSs per sub area in 4G and 5G traffic scenarios

user peak traffic offered to the sub-area, we achieve the values n_{RRU} and n_{RBS} reported in the first column of Table 4.3.

If RRU switching off strategies were not applied, it would be needed to guarantee a number of CPRI circuits equal to the number n_{AS}^{CPRI} of hardware elements generating CPRI traffic and tied to the AS. The values of n_{AS}^{CPRI} is equal to n_{RRU}^{AS} that is given by T times the value of n_{RRU}. In this case of 4G traffic scenario, we achieve a value of 351 for n_{AS}^{CPRI}.

Conversely a remarkable reduction in CPRI circuits is possible to achieve if switching off algorithms are adopted. Based on a traffic profile and an expected traffic demand, the switching off algorithm leads to do a network planning of the active elements in each hour interval in order to satisfy that expected traffic demand with a certain blocking probability.

In the performance analysis, the survivor function of the variable N_{AS}^{k} for each stationary interval and, by applying the procedure mentioned in Subsection 4.4.1, the number of CPRI circuits to be supported between the Access Switch and the CO have been evaluated. The survivor functions of N_{AS}^{k} are diagrammed in Fig. 4.9 for the values of k equal to 5, 8, 12 and 20. In particular notice from Fig. 4.5 how k=12 corresponds to the case of the PHI. Both the analytical and simulation results are reported in the figure.

As a consequence, the number of needed circuits in PHI gives informations for dimensioning the transport network that has to connect a certain number of ASs to the Central Office.

First of all we can notice how the analytical results are in good agreement with the simulation ones. The analytical model has been also validated for other case studies not shown in this chapter.

The application of the methodology illustrated in Subsection 4.4.1 and applied with $\alpha = 1 - 10^{-7}$ leads to dimensioning values of the number $nc_{AS,CPRI}^{k}$ of CPRI flows @2.5 *Gbps* equal to 72, 121, 125 and 38 for k equal 5, 8, 12 20 respectively. All of the dimensioning values of $nc_{AS,CPRI}^{k}$ $(k = 0, 1, \cdots, N-1)$ are reported in Fig. 4.10. These values explain very well the advantages in

the application of a switching off technique with respect to the case in which the dimensioning is performed on the number RRUs installed. For instance when k=12, that is in the PHI, the percentage advantage in terms of CPRI circuits is in the order of 64%.

Furthermore, in the Fig 4.10, it is reported the validation of the analytic results obtained through a simulation campaign.

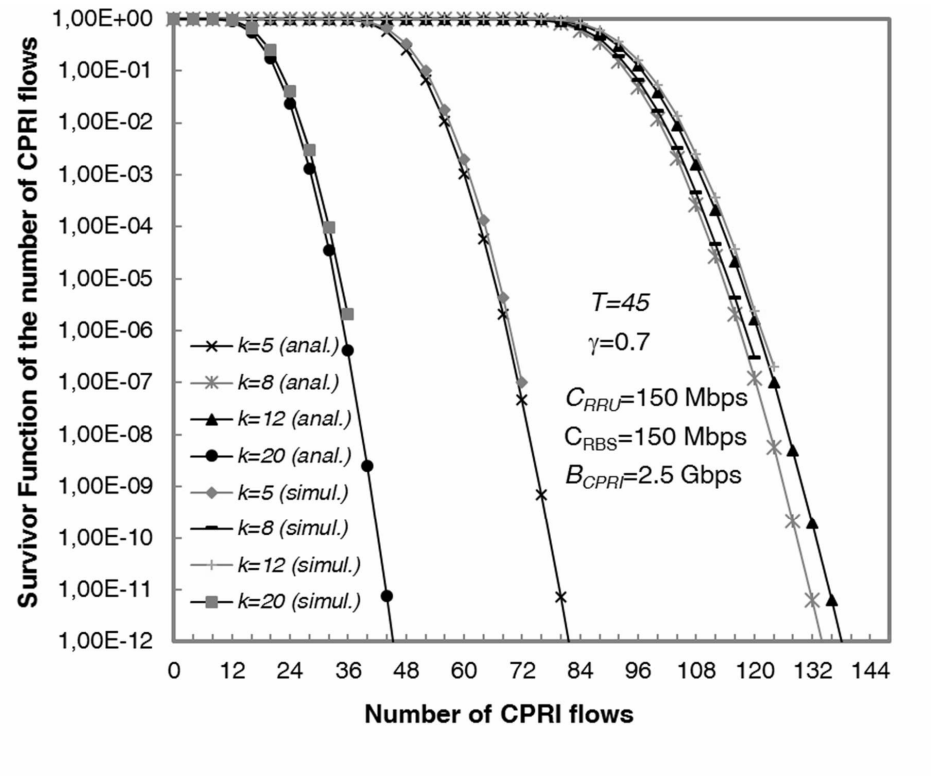

Figure 4.9: Survivor Function of the random variables N_{AS}^{k} for k equal to 5, 8, 12 and 20 in a 4G traffic scenario. Both analytical and simulation results are reported.

The results for the dimensioning of the number $nc_{AS,GE}^{k}$ of GEthernet circuits are also reported in Fig 4.11. In this figure, it is shown the number of GEthernet circuits needed between the AS and the CO in each daily time interval. We can see a remarkable reduction in number of GEthernet circuits in the daily intervals when the traffic is very low. For instance in the time interval $k = 2$ only 3 GEthernet circuits are needed instead of 14 if the dimensioning were dimensioned according to the capacity of micro RBSs installed.

Next some results for a 5G traffic scenario are presented. In this case the traffic density is much higher. To handle this remarkable traffic amount, the

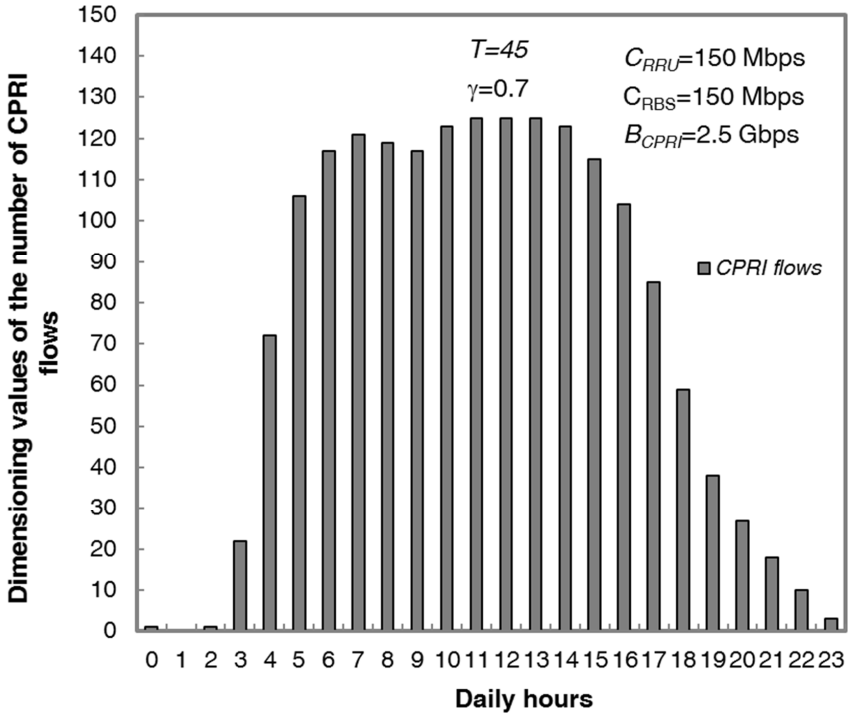

Figure 4.10: Dimensioning values $nc^k_{AS,CPRI}$ as a function of the daily intervals in a 4G traffic scenario

choice of employing network elements able to provide larger capacity has been done, thus an LTE bandwidth equal to 20 MHz and MIMO $8x8$ are employed for each station, that leads to a capacity C_{RBS} and C_{RRU} equal to 600 $Mbps$. In this case, RRU generates one CPRI flow @10 $Gbps$ [11]. The number n_{RRU} and n_{RBS} of RRUs and micro RBSs respectively needed per sub-area and dimensioned according to the procedure of Appendix A.3.3 are reported in the second column of Table 4.3. The dimensioning values $nc^k_{AS,CPRI}$ and $nc^k_{AS,GE}$ $(k = 0, 1, ..., N-1)$ are reported in Figs 4.13 and 4.14. Even in this case we can see how a much more severe dimensioning is needed. Though the switching off technique allows for a remarkable reduction in number of 10 $Gbps$ CPRI circuits, we notice that the traffic amount required is very high and challenging solutions are required for the network design.

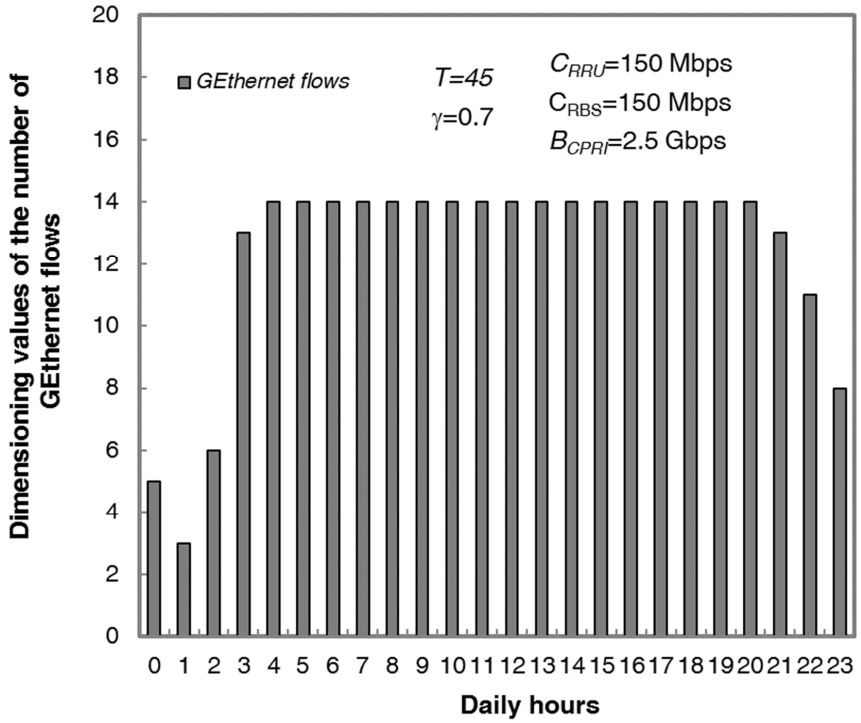

Figure 4.11: Dimensioning values $nc^k_{AS,GE}$ as a function of the daily intervals in a 4G traffic scenario

4.5.4 Optimal Bandwidth/Power Consumption Trade-Off

Next some results evaluated by the model reported in Section 4.3 are reported. In the Xhaul solution analysis as in the case of the fronthaul solution, the RBS power consumption P_{RBS} is considered equal to 300 Watt ([91, 92]) and the same value for the total power consumption $P_{RRU,BBU}$ of a CPRI network element is assumed. In the same way, $P_{RRU,BBU}$ is expressed by:

$$P_{RRU,BBU} = P_{RRU} + P_{server}/K_{BBU} + P^{BBU}_{ins}$$

The value of K_{BBU} is chosen equal to 4 while the constant server power P_{server} is fixed equal to 30% of the maximum server power. Furthermore, also in this case, it is denoted with δ the ratio of the radio power consumption P_{RRU} to the total power consumption $P^{tot}_{RRU,BBU}$. It is important to note that the RRU is always on, thus only the baseband processing component gives a variable contribution to the total power consumption. Here the objective is to evaluate the optimum value of γ allowing for a right trade-off between

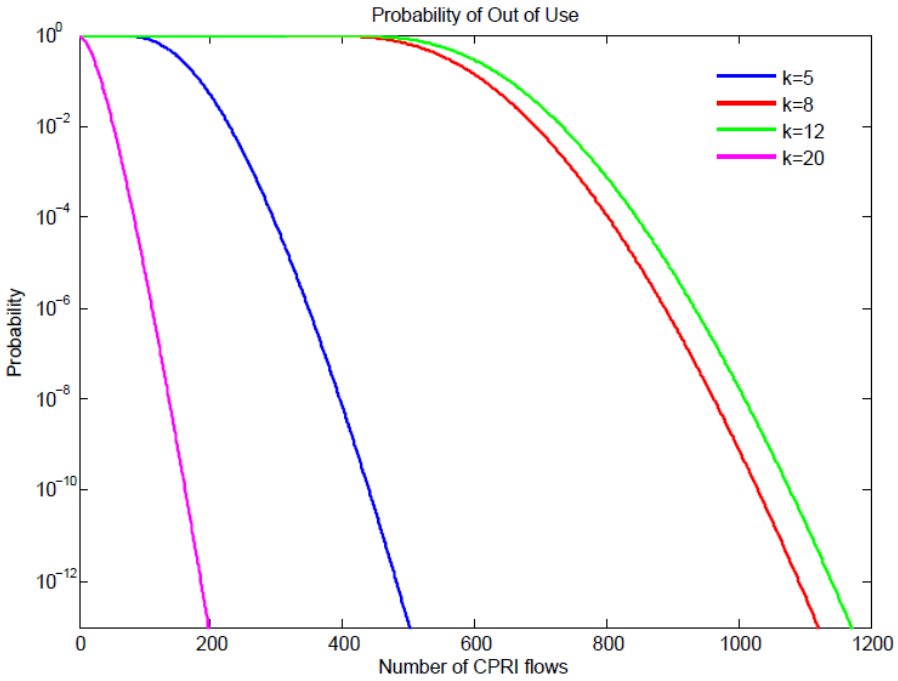

Figure 4.12: Survivor Function of the random variables N_{RS}^{k} for k equal to 5, 8, 12 and 20 in a 5G traffic scenario

bandwidth and power consumption. Obviously the study depends on the values of the parameters μ_{BW} and μ_{PWR} introduced in Section 4.3 and characterizing the costs per bandwidth unit (1 Gbps) and per power unit (1 W) respectively. In particular we have noticed that when μ_{BW}=1, the region in which the trade-off exists is when μ_{PWR} ranges from 0.001 to 0.86. In fact when μ_{PWR} is smaller (larger) than 0.001 (0.86), the bandwidth cost (power cost) is dominant and we have the trivial solution γ=0 (γ=1), in which only micro RBSs (RRUs) are used.

In Fig. 4.15 the bandwidth and power consumption costs are reported and evaluated given by the two contributions of the second hand of expression (4.2) for μ_{BW}=1, μ_{PWR}=0.01, δ=0.5 and when T=45 sub-areas are handled by an AS. In Fig. 4.15 it is also presented the total cost expressed by (4.2). As it is possible to note, the power consumption decreases when the γ ratio of the number n_{RRU} of RRUs to the total number of radio stations increases. In fact when this increase occurs a larger number of RRUs is used in place of RBSs and it is possible to save the energy consumption related to the deactivation of BBU instances that are not used when the traffic is low. At the same time we notice that the increase of γ leads to bandwidth cost increases very quickly due to the high bandwidth required by the CPRI flows. As reported in Fig. 4.15,

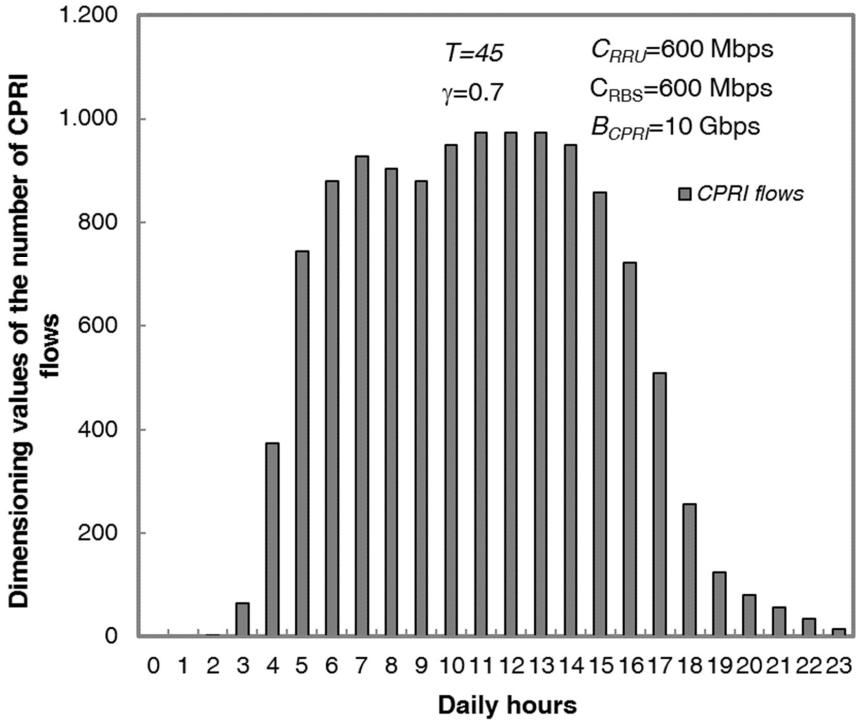

Figure 4.13: Dimensioning values $nc^k_{AS,CPRI}$ as a function of the daily intervals in a 5G traffic scenario

the total cost initially decreases, then starts to grow. As a consequence, we can notice a minimum point that represents the trade-off between bandwidth and power cost. For the case study considered, the minimum point is achieved for a value of γ equal to 0.4.

The bandwidth, power and total costs are reported as a function of γ and for T varying from 5 to 225 in Figs 4.16, 4.17 and 4.18 respectively. The value of δ is chosen equal to 0.5. We can notice from Figs 4.16-4.18 how the bandwidth, the power consumption and total costs decrease how the number T of sub-areas handled by any AS is increased. This is due to the high statistical multiplexing gain especially for the bandwidth used. Owing to the central limit theorem, the bandwidth and the power consumption tend to deterministic values for T tending to infinity and for this reason the decrease of the bandwidth, power consumption and the total costs reduces for values of T greater than 75 and tend to an asymptotic value. We also notice from Figs 4.16-4.18 that the minimal point tends to move towards higher values of γ for T increasing. For instance the optimal values of γ are 0.26 and 0.48 for T equal to 10 and 75 respectively. This shifting is due to the higher

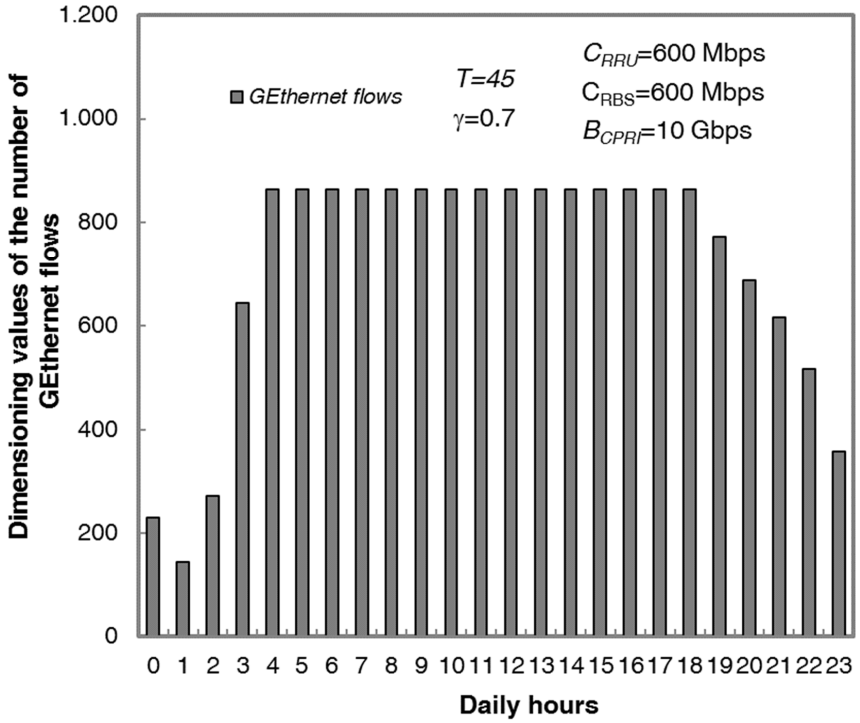

Figure 4.14: Dimensioning values $nc^k_{AS,GE}$ as a function of the daily intervals in a 5G traffic scenario

decrease in bandwidth with respect to power consumption when the number T of sub-areas handled by an AS is increased.

As further contribution to the investigation done in this work, in Fig. 4.19 the total cost is reported as a function of γ when T=45 and for values of δ equal to 0.20, 0.40, 0.60 and 0.80. We can notice from Fig. 4.19 how the minimal points moves towards lower values of γ for δ increasing. As a matter of example, the minimum values of γ equal 0.55 and 0.42 for T equal to 0.20 and 0.80 respectively. The reason is due to higher radio power consumption P_{RRU} of an RRU that makes less power efficient the use of RRUs.

Finally, the conducted analysis considers the impact on the cost of a spatial correlation of the traffic distribution. In particular, the case in which the spatial correlation coefficient has a negative exponential trend [93] as a function of the distance between sub-areas has been studied. Next it is denoted with ρ the correlation coefficient of the traffic of two adjacent sub-areas. Fig. 4.20 shows the survivor function of the number of needed CPRI flows when an AS handles T=45 sub-areas and for values of ρ varying from 0 to 0.6. The 5G traffic scenario is considered and the values of k equal to 12 and 20 are

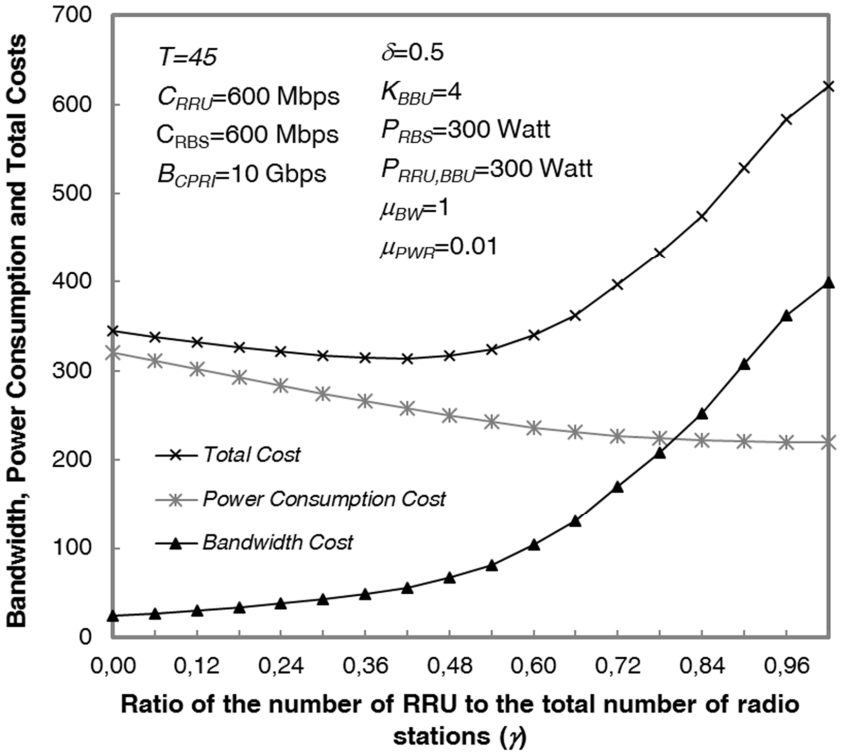

Figure 4.15: Bandwidth, power consumption and total costs as a function of the ratio γ of the number of RRUs to the total number of radio stations. The AS handles T=45 sub-areas and the ratio δ of the radio power consumption P_{RRU} to the total power consumption $P_{RRU,BBU}$ of an RRU is chosen equal to 0.5.

considered. We can notice that higher dimensioning values of the number of CPRI circuits are needed for ρ increasing. As a matter of example if we fix $\alpha = 1 - 10^{-6}$, the number of needed CPRI circuits is equal to 936, 1224, 1440 and 1584 for ρ equal 0, 0.2, 0.4 and 0.6 respectively.

In Fig. 4.21 the total cost is depicted as a function of γ for the same values of Fig. 4.19 and when δ is chosen equal to 0.5. The values of ρ from 0 to 0.5 are considered. In the case of higher traffic correlation, we can notice that the value of γ in which the cost is minimum tends to move towards lower values. For instance, the minimum values of γ equal 0.48 and 0.30 for ρ equal to 0 (no correlation) and 0.5 (maximum correlation) respectively. This is due to the increase in requested bandwidth that leads to the use of RRUs less convenient with respect to the one of RBSs.

Furthermore, in fig 4.20 the total cost is reported as a function of ρ. In the case of correlated traffic, we note that the minimum point tends to move towards lower values for ρ increasing. For instance, the minimum values of

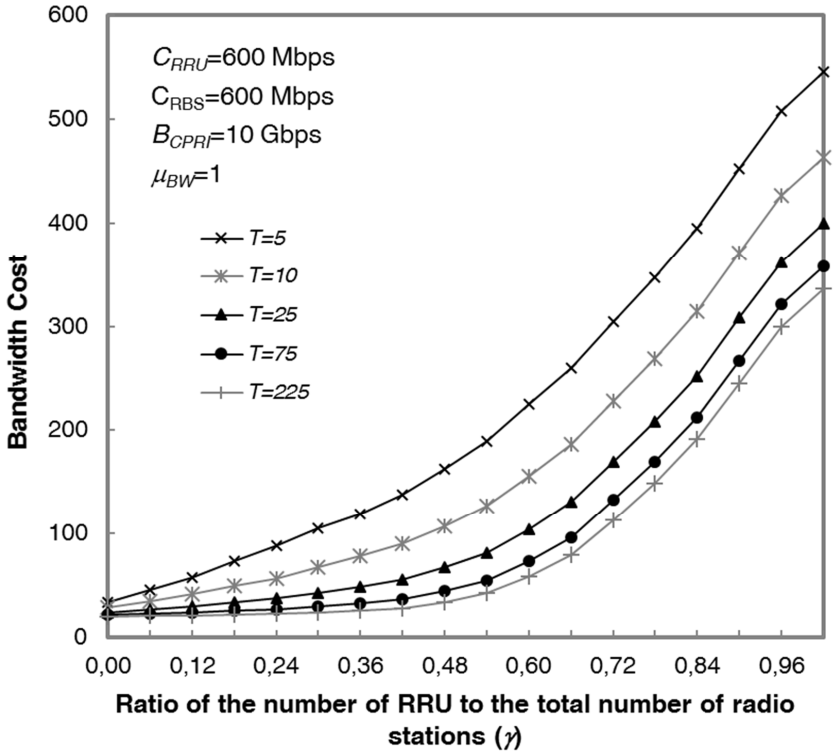

Figure 4.16: Bandwidth cost as a function of the ratio γ of the number of RRUs to the total number of radio stations. The ratio δ of the radio power consumption P_{RRU} to the total power consumption $P_{RRU,BBU}$ of an RRU is chosen equal to 0.5 and the AS handles a number T of sub-areas varying from 5 to 225.

γ equal 0.48 and 0.30 for ρ equal to 0 (no correlation) and 0.5 (maximum correlation) respectively. This is due to the assumptions that the RBSs are always active and give a basic capacity thus, if their number is higher, the access network capacity could be enough to menage more traffic in case of correlated event.

4.6 Conclusions

In this chapter, a dimensioning procedure has been proposed to evaluate the number of CPRI and GEthernet circuits that a network has to guarantee between an Access Switch and the CO. The AS handles the traffic generated by a set of sub-areas. The user traffic is managed by both micro RBSs and RRUs that generate GEthernet and CPRI flows respectively. The dimensioning procedure allows for a saving of needed CPRI circuits with respect to the case in which the number of CPRI circuits is statically fixed to the number

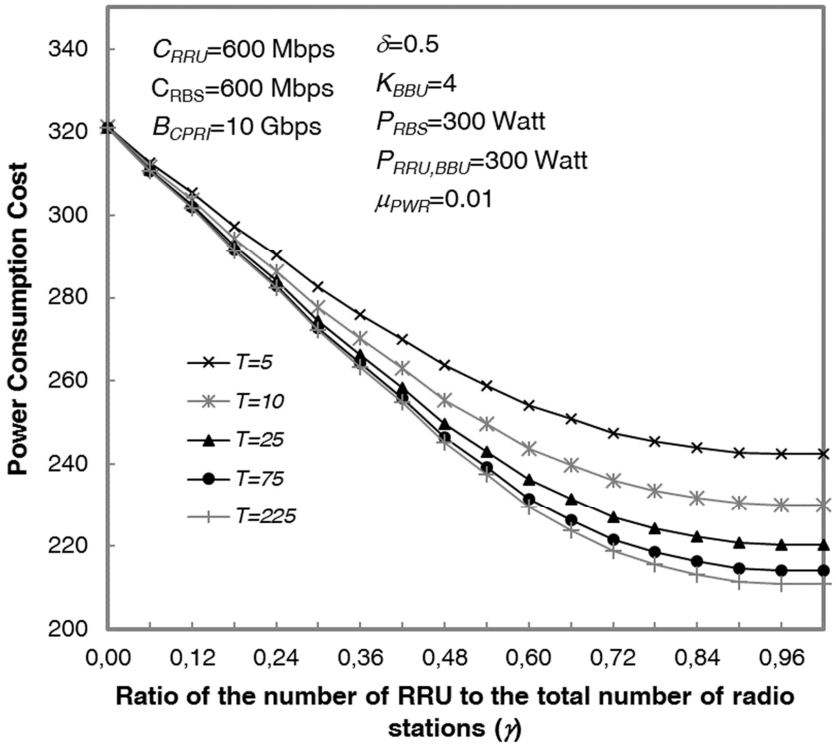

Figure 4.17: Power consumption cost as a function of the ratio γ of the number of RRUs to the total number of radio stations. The ratio δ of the radio power consumption P_{RRU} to the total power consumption $P_{RRU,BBU}$ of an RRU is chosen equal to 0.5 and the AS handles a number T of sub-areas varying from 5 to 225.

of RRUs installed in all of the sub-areas handled by the Access Switch and dimensioned in each area according to the traffic amount during the Peak Hour Interval. This CPRI circuits saving is due to two reasons:

i) the application of an algorithm of BBU instance deactivation applied when the offered traffic decreases;

ii) the statistical multiplexing advantages that leads to a less severe dimensioning, even during the Peak Hour Interval, due to the fact that the AS has to provide CPRI circuits for an aggregate of sub-areas while the number of RRUs installed is dimensioned according to the traffic amount offered to every single sub area.

The analysis in the case of the fronthaul network shows how the bandwidth saving percentage varies from 45% to 70%. In the case of the Xhaul architecture, the obtained results show how the introduced dimensioning procedure allows, even during the Peak Hour Interval, for remarkable gains that

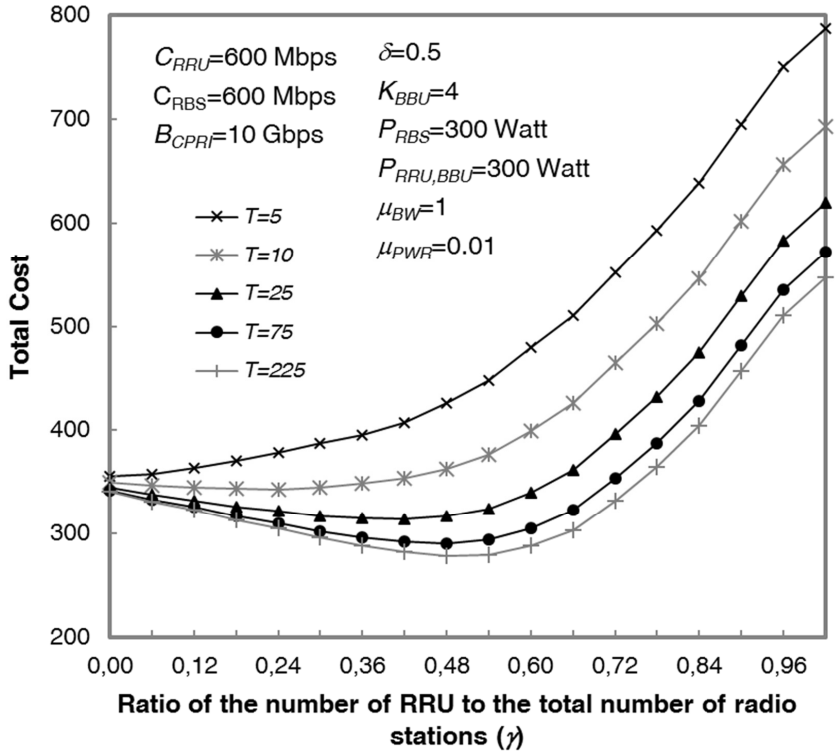

Figure 4.18: Total cost as a function of the ratio γ of the number of RRUs to the total number of radio stations. The ratio δ of the radio power consumption P_{RRU} to the total power consumption $P_{RRU,BBU}$ of an RRU is chosen equal to 0.5 and the AS handles a number T of sub-areas varying from 5 to 225.

can reach about 60% and 70% in 4G and 5G traffic scenarios respectively. Furthermore, in both cases, due to statistical multiplexing effects within large sub-areas clusters, the running of the BBU instances in pools of shared servers leads to a power decrease as much higher as the number of sub-area handled by any Access Switch.

By means of an analytical model, a bandwidth/power trade-off solution of the Xhaul architecture has been evaluated. The proposed study has shown how the choice of the right mix of RRU/RBS in a sub-area allows for the minimization of the total cost expressed in terms of bandwidth and power consumption costs. Furthermore it has shown how the optimal mix depends on some parameters as the number of sub-areas handled by any AS, the radio power consumption of an RRU, etc. For instance, the performance evaluation shows that the optimal mix is composed by the 35% of RRUs in the case in which the AS handles 45 sub-areas and the radio power consumption of an RRU is the 20% of the total power consumption of a CPRI network element.

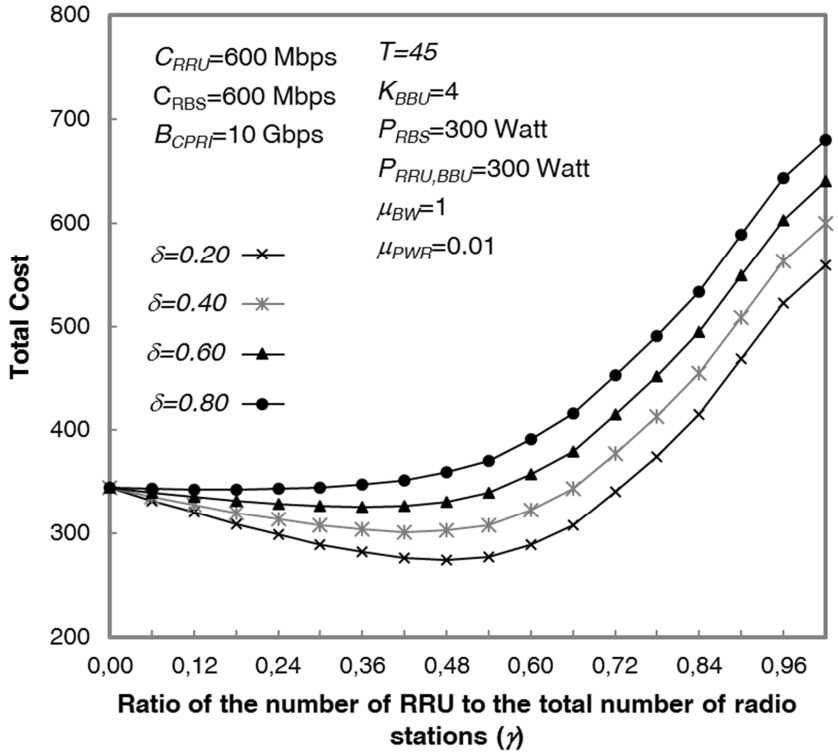

Figure 4.19: Total cost as a function of the ratio γ of the number of RRUs to the total number of radio stations. The AS handles a number T of sub-areas equal to 45 and the ratio δ of the radio power consumption P_{RRU} to the total power consumption $P_{RRU,BBU}$ of an RRU equals 0.20, 0.40, 0.60 and 0.80.

The impact on the cost in the case of traffic correlation has been also evaluated. The reported results show how a higher correlation leads to more severe bandwidth dimensioning with the consequence of making less convenient the use of RRUs.

Furthermore, the analysis in the case of correlated traffic distributions for the sub-areas shows how the proposed procedure leads to remarkable gains even if the dimensioning could be more severe than in the case in which the user peak traffic generated in the sub-areas are i.i.d. variables.

Other case studies will be investigated in future analysis to confirm the aforementioned conclusions. As future research items the impact of these dimensioning procedures on the network resources (number of rings, number of ASs, number of wavelengths, crosspoints size, Ethernet and CPRI switches size,...) will be evaluated.

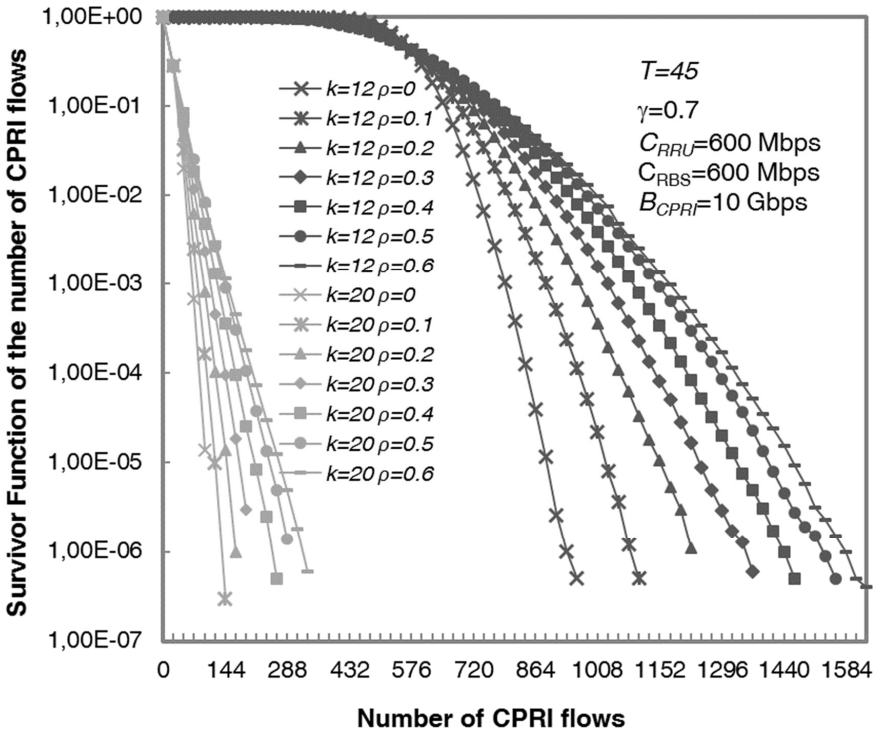

Figure 4.20: Survivor Function of the random variables N_{AS}^{k} for k equal to 12 and 20 in a 5G traffic scenario where the spatial correlation parameter ρ varies from 0 to 0.6

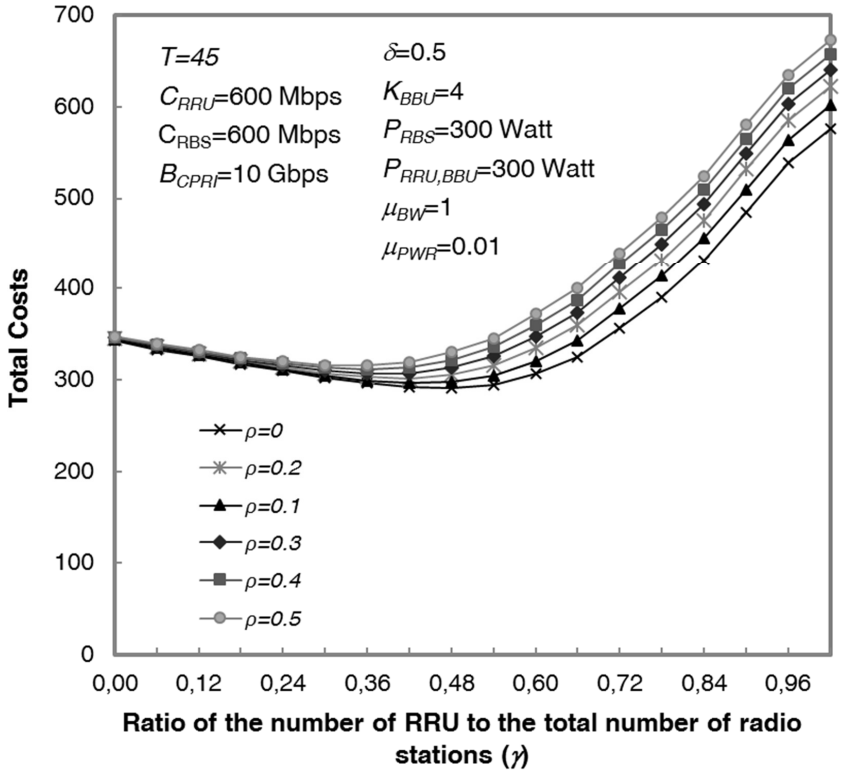

Figure 4.21: Total cost as a function of the ratio γ of the number of RRUs to the total number of radio stations. The AS handles a number T of sub-areas equal to 45, the ratio δ of the radio power consumption P_{RRU} to the total power consumption $P_{RRU,BBU}$ of an RRU equals to 0.50 and the spatial correlation parameter ρ varies from 0 to 0.5

Chapter 5

Conclusions and Outlooks

In this thesis, the trend evolution and the road toward the 5G networks have been explored. It has been analyzed the transition from the vision of a transparent all-optical network to a more versatile and pragmatic idea of network that can handle efficiently different radio access technologies, whose the next generation network will be the best expression.

Some of the key drivers of this evolution are the increase of the mobile networks capacity, the data rates and the number of devices simultaneously connected, and the requirements for extremely low latency to provide for a better user experience, energy efficiency, or the centralization of control in order to accommodate more complex network planning and optimization and to simplify the hardware enabling the virtualization of the network functions. In adding to these ones, we could consider the capacity of the future network to reconfigure itself in order to achieve some of the goals listed above. It is clear to understand that the network needs to be as flexible as possible to manage in the same architecture the several types of radio access technologies.

Flexibility is, in facts, one of the key points of this research. The joint use of OTN/WDM switching is one of the available solutions to manage the very heterogeneous technologies of the next generation access network. The advantages introduced by the OTN/WDM integrated switching are related to the finer granularity of this technology compared to the all-optical switches. This benefits could be exploit to obtain high level of efficiency and, of course, flexibility.

For these reasons, a low complex integrated OTN/WDM switch node has been studied and evaluated. In this analysis, some architectures are considered and the savings in terms of number of components has been evaluated through the formulations of routing and assignment problems and the in-

troduction of heuristics for simulations. Network blocking performance have been evaluated for different metropolitan networks and in static and dynamic scenarios. It has also been estimated the right spatial speedup that the architecture needs in order to compensate the performance degradation due the switch internal blocking and save components, thus allowing for hardware complexity reduction, with respect to the case of Strict Sense Non Blocking switch.

The second part of the thesis deals with the investigation of a network architecture, called "Xhaul", that unifies fronthaul and backhaul networks in a common connectivity segment. A dimensioning procedure has been proposed to evaluate the number of CPRI (fronthaul) and GEthernet (backhaul) circuits that a network has to guarantee between an Access Switch and the Central Office. In particular, this procedure allows for a saving of needed CPRI circuits with respect to the case in which the number of CPRI circuits is statically fixed. The achievement of this bandwidth efficiency is due to two important reasons: the application of BBU instance deactivation policies when the offered traffic decreases, and the statistical multiplexing advantages that leads to a less severe dimensioning, even during the Peak Hour Interval. The analysis shows how the introduced procedure allows for remarkable gains that can reach about 60% and 70% in 4G and 5G traffic scenarios respectively.

By means of an analytical model, a bandwidth/power trade-off solution of the Xhaul architecture has been evaluated. The proposed study has shown how the choice of the right mix of RRU/RBS in a sub-area allows for the minimization of the total cost expressed in terms of bandwidth and power consumption costs. Furthermore it has shown how the optimal mix depends on some parameters as the number of sub-areas handled by any AS, the radio power consumption of an RRU, etc. For instance, the performance evaluation shows that the optimal mix is composed by the 35% of RRUs in the case in which the AS handles 45 sub-areas and the radio power consumption of an RRU is the 20% of the total power consumption of a CPRI network element.

The impact on the cost in the case of traffic correlation has been also evaluated. The reported results show how a higher correlation leads to more severe bandwidth dimensioning with the consequence of making less convenient the use of RRUs.

Furthermore, the analysis in the case of correlated traffic distributions for the sub-areas shows how the proposed procedure leads to remarkable gains, even if the dimensioning could be more severe than in the case in which the

user peak traffic generated in the sub-areas are i.i.d. variables.

Other case studies will be investigated in future analysis to confirm the aforementioned conclusions. As future research items, it will be evaluated the impact of these dimensioning procedures on the network resources (number of rings, number of ASs, number of wavelengths, crosspoints size, Ethernet and CPRI switches size,etc.).

Appendix A

Appendices

A.1 Proof of the lemma 1 on the SSNB condition of the switch core

Lemma 1: Under the constraint of W multiple of H, the proposed switch core architecture is SSNB if the speedup S is greater than or equal to

$$S_{SSNB} = \lceil \frac{K}{\lfloor \frac{K}{F} \rfloor} \rceil$$

Proof. The assumption is that at a given instant the worst traffic conditions according to which:

i) only SH-ODU traffic is offered to the switch;

ii) the maximum number $NWF - 1$ of L-ODUs is already handled by the switch and hence there is one only input wavelength and one only output wavelength that can carry one L-ODU.

These wavelengths are referred to as λ_i^f and λ_o^f respectively. We have to determine the minimum value S_{SSNB} of the spatial speedup so that there are sufficient switch resources to carry the L-ODU from λ_i^f to λ_o^f.

Let us suppose that λ_i^f to λ_o^f are an input and an output of the OTN switches denoted as $IOS_{x,y}$ and $OSS_{z,t}$ respectively. The minimum value S_{SSNB} is obtained when the following two conditions occur:

1. the $NWF-1$ L-ODUs already handled by the switch, engage the maximum number $N_{OM}^{IOS_{x,y}}$ and $N_{IM}^{OOS_{z,t}}$ of outputs and inputs of $IOS_{x,y}$ and $OOS_{z,t}$ respectively;

2. one input and one output of $IOS_{x,y}$ and $OOS_{z,t}$ respectively are still available.

The OTN switching modules $IOS_{x,y}$ and $OOS_{z,t}$ handle $\frac{W}{H}$ input and output wavelengths channels respectively and $\frac{W}{H}F-1$ L-ODUs. In the worst case these L-ODUs are carried on different interstage links and hence need the engagement of $N_{OM}^{IOS_{x,y}}$=$N_{IM}^{OOS_{z,t}}$=$\frac{W}{H}F-1$ outputs and inputs of $IOS_{x,y}$ ($OOS_{z,t}$) respectively.

The evaluation of $N_{OM}^{IOS_{x,y}}$ and $N_{IM}^{OOS_{z,t}}$ and the conditions 1) and 2) lead to the condition K=$\frac{W}{H}F$ and that is to the following condition for S_{SSNB}:

$$S_{SSNB} = \left\lceil \frac{K}{\lfloor \frac{K}{F} \rfloor} \right\rceil \tag{A.1}$$

□

A.2 Proof of the lemma 2 on the SSNB condition of the space switching module

Lemma 2: A $U \times U$ switching module with a three stages NBSS Clos network structure can be realized with the least number $N_{Q\times Q}$ of $Q \times Q$ $(U > Q)$ switching modules given by:

$$N_{Q\times Q} = min_{n\in\Theta}\left(2\left\lceil\frac{\lceil\frac{U}{n}\rceil}{\lfloor\frac{Q}{2n-1}\rfloor}\right\rceil + \left\lceil\frac{2n-1}{\left\lfloor\frac{Q}{\lceil\frac{U}{n}\rceil}\right\rfloor}\right\rceil\right) \tag{A.2}$$

where Θ is a set of positive integer numbers given by:

$$\Theta = \{i \in Z^+ \ / \ Q \geq max(2i-1, \left\lceil\frac{U}{i}\right\rceil)\} \tag{A.3}$$

Proof. To prove expression (A.2), in Fig. A.1 it is reported a three stages SSNB Clos network with $\lceil\frac{U}{n}\rceil$ $n \times (2n-1)$ switching elements in the first and third stage and $(2n-1)$ $\lceil\frac{U}{n}\rceil \times \lceil\frac{U}{n}\rceil$ switching elements in the second stage.

While the parameter U is given, we can optimize the choice of the parameter n. The Clos network is realized with the available $Q \times Q$ switching modules by aggregating switching elements of the Clos network as indicated in Fig. A.1. Thus the number $N_{Q\times Q}(n)$ of $Q \times Q$ switching modules for a given n could be expressed as:

$$N_{Q\times Q}(n) = N^{1st}_{Q\times Q}(n) + N^{2nd}_{Q\times Q}(n) + N^{3rd}_{Q\times Q}(n) \tag{A.4}$$

where $N^{1st}_{Q\times Q}(n)$, $N^{2nd}_{Q\times Q}(n)$ and $N^{3rd}_{Q\times Q}(n)$ are the number of $Q\times Q$ switching modules needed for the first, second and third stage of the Clos Network for a given n. $N^{1st}_{Q\times Q}(n)$ and $N^{3rd}_{Q\times Q}(n)$ can be expressed according to the following remarks:

i) each $Q \times Q$ switching module can implement up to $\lceil\frac{Q}{2n-1}\rceil$ $n \times (2n-1)$ switching elements of the first and third stage;

ii) these stages contain each one a number $\lceil\frac{U}{n}\rceil$ of switching elements.

Hence we can write:

$$N^{1st}_{Q\times Q}(n) = N^{3rd}_{Q\times Q}(n) = \left\lceil\frac{\lceil\frac{U}{n}\rceil}{\lfloor\frac{Q}{2n-1}\rfloor}\right\rceil \tag{A.5}$$

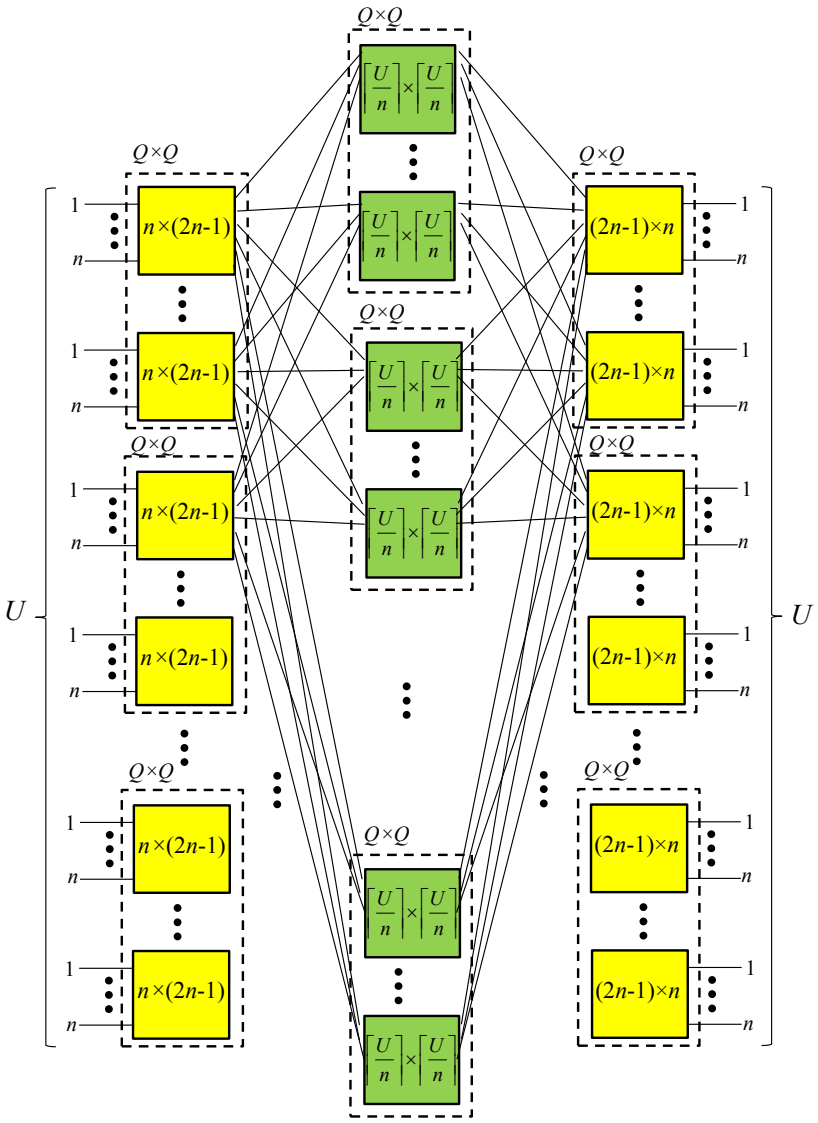

Figure A.1: Realization of the $U \times U$ space switching module with $Q \times Q$ ($U > Q$) switching modules.

A.2 Proof of the lemma 2 on the SSNB condition of the space switching module

To guarantee that the introduction of the $Q \times Q$ switching modules does not introduce any blocking, we have to impose that the $Q \times Q$ switching module allow for the aggregation of at least one $n \times (2n-1)$ switching element. That leads to the following condition:

$$Q \geq 2n - 1 \tag{A.6}$$

By analogy to expressions (A.5) and (A.6), we can write for the second stage:

$$N_{Q\times Q}^{2nd}(n) = \left\lceil \frac{2n-1}{\left\lfloor \frac{Q}{\lceil \frac{U}{n} \rceil} \right\rfloor} \right\rceil \tag{A.7}$$

$$Q \geq \left\lceil \frac{U}{n} \right\rceil \tag{A.8}$$

Finally by inserting (A.5) and (A.7) in (A.4) and minimizing with respect to the parameter n we obtain (A.2). By taking into account (A.6) and (A.8), it follows that the optimization of n has to be searched in the set given by (A.3). □

A.3 Xhaul Evaluation Analysis

A.3.1 Evaluation of the probabilities $p_{N_{AS}^k}(j)$ of the random variable N_{AS}^k

If as reference we consider an Access Switch that handles the traffic of T sub-areas, and we denote with N_t^k the number of CPRI circuits needed for the sub-area SA_t $(t = 1, ..., T)$, the following expression for N_{AS}^k can be written:

$$N_{AS}^k = \sum_{t=1}^{T} N_t^k \qquad (k = 0, 1, ...N-1) \tag{A.9}$$

The lack of traffic correlation assumed, leads to i.i.d random variables N_t^k $(t = 1, ..., T)$. Then we can write the following expression (A.10) for the probabilities N_t^k:

$$p_{N_{AS}^k}(j) = \otimes^T p_{N_{SA}^k}(j) \;\; j = 1, ..., Tn_{RRU} \;\; k = 0, 1, ...N-1 \tag{A.10}$$

wherein $p_{N_{SA}^k}(h)$ denotes the probabilities of N_t^k and the symbol $\otimes^T$ denotes the convolution operator applied T times.

For the evaluation of the probability $p_{N_{SA}^k}(h)$ $(h = 0, 1, ..., n_{RRU})$, that is the probability that h RRUs are used in the target sub-area, we remember our assumption of minimizing the number of CPRI circuits that leads to employing as much as possible the capacity of micro RBSs and only when this capacity is occupied, RRU capacity is used.

Next we consider three cases:

i) $h = 0$;

ii) $1 \leq h \leq n_{RRU} - 1$;

iii) $h = n_{RRU}$.

In the case $h = 0$, we can observe that N_{SA}^k is equal to 0 up to when the traffic A^k offered to the sub-area is smaller than or equal to $n_{RBS}\ C_{RBS}$ that is the total sum of the capacities of the n_{RBS} micro RBSs assigned to the target sub-area.

In the case $1 \leq h \leq n_{RRU} - 1$, we can observe that N_{SA}^k is equal to h when the traffic A^k offered to the sub area is in the interval $[n_{RBS}C_{RBS} + (h-1)C_{RRU}, n_{RBS}\ C_{RBS} + h\ C_{RRU}]$.

In the case $h = n_{RRU}$, we can observe that N^k_{SA} is equal to n_{RRU} when the offered traffic is higher than or equal to $n_{RBS}C_{RBS} + n_{RRU}C_{RRU}$.

According to the observations above, the expression A.11 could be obtained for the probabilities $p_{N^k_{SA}}(h)$ $(h = 0, 1, ..., n_{RRU})$. Finally by inserting (A.11) in (A.10), we can evaluate the probabilities $p_{N^k_{AS}}(j)$ $(j = 0, 1, ..., Tn_{RRU})$ of the random variable N^k_{AS}.

A.3.2 Evaluation of the probabilities $p_{N^k_{AS,E}}(j)$ of the random variable $N^k_{AS,E}$

If as reference we consider an Access Switch that handles the traffic of T sub-areas, $N^k_{AS,E}$ denotes the number of GEthernet flows that depends on the traffic generated by the micro RBSs located in the sub-areas. To evaluate the probabilities $p_{N^k_{AS,E}}(j)$ we need to knowledge the total traffic amount (Gbps) $A^k_{AS,E}$ expressed in Gbps and emitted by the micro RBSs handled by the AS. If we denote with $A^k_{SA_t}$ the traffic amount generated by the micro RBSs located in the sub area SA_t $(t = 1, ..., T)$, the following expression holds:

$$A^k_{AS,E} = \sum_{t=1}^{T} A^k_{SA_t} \qquad (k = 0, 1, ..., N-1) \tag{A.13}$$

It is assumed that the random variables $A^k_{SA_t}$ $(t = 1, ..., T)$ independent and identically distributed (i.i.d.) with log-normal distributions of parameters (μ^k, σ^k). In this case it has been proved that the probability density $p_{A^k_{AS,E}}(x)$ of $A^k_{AS,E}$ can be approximated as log-normal probability density of parameters $(\mu^k_{AS}, \sigma^k_{AS})$ given by the following expressions [94]:

$$\sigma^k_{AS} = \sqrt{\log_e(\frac{1}{T}(e^{(\sigma^k)^2} - 1) + 1)} \tag{A.14}$$

$$\mu^k_{AS} = \log_e(Te^{\mu^k}) + 0.5((\sigma^k)^2 - (\sigma^k_{AS})^2) \tag{A.15}$$

At this point we can evaluate the probabilities $p_{N^k_{AS,E}}(j)$ $(j = 1, ..., \lceil Tn_{RBS}C_{RBS} \rceil)$ from the probability densities $p_{A^k_{AS,E}}(x)$ of the random variable $A^k_{AS,E}$. We can follow the same approach applied in Appendix-A.3.1 and obtain the expression (A.12).

$$p_{N_{SA}^k}(h) = \begin{cases} \frac{1}{2}erfc(-\frac{\log_e(n_{RBS}C_{RBS})-\mu^k}{\sigma^k\sqrt{2}}) & h=0 \\ \frac{1}{2}erfc(-\frac{\log_e(n_{RBS}C_{RBS}+hC_{RRU})-\mu^k}{\sigma^k\sqrt{2}}) - \frac{1}{2}erfc(-\frac{\log_e(n_{RBS}C_{RBS}+(h-1)C_{RRU})-\mu^k}{\sigma^k\sqrt{2}}) & h=1,\cdots,n_{RRU}-1 \\ 1-\frac{1}{2}erfc(-\frac{\log_e(n_{RBS}C_{RBS}+n_{RRU}C_{RRU})-\mu^k}{\sigma^k\sqrt{2}}) & h=n_{RRU} \end{cases} \tag{A.11}$$

$$p_{N_{AS,E}^k}(j) = \begin{cases} \frac{1}{2}erfc(\frac{\mu_{AS}^k}{\sigma_{AS}^k\sqrt{2}}) & if \;\; j=1 \\ \frac{1}{2}erfc(-\frac{\log_e j-\mu_{AS}^k}{\sigma_{AS}^k\sqrt{2}}) - \frac{1}{2}erfc(-\frac{\log_e(j-1)-\mu_{AS}^k}{\sigma_{AS}^k\sqrt{2}}) & if \;\; 2\leq j\leq \lceil Tn_{RBS}C_{RBS}\rceil - 1 \\ 1-\frac{1}{2}erfc(-\frac{\log_e(\lceil Tn_{RBS}C_{RBS}\rceil-1)-\mu_{AS}^k}{\sigma_{AS}^k\sqrt{2}}) & if \;\; j=\lceil Tn_{RBS}C_{RBS}\rceil \end{cases} \tag{A.12}$$

A.3.3 Network Resource Dimensioning Procedure of the number of micro RBSs and RRUs used

The procedure consists in dimensioning the number of network elements (micro RBSs and RRUs) so as to guarantee that the provided capacity satisfies the α-th of the peak traffic generated in the Peak Hour Interval (PHI). Next some definitions are done:

- k_p: index of the Peak Hour Interval for the sub area traffic profile;
- A_{k_p}: random variable characterizing the peak traffic generated during the PHI in a sub-area; its distribution is log-normal with parameters μ^{k_p} and σ^{k_p};

Having fixed the ratio γ of the number n_{RRU} of RRU to the total number $n_{RBS} + n_{RRU}$ of radio stations installed, for the dimensioning of the number n_{RRU}, n_{RBS} of RRUs and micro RBSs respectively we can observe that the entire capacity of a sub-area is given by the following expression:

$$C = n_{RRU}[\frac{(1-\gamma)}{\gamma} C_{RBS} + C_{RRU}] \tag{A.16}$$

In order to guarantee the α-th percentile of the peak traffic in a sub-area during the PHI, we have to choose the smallest n_{RRU} such that the following expression holds:

$$\begin{aligned} Pr(A_{k_p} \leq n_{RRU}[\frac{(1-\gamma)}{\gamma} C_{RBS} + C_{RRU}]) = \\ = \frac{1}{2} erfc(-\frac{\log_e n_{RRU}[\frac{(1-\gamma)}{\gamma} C_{RBS} + C_{RRU}] - \mu^{k_p}}{\sigma^{k_p}\sqrt{2}}) \\ \geq 0.01 \cdot \alpha \end{aligned} \tag{A.17}$$

The number n_{RBS} of micro RBSs is given by:

$$n_{RBS} = \lceil \frac{(1-\gamma)}{\gamma} n_{RRU} \rceil \tag{A.18}$$

A.4 List of Acronyms

AS Access Switch
BBU BaseBand Unit
C&M Control and Management
CO Central Office
CoMP Coordinated MultiPoint
CPRI Common Public Radio Interface
C-RAN Cloud Radio Access Network
CWDM Coarse Wavelength Division Multiplexing
DWDM Dense Wavelength Division Multiplexing
FMC Fixed and Mobile Convergence
GEth Gigabit Ethernet
IQ In-phase Quadrature
LTE Long Term Evolution
MAC Media Access Control
MBS Macro Base Station
MIMO Multiple Input Multiple Output
NFV Network Function Virtualization
NGPON2 Next Generation Passive Optical Network
OBSAI Open Base Station Architecture Initiative
ODU Optical Data Unit
OEO Optical/Electrical/Optical
OTN Optical Transport Network
PIC Photonic Integrated Circuit
PON Passive Optical Network
QAM Quadrature Amplitude Modulation
RANaaS RAN-as-a-Service
RBS Radio Base Station
ROADM Reconfigurable Optical Add Drop Multiplexer
RoF Radio-over-Fiber
RRH Remote Radio Head
RRU Remote Radio Unit
SCM SubCarrier Modulation
SDN Software Defined Network
SFP Small Form factor Pluggable
SMP Split MAC Physical

SPP Split Physical Processing
SSNB Strict Sense Non Blocking
TCO Total Cost of Ownership
WDM Wavelength Division Multiplexing

Bibliography

[1] *PM5440 DIGI 120G PMC-Sierra Product.* [Online]. Available: http://pmcs.com/products/optical_networking/otn/multi-service_otn_processors/pm5440/

[2] *VSC3144 Vitesse Product.* [Online]. Available: https://www.vitesse.com/products/product/VSC3144

[3] NGMN, "5g white paper," white paper. [Online]. Available: https://www.ngmn.org/

[4] C. M. R. Institute, "C-ran the road towards green ran white paper," white paper. [Online]. Available: http://labs.chinamobile.com/

[5] A. Checko, H. Christiansen, Y. Yan, L. Scolari, G. Kardaras, M. Berger, and L. Dittmann, "Cloud ran for mobile networks a technology overview," *IEEE Communications Surveys & Tutorials*, no. 17, pp. 405 – 426, 2015.

[6] ADVA, "Fronthaul networks - a key enabler for lte-advanced," white paper.

[7] Infinera, "The evolution of mobile fronthaul to support ran architecture migration to 5g," white paper.

[8] *Common Public Radio Interface (CPRI) Specification V6.1*, 2014. [Online]. Available: http://www.cpri.info/spec.html

[9] *Open Base Station Architecture Initiative (OBSAI)*, 2013. [Online]. Available: http://www.obsai.co/specifications.html

[10] *Open Radio equipment Interface (ORI)*, 2014. [Online]. Available: http://www.etsi.org/technologies-clusters/technologies/ori

[11] JDSU, "Cloud-ran deployment with cpri fronthaul technology," white paper.

[12] D. Breuer, E. Weis, S. Krau, J. Belschner, and F. Geilhardt, "Assessment of future backhaul and fronthaul networks for hetnet architectures," in *International Conference on Transparent Optical Networks*, Budapest (Hungary), July 2015.

[13] A. De La Oliva, X. Costa Prez, A. Azcorra, A. Di Gigli, F. Cavaliere, D. Tiegelbekkers, J. Lessmann, T. Haustein, A. Mourad, and P. Iovanna, "Xhaul toward an integrated fronthaul/backhaul architecture in 5g networks," *IEEE Wireless Communication*, no. 22, pp. 32–40, October 2015.

[14] V. Eramo, M. Listanti, R. Sabella, and F. Testa, "Definition and performance evaluation of a low-cost/high-capacity scalable integrated otn/wdm switch," *IEEE Journal of Optical Communications and Networking*, no. 4, pp. 1033–1045, April 2012.

[15] V. Eramo, M. Listanti, F. Lavacca, P. Iovanna, G. Bottari, and F. Ponzini, "Trade-off between power and bandwidth consumption in a reconfigurable xhaul network architecture," *IEEE Access*, accepted to publication.

[16] S. Gosselin, A. Pizzinat, X. Grall, D. Breuer, E. Bogenfeld, J. T. Gijn, A. Hamidian, and N. Fonseca, "Fixed and mobile convergence: Which role for optical networks?" in *Optical Fiber Communications Conference*, March 2015.

[17] H. Al-Ahmed, C. Cicconetti, A. De La Oliva, V. Mancuso, M. Reddy Sama, and S. Seite, P. Shanmugalingam, "An sdn-based network architecture for extremely dense wireless networks," in *IEEE SDN for Future Networks and Services (SDN4FNS)*, Trento, Italy, 2013, pp. 105–108.

[18] T. Pfeiffer, "Next generation mobile fronthaul and midhaul architectures," *IEEE Journal of Optical Communication and Networking*, no. 7, 2015.

[19] H. Son and S. Shin, *Fronthaul size: Calculation of maximum distance between RRH and BBU*, April 2014. [Online]. Available: http://www.cpri.info/spec.html

[20] U. Dotsch, M. Doll, H. Mayer, F. Schaich, J. Segel, and P. Seh, "Quantitative analysis of split base station processing and determination of advantageous architectures for lte," *IEEE Communications Surveys & Tutorials*, no. 18, pp. 105–128, March 2013.

[21] A. Maeder, M. Lalam, A. De Domenico, E. Pateromichelakis, D. Wubben, J. Bartelt, R. Fritzsche, and P. Rost, "Towards a flexible functional split for cloud-ran networks," in *European Conference on Networks and Communications*, September 2014.

[22] T. Diallo, B. Le Guyader, A. Pizzinat, S. Gosselin, P. Chanclou, F. Saliou, and A. Abdelfattath, "A complete fronthaul cwdm single fiber solution including improved monitoring scheme," in *European Conference on Networks and Communications (EuCNC)*, 2015.

[23] M. Zhu, X. Liu, N. Chand, F. Effemberg, and G. Chang, "High-capacity mobile fronthaul supporting lte-advanced carrier aggregation and 8x8 mimo," in *Optical Fiber Conference (OFC)*, San Diego (California), March 2015.

[24] M. Morant, A. Macho, and R. Llorente, "Optical fronthaul of lte-advanced mimo by spatial multiplexing in multicore fiber," in *Optical Fiber Conference (OFC)*, San Diego (California), March 2015.

[25] B. Lannoo, A. Dixit, D. Colle, J. Bauwelinck, B. Dhoedt, B. Jooris, I. Moerman, M. Pickavet, H. Rogier, P. Simoens, G. Torfs, D. Vande Ginste, and P. Demeester, "Radio-over-fibre for ultra-small 5g cells," in *International Conference on Transparent Optical Networks*, Budapest (Hungary), July 2015.

[26] G. Britton, B. Kubert, and J. Chapin, "Rf over ethernet for wireless infrastructure," in *Software Defined Rdio Technical Conference*, 2005.

[27] C. Liu, K. Sundaresan, M. Jiang, S. Rangarajan, and G.-K. Chang, "The case for re-configurable backhaul in cloud-ran based small cell networks," in *IEEE INFOCOM*, March 2013.

[28] P. Monteiro, D. Viana, J. da Silva, D. Riscado, M. Drummond, A. Oliveira, N. Silva, and P. Jesus, "Mobile fronthaul rof transceivers for c-ran applications," in *International Conference on Transparent Optical Networks*, Budapest (Hungary), July 2015.

[29] S. Hyun Cho, H. Chung, C. Han, S. Lee, and J. Lee, "Experimental demostrations of next generation cost-effective mobile fronthaul with ifof technique," in *Optical Fiber Conference (OFC)*, San Diego (California), March 2015.

[30] *Radio-over-Ethernet Project (IEEE 1914.3)*. [Online]. Available: https://standards.ieee.org/develop/project/1914.3.html

[31] T. Pfeiffer, "Next generation mobile fronthaul architectures," in *Optical Fiber Conference (OFC)*, San Diego (California), March 2015.

[32] D. Chitimalla, K. Kondepu, L. Valcarenghi, and B. Mukherjee, "Network function virtualization: Challenges and directions for reliability assurance," in *Advanced Networks and Telecommuncations Systems (ANTS), 2015 IEEE International Conference on*, Dec. 2015.

[33] P. Assimakopoulos, M. K. Al-Hares, and N. J. Gomes, "Switched ethernet fronthaul architecture for cloud-radio access networks," *IEEE/OSA Journal of Optical Communications and Networking*, vol. 8, pp. B135–B146, December 2016.

[34] I. Chih-Lin, J. Huang, R. Duan, C. Cui, J. Jiang, and L. Li, "Recent progress on c-ran centralization and cloudification," *IEEE Access*, vol. 2, pp. 1030–1039, 2014.

[35] J. Lorca and L. Cucala, "Lossless compression technique for the fronthaul of lte/lte-advanced cloud-ran architectures," in *2013 IEEE 14th International Symposium on "A World of Wireless, Mobile and Multimedia Networks" (WoWMoM)*, June 2013.

[36] U. Dötsch, M. Doll, H.-P. Mayer, F. Schaich, J. Segel, and P. Sehier, "Quantitative analysis of the split base station processing and determination of advantageous architectures for lte," *Bell Labs Technical Journal*, vol. 18, pp. 105–128, 2013.

[37] M. Peng, C. Wang, V. Lau, and H. Poor, "Fronthaul-constrained cloud radio access networks: insights and challenges," *IEEE Wireless Communication*, vol. 22, no. 2, pp. 152–160, 2015.

[38] L. Valcarenchi, K. Kondepu, and P. Castoldi, "Analytical and experimental evaluation of cpri over ethernet dynamic rate reconfiguration," in *INFOCOM 2016, 25th IEEE International Conference on Computer Communications Proceedings*, Kuala Lumpur (Malaysia), May 2016.

[39] J. Liu, S. Xu, S. Zhou, and Z. Niu, "Redesigning fronthaul for next-generation networks: beyond baseband samples and point-to-point links," *IEEE Wireless Communication*, vol. 22, no. 5, pp. 90–97, 2015.

[40] C.-Y. Chang, R. Schiavi, N. Nikaein, T. Spyropoulos, and C. Bonnet, "Impact of packetization and functional split on c-ran fronthaul performance," in *INFOCOM 2016, 25th IEEE International Conference on Computer Communications Proceedings*, Kuala Lumpur (Malaysia), May 2016.

[41] M. Fiorani, P. Monti, B. Skubic, J. Martensson, L. Valcarenghi, P. Castoldi, and L. Wosinska, "Challenges for 5g transport networks," in *International Conference on Advanced Networks and Telecommuncations Systems (IEEE ANTS)*, 2014.

[42] M. Raza, M. Fiorani, B. Skubic, J. Martensson, L. Wosinska, and P. Monti, "Power and cost modeling for 5g transport networks," in *International Conference on Transparent Optical Networks*, Budapest (Hungary), July 2015.

[43] L. Wang and S. Zhou, "On the fronthaul statistical multiplexing gain," *IEEE Communication Letters*, pp. 1–1, January 2017.

[44] D. Sabella, P. Rost, Y. Sheng, E. Pateromichelakis, U. Salim, P. Guitton-Ouhamou, M. Di Girolamo, and G. Giuliani, "Ran as a service: Challenges of designing a flexible ran architecture in a cloud-based heteroge-

neous mobile network," in *Future Network & Mobile Summit (FutureNetworkSummit) 2013*, July 2013.

[45] S. Nishihara, S. Kuwano, K. Miyamoto, J. Terada, and A. Otaka, "Study on protocol and required bandwiidth for 5g mobile fronthaul in c-ran architecture with mac-phy split," in *The 22nd Asia-Pacific Conference on Communication (APCC2016)*, August 2016.

[46] K. Miyamoto, S. Kuwano, T. Shimizu, J. Terada, and A. Otaka, "Performance evaluation of ethernet- based mobile fronthaul and wireless comp in split-phy processing," *IEEE/OSA Journal of Optical Communications and Networking*, vol. 9, pp. A46 – A54, Jan. 2017.

[47] K. Miyamoto, S. Kuwano, J. Terada, and A. Otaka, "Split-phy processing architecture to realize base station coordination and transmission bandwidth reduction in mobile fronthaul," in *Optical Fiber Communications Conference*, March 2015.

[48] I. Katib and D. Medhi, "A study on layer correlation effects through a multilayer network optimization problem," in *The 23rd International Teletraffic Congress (ITC)*, San Francisco (California), September 2011.

[49] I. Katib and D. Medhi, "Optimizing node capacity in multilayer networks," *IEEE Communications Letters*, vol. 15, pp. 581–583, May 2011.

[50] I. Katib and D. Medhi, "A network protection design model and a study of three-layer networks with ip/mpls, otn and dwdm," in *8th International Workshop on the Design of Reliable Communication Networks (DRCN)*, Kracow (Poland), October 2011.

[51] J. Santos, J. Pedro, P. Monteiro, and J. Pires, "Optimization framework for supporting 40 gb/s and 100 gb/s services over heterogeneous optical transport networks," *Journal of Networks*, vol. 7, pp. 783–790, May 2012.

[52] J. Santos, J. Pedro, P. Monteiro, and J. Pires, in *IEEE International Conference on Communications (ICC*, Kyoto (Japan).

[53] J. Santos, J. Pedro, P. Monteiro, and J. Pires, "Simplified framework for optimal support of 40 gb/s and 100 gb/s services over otn exploiting grooming and vcat," in *Conference on Optical Fiber Communication and the National Fiber Optic Engineers Conference (OFC/NFOEC)*, San Diego (California), March 2010.

[54] ITU-T, *Interfaces for the Optical Transport Network (OTN)*, 2009, recommendation G.709/Y.1331.

[55] P. Mahajan, "The economics of using ip over otn in core networks,," in *World Telecommunications Congress (WTC)*, Berlin (Germany), June 2014.

[56] A. Deore, O. Turkcu, S. Ahuja, S. J. Hand, and S. Melle, "Total cost of ownership of wdm and switching architectures for next-generation 100gb/s networks," *IEEE Communication Magazine*, no. 50, pp. pp. 179–187, November 2012.

[57] S. Melle, A. Deore, O. Turkcu, S. Ahuja, and S. Hand, "Titolo sconosciuto," in *Comparing optical and OTN switching architectures in next-gen 100Gb/s networks,*, Anaheim (California), March 2013.

[58] W. Bo, Q. Shaofeng, F. Zhiyong, C. Shiyi, Z. Han, X. Junling, D. Chiwu, G. Liu, D. Ning, and X. QianJin, "Green and agile petabit optical sub-wavelength switching prototype for the future otn multi-chassis switch cluster,," in *Optical Fiber Communications Conference*, Anaheim (California), March 2013.

[59] T. Hashiguchi, Y. Takita, K. Tajima, and T. Naito, "Designs of otn-level shared mesh restoration in wdm networks,," in *Design of Reliable Communication Networks Conference*, Budapest (Hungary), March 2013.

[60] I.-T. R. G.709, "Interfaces for the optical transport network (otn)," Tech. Rep., 2003.

[61] I.-T. R. G.798, "Characteristics of optical network hierarchy equipment functional blocks," Tech. Rep., 2004.

[62] I.-T. R. G.872, "Architecture of optical transport networks," Tech. Rep., 2001.

[63] R. Jensen, "Optical switch architectures for emerging colorless/directionless/contentionless roadm networks," in *Conference on Optical Fiber Communication and the National Fiber Optic Engineers Conference (OFC/NFOEC)*, Los Angeles (California), March 2011.

[64] S. Tibuleac and M. Filer, "Trends in next-generation roadm networks," in *37th European Conference and Exhibition on Optical Communication (ECOC)*, Geneva (Italy), September 2011.

[65] J. Strand, "Integrated route selection, transponder placement, wavelength assignment, and restoration in an advanced roadm architecture," *IEEE Journal Optical Communications and Networking*, vol. 4, pp. 282–288, March 2012.

[66] S. Woodward, M. Feuer, I. Kim, X. Palacharla, P.and Wang, and D. Bihon, "Service velocity: Rapid provisioning strategies in optical roadm networks," *IEEE Journal Optical Communications and Networking*, vol. 4, pp. 92–98, February 2012.

[67] M. Feng, K. Hinton, R. Ayre, and R. Tucker, "Reducing ngn energy consumption with ip/sdh/wdm," in *1-st International Conference on Energy-Efficient Computing and Networking (e-Energy)*, Athens (Greece), October 2011.

[68] J. Baliva, K. Hinton, R. Ayre, W. Sorin, and R. Tucker, "Energy consumption in optical ip networks," *IEEE Journal Lightwave of Technology*, vol. 27, pp. 2391–2401, July 2009.

[69] G. Shen and R. Tucker, "Energy minimized design for ip over wdm optical networks," *IEEE Journal Optical Communications and Networking*, vol. 1, pp. 176–186, June 2009.

[70] F. Kish, "Current status of large-scale inp photonic integrated circuits,," *IEEE Journal of Selected Topics in Quantum Electronics*, no. 17, pp. 1470–1489, March/April 2011.

[71] S. Melle, "Building agile optical networks,," in *Optical Fiber Communications Conference*, San Diego (California), March 2008.

[72] P. Iovanna, R. Sabella, F. Testa, A. Testa, P.and Germoni, and M. Casanova, "Digital vs. all-optical networking in packet-optical integrated transport: a lifecycle cost-benefit analysis," in *37th European Conference and Exhibition on Optical Communication (ECOC)*, Geneva (Italy), September 2011.

[73] P. Iovanna, F. Testa, R. Sabella, A. Bianchi, M. Puleri, M. Casanova, and A. Germoni, "Packet-optical integration nodes for next generation transport networks," *IEEE Journal Optical Communications and Networking*, vol. 4, pp. 821 – 835, 10 2012.

[74] G. Eilenberger, "Integrated electrical/optical switching for future energy efficient packet networks," in *Conference on Optical Fiber Communication and the National Fiber Optic Engineers Conference (OFC/NFOEC)*, Los Angeles (California), March 2011.

[75] G. Zhang and S. Xiong, Q.and Shen, "Novel multi-granularity optical switching node with wavelength management pool resources," in *4-th Asia- Pacific Photonics Conference (APMP 2009)*, Bejing (China), April 2009.

[76] S. Gringeri, B. Basch, V. Shukla, R. Egorov, and T. Xia, "Flexible architectures for optical transport nodes and networks," *IEEE Communication Magazine*, vol. 48, pp. 40–50, July 2010.

[77] P. Belotti, K. Kompella, L. Ceuppens, and L. Noronha, "Transport networks at a crossroads, the roles of mpls and otn in packet transport networks," in *Conference on Optical Fiber Communication and the National Fiber Optic Engineers Conference (OFC/NFOEC)*, Los Angeles (USA), March 2011.

[78] S. Melle and V. Vusirikala, "Network planning and architecture analysis of wavelength blocking in optical and digital roadm networks," in *Conference on Optical Fiber Communication and the National Fiber Optic Engineers Conference (OFC/NFOEC)*, Anaheim (California), March 2007.

[79] S. Melle and V. Vusirikala, "Analysis of wavelength blocking in large metro core network using optical and digital roadm transport system,," in *33rd European Conference and Exhibition on Optical Communication*, Berlin (Germany), September 2007.

[80] V. Eramo, M. Listanti, R. Sabella, and F. Testa, "Study of otn switching resource assignment policies in integrated otn/wdm nodes," in *International Conference on Transparent Optical Networks*, Cartagena (Spain), July 2013.

[81] V. Eramo, M. Listanti, R. Sabella, and F. Testa, "Integrated otn/wdm switching architecture equipped with the minimum number of otn switches," *IEEE Journal of Optical Communications and Networking*, no. 6, pp. 138–151, February 2014.

[82] V. Eramo, M. Listanti, F. Lavacca, R. Sabella, and F. Testa, "Blocking performance of metropolitan optical networks equipped with low complexity integrated otn/wdmswitches," in *International Conference on Transparent Optical Networks*, Graz (Austria), July 2014.

[83] V. Eramo, M. Listanti, F. Lavacca, R. Sabella, and F. Testa, "Performance evaluation of integrated otn/wdm metropolitan networks in static and dynamic traffic scenario," *IEEE Journal of Optical Communications and Networking*, no. 7, pp. 761–775, July 2015.

[84] K. Zhu and B. Mukherjee, "Traffic grooming in an optical wdm mesh network,," *IEEE Journal on Selected Areas in Communications*, no. 20, pp. 122–133, January 2002.

[85] V. Eramo, M. Listanti, F. Lavacca, R. Sabella, and F. Testa, "Blocking performance of cost efficient integrated otn/wdm metropolitan networks in static traffic scenario," in *2015 International Conference on Optical Network Design and Modeling (ONDM)*, Pisa (Italy), May 2015.

[86] S. Melle and V. Vusirikala, "Network planning and architecture analysis of wavelength blocking in optical and digital roadm networks,," in *Optical Fiber Communications Conference*, Anhamein (California), March 2007.

[87] Y. Takita, T. Hashiguchi, K. Tajima, and T. Naito, "Investigation of traffic grooming characteristics for otn/wdm networks," in *The 18th Opto-Electronics and Communications Conference*, Kyoto (Japan), July 2013.

[88] V. Eramo, M. Listanti, F. Lavacca, R. Sabella, and F. Testa, "Performance improvement evaluation of otn/wdm metropolitan nodes provided with spatial speed-up," in *International Conference on Transparent Optical Networks*, Budapest (Hungary), July 2015.

[89] D. Lee and S. Zhou, "Spatial modeling of the traffic density in cellular networks," *IEEE Wireless Communication*, no. 21, pp. 80–88, 2014.

[90] *ManyCities*. [Online]. Available: http://www.manycities.org/

[91] M. Imran and *et al.*, "Energy efficiency analysis of the reference systems, areas of improvements and target breakdown," in *EU Project EARTH Deliverable D2.3*, Jan 2012.

[92] M. Fiorani, S. Tombaz, F. Farias, L. Wosinska, and P. Monti, "Joint design of radio and transporrt for green residential access networks," *IEEE Journal on Selected Area in Communications*, April 2016.

[93] X. e. Chen, "Analyzing and modeling spatio-temporal dependence of cellular traffic at city scale," in *IEEE International Conference on Communications 2015*, London (England), June 2015.

[94] B. Cobb and R. Salmeron, "Approximating the distribution of a sum of log-normal random variables," in *Sixth European Workshop on Probabilistic Graphical Models*, Granada (Spain), 2012.